

DESIGN AND DEVELOPMENT OF FORCE TRANSDUCERS FOR INDUSTRIAL APPLICATIONS

by

RAJESH KUMAR

(2K11/PhD/ME/04)

Department of Mechanical Engineering

Submitted

in fulfilment of the requirements of the degree of

Doctor of Philosophy

to the



Delhi Technological University


Bawana Road, Delhi-110042 (India)

November-2018

CERTIFICATE

This is to certify that the thesis entitled "Design and Development of Force Transducers for Industrial Applications" being submitted by Rajesh Kumar (Regn. No. 2k11/PhD/ Mech. Engg./04) in the Department of Mechanical, Production & Industrial Engineering, Delhi Technological University, Delhi, India for the award of Degree of 'Doctor of Philosophy' in Mechanical Engineering, is a bonafide research work carried out by him under my supervision and guidance. His thesis has reached the standard of fulfilling the requirements of regulations relating to degree. The thesis is an original piece of research work and embodies the findings made by the research scholar himself.

The results presented have not been submitted in part or in full to any other University/ Institute for the award of any degree or diploma.


(Dr. Sagar Maji)

Supervisor

Professor,

Department of Mechanical, Production &
Industrial Engineering,

Delhi Technological University,
Delhi - 110 042, India.


(Dr. B. D. Pant)

Co-Supervisor

Emeritus Scientist

CSIR-Central Electronics Engineering
Research Institute, Pilani.

Rajasthan- 333 031, India.

And

Professor

AcSIR, New Delhi, India.

ACKNOWLEDGEMENTS

Completing any work of great proportions is no easy task. The immense pain which any researcher undergoes as part of doing quality research work is beyond explanation. At the outset, I am very thankful to the Almighty for bestowing me with good health to carry out a worthwhile research work. It is my privilege to express my sincere gratitude to all the persons who played a very vital role in giving direction and helping me in achieving the objectives of the research.

I am extremely thankful to my research supervisor **Professor S. Maji** and **Dr. B.D. Pant** for giving me an opportunity to work under their able supervision. It is their complete confidence in me that paved the way for this research work. I am very much obliged to them for their active support throughout the course of my research work. I am very privileged to have them as my supervisors not only for this thesis but also for future endeavors in life. The guidance, support, motivation, flexible behaviour, and help extended to me during my Ph.D. work from my supervisors were valuable and unforgettable for me. I would also like to extend my gratitude to **Dr. Ranjana Mehrotra**, Chief Scientist and **Dr. Sanjay Yadav**, Senior Principal Scientist, CSIR – National Physical Laboratory, New Delhi, who helped me in the research work. His continuous support and a very long experience related to the Physico-mechanical metrology were very wonderful during the course of research work.

I am also thankful to **Dr. Harish Kumar**, Assistant Professor, NIT, Delhi, Narela, for his support and motivation in accomplishing this work. I offer my sincere thanks to **Prof. R S Mishra**, Delhi Technological University, Bawana, Delhi for consistent motivation and

support. I would like to extend my sincere thanks to **Dr. D K Aswal**, Director, CSIR – National Physical Laboratory, New Delhi for their support to pursue Ph. D.

But most of all, I would like to offer my thanks to my family. I am grateful to God for blessing me with such a wonderful family. It is my mother **Mrs. Omwati** and my Father **Mr. Vinod Kumar**, who always inspired me. My wife **Purnima** fills my thoughts and there is no other person with whom I would have wish to share this incredible adventure called life. There is no compensation sufficient for the sacrifices she has made and the burdens she has carried as a result of my decision to pursue this support, patience and loving participation in accomplishing this task. I am also very thankful to my daughter **Kriti** and my son **Jayant Kumar**, the time given to research work could be spent with them, and they would have missed my attention during the research work. Last but not the least; I thank all my relatives and well-wishers for their wishes.

November, 2018

(**Rajesh Kumar**)

ABSTRACT

The precise and accurate force measurement performs an extremely important job during a variety of industrial applications, which helps in quality control of the product development and to optimize different material synthesis processes, thus necessitating its precise and accurate measurement. From the investigation of global research, it is noticed that the majority of investigation linked to force measurement has been done to design and develop a variety of force transducers. A limited investigation has been made to talk about different facets of primary force standard as well as secondary force calibration machines.

With day by day growing technological demands of quality systems (ISO 9000/IS 14000) and call for more precise & accurate measurement of force for quality products, the force transducers are developed. Force transducers play a very significant role in maintaining uniformity in force measurements and proficiency testing within the country by providing unbroken chain of measurement traceability of force from primary force standard machines/force calibration machines to the uniaxial testing machines (UTM) of user industries and NABL accredited calibration laboratories. Although the force transducers have been developed related to various field applications, however the majority of the development has been regard to meet the demand of particular applications and barely any attention is given for development of force transducer to serve up as force transfer standards.

Considering the past research shortcomings into account, the present investigation aims to develop some force transducers intended for applications of static force measurement. The circular diaphragm shaped steel force transducers are developed on the basis of classical plate theory (CPT) of bending of circular plate and investigated for deflection and

stress/strain under action of centrally applied forces. Another very small MEMS circular diaphragm load sensor of silicon is developed on the basis of deflection theorem related to small MEMS sensors. Rigorous validations have been taken into account for the findings of analytical approach with the computational investigations e.g. finite element analysis. Deviations are found among the analytical and computational findings. The one of the elastic sensing element are fabricated of steel (EN24) by conventional technique, along with another very small elastic sensing element of silicon are fabricated through MEMS technology. Both the elastic sensing elements are strain gauged on the most suitable locations find out on the basis of FEM software. The strain gauges are then configured in a Wheatstone bridge circuit. The force transducers thus developed are then metrological characterized as per the calibration procedures based on standards like ISO-376 & IS- 4169 and their measurement uncertainty are evaluated.

The force transducer under reference will be of great importance both as force proving and measuring instruments for NABL accredited laboratories to maintain traceability to national force primary standard and for proficiency testing in the country. The present research will also enable the metrology personals to design, develop and metrological investigate the force transducers in a rationalized manner.

TABLE OF CONTENTS

Title	Page
Certificate	i
Acknowledgement	ii
Abstract	iv
Table of Contents	vi
List of Figures	xii
List of Tables	xvi
Symbols	xviii
List of Publications	xx

Chapter 1	Introduction	
	1.1 Force Introduction	1
	1.1A Role in Standardization	3
	1.1B Realization of Force	4
	1.2 Force Proving Device	4
	1.2 A Category of Dial Gauge based Force Measuring Devices	6
	1.2 B Standardizing Box	8
	1.2 C Development of Force Transducers based on Hall Effect & Tuning Fork type)	9
	1.2 D Strain Gauged Force Transducer	10
	1.3 Limitations of Present Industrial Force Proving Instruments	13

1.3.1	Motivation	13
1.3.2	Salient features of silicon force transducers	15
1.4	Research Objectives	15
1.5	Specific Research Objectives	16
1.6	Research methodology	17
1.7	Thesis Organization	17
1.8	Summary	20

Chapter 2

Literature Review

2.1	Introduction	21
2.2	Analogue Force Transducers (Dial Gauged)	21
2.3	Digital Strain Gauged Force Transducers	22
2.4	Force Transducers (Tuning Fork Type)	25
2.5	Silicon based Force Transducers	26
2.6	Modified Ring shaped Analogue Force Transducers	28
2.7	Force Transducer based on Agriculture need	32
2.8	Force Transducers based on Special Purpose/Need	33
2.9	Computational Studies of Force Transducers	36
2.10	Procedures of calibration	37
2.11	Force Calibration Methods	39
2.12	National Measurement Facilities of force in India at NPL, New Delhi	43
2.13	Commercially available Force Transducers	48

2.14	Shortcomings of the Past Research	49
2.15	Summary	51
Chapter 3	Design of diaphragm based Force Transducers through analytical approach	
3.1	Introduction	52
3.2	Analytical Approaches	52
3.2.1	Classical Plate Theory	52
3.2.1A	Types of plate theories	53
3.2.1B	Assumptions of Thin Plate Theory	53
3.3	Analytical model for Steel Force transducer	56
3.4	Analytical model for MEMS Silicon Force transducer	58
3.5	Summary	61
Chapter 4	Computational studies of diaphragm based Force Transducers	
4.1	Introduction	62
4.2	FE Model of the Steel Force Transducer	62
4.3	Key Outcomes of FE Analysis of Steel Force Transducer	64
4.4	FE Model of the MEMS Silicon Force Sensor	69
4.5	Key Outcomes of FE Analysis of Silicon Force Sensor	72
4.6	Summary	79

Chapter 5	Fabrication and Metrological Investigation of the EN 24 steel grade based Diaphragm Force Transducer	
5.1	Introduction	81
5.2	Fabrication of Steel Diaphragm Force Transducer	81
5.3	Bonding of Strain Gauges	82
5.4	Investigations of a of Steel diaphragm for Metrological characteristics	85
5.4.1	Calibration method according to Standard ISO 376- 2004/ 2011	86
5.4.2	Calibration method according to Standard IS : 4169-88, re-affirmed 2003	88
5.5	Summary	101
Chapter 6	Fabrication and performance evaluation of MEMS based diaphragm force sensor	
6.1	Introduction	102
6.2	Fabrication Approach	104
6.2.1	Selection of materials	104
6.2.2	MEMS Fabrication Processes	105
6.3	Materials chosen for the device	108
6.4	Mask details and layout	109
6.5	Process flow chart	111
6.6	Device fabrication	114

6.6.1	Wafer selection	114
6.6.2	Silicon Wafer Cleaning Processes	116
6.6.3	Piranha and Nitric Acid cleaning	117
6.6.4	Thermal oxidation	119
6.6.5	Growth of Quality Oxide for electrical isolation of Piezoresistors	122
6.6.6	Polysilicon Deposition for Piezoresistors.	123
6.6.7	Phosphorous Diffusion in Polysilicon	124
6.6.8	Polysilicon Oxidation and Annealing	125
6.6.9	Polysilicon patterning and formation of piezoresistors	126
6.6.10	Photolithography: Mask-1	126
6.6.11	RIE of PolySi	128
6.6.12	Oxide etching for Diaphragm	128
6.6.13	PECVD oxide deposition	129
6.6.14	Contact opening in PECVD oxide	130
6.6.15	Metalisation	130
6.6.16	Formation of Si Diaphragm	130
6.6.17	Patterning of Aluminum	134
6.6.18	Anodic Bonding with Pyrex Glass	135
6.6.19	Dicing of the Fabricated Chips	135
6.7	Packaging of the Device	136
6.8	Investigations of a of Silicon diaphragm for Metrological characteristics	137
6.9	Summary	141

Chapter 7	Conclusion and Future Scope of Work	
7.1	Introduction	142
7.2	Summary of these Investigations Findings	142
7.3	Study-wise Learning's and Conclusions	143
7.4	Key conclusion of Research	146
7.5	Research's Socio-Economic Impact	147
7.6	Important investigation Contribution	149
7.7	Limitations of the Investigative Work	150
7.8	Scope for Future Research Work	152
7.9	Summary	153
	Bibliography	155
	Bio-data	169

LIST OF FIGURES

FIGURE NO.	TITLE	PAGE
Figure 1.1	Different applications of force transducers	2
Figure 1.2	Unbroken chain of traceability of force measurement	3
Figure 1.3	Dial Gauged Instruments: (a) Analogue Ring Shaped Force Proving Instrument (b) Bow Dynamometer (c) Amsler loop dynamometer (d) Dynamometer of make (A. Macklow-Smith Ltd.)	6
Figure 1.4	A mercury based Standardizing Box	8
Figure 1.5	A Tuning Fork type Force Transducer [14]	10
Figure 1.6	A typical strain gauged force transducer with Wheatstone bridge and a typical strain gauge [11]	10
Figure 1.7	Bridge Circuit with compensation resistors	13
Figure 1.8	Research Methodology Flowchart	17
Figure 2.1	A silicon load cell with thin-film strain gauges [33]	28
Figure 2.2	Dead Weight Force Machine (2 MN) at PTB, Germany [95]	40
Figure 2.3	Dead Weight cum Lever Multiplication Force Standard Machine (1 MN) at NPL, India [100]	41
Figure 2.4	Hydraulic Multiplication Force Machine (3 MN) (Courtesy M/s GTM, Germany)	42
Figure 2.5	Low force measurement machine, PTB, Germany	43
Figure 2.6	Dead Weight Standard Force Machine (50 N) NPL	45
Figure 2.7	Dead weight Force Machine (50 kN) at NPL [98]	46

Figure 2.8	Force Standard Machine (1 MN) at NPL	47
Figure 2.9	Hydraulic Multiplication Force Machine (1 MN) at NPL	48
Figure 3.1	Cartesian axes with plate	54
Figure 3.2	Diagram view of Steel force transducer	55
Figure 3.3	Maximum deflection simulation plot for Steel transducer	58
Figure 3.4	Schematic view of MEMS silicon force transducer	58
Figure 3.5	Maximum deflection simulation plot for MEMS transducer	60
Figure 4.1	3-D CAD model of the Steel force transducer	63
Figure 4.2	Meshing of steel diaphragm	64
Figure 4.3	Force application at the centre of the diaphragm	64
Figure 4.4	Stress for steel force transducer at 5 kN load	65
Figure 4.5	Stress distribution for steel force transducer	65
Figure 4.6	Strain for steel force transducer at 5 kN load	66
Figure 4.7	Strain distribution for steel force transducer	66
Figure 4.8	Deflection plot for steel transducer	67
Figure 4.9	Dimensional cross-section view of diaphragm force sensing element	70
Figure 4.10	3-D Silicon force sensor CAD model	71
Figure 4.11	Meshing of the Silicon force sensor	71
Figure 4.12	Force application at the centre of the silicon diaphragm	72
Figure 4.13	Stress of MEMS force sensor	73
Figure 4.14	Stress distribution of silicon sensor	73
Figure 4.15	Strain of MEMS sensor	74
Figure 4.16	Strain distribution of MEMS force Sensor	75
Figure 4.17	Deflection plot for silicon force sensor	76
Figure 4.18	Computational deflection data of silicon force sensor	77

Figure 4.19	Comparison between computational and theoretical results of silicon force sensor	79
Figure 5.1	A typical Wheatstone bridge [10]	84
Figure 5.2	Arrangements of Strain Gauges	84
Figure 5.3	Strain Gauged Force Transducer	84
Figure 5.4	Experimental setup for steel diaphragm force transducer at force machine of 50 kN dead weight at NPL, New Delhi	85
Figure 5.5	5 kN force transducer metrological characterization according to IS 4169-1988 (reaffirmed 2003) [116]	96
Figure 5.6	5 kN force transducer metrological characterization according to ISO 376-2004 [116]	97
Figure 5.7	Schematic diagram of array of strain gauges (R: Radial; T: Tangential) with connectivity of strain gauges	99
Figure 6.1	Block diagram of the cross-section of the device with different dimensions	103
Figure 6.2	Snapshot of the combined mask layout	111
Figure 6.3	Process Flow Chart	113-114
Figure 6.4	Specialty Chemical Bench for cleaning (RCA cleaning in progress)	118
Figure 6.5	(a) Wafer cleaning in Piranha. (b) Removal of native oxide in dilute HF	119
Figure 6.6	MRL Oxidation furnace Model SBR 1503 used in this work	121
Figure 6.7	DELTA 80 BM Spin Coater used in the present work	127
Figure 6.8	SUSS MA6 Mask Aligner used in the present work	127
Figure 6.9	(a) Wafers loading in RIE machine (b) Plasma etching during process	128

Figure 6.10	DEKTEK Surface Profiler: Measurement of Etch Depth of Si	131
Figure 6.11	AMS 100 DRIE Tool (Alcatel Micro Machining System)	131
Figure 6.12	Si Circular Diaphragm with cavity etched from backside of the wafer using DRIE	134
Figure 6.13	Fully processed 150 mm Si wafer	135
Figure 6.14	Diced Chips: Si Force Sensor	136
Figure 6.15	PCB Layout for packaging of Force Sensor	137
Figure 6.16	PCB Layout with Force Sensor image	137
Figure 6.17	Force Sensor packaged on PCB and packed cover with epoxy with open diaphragm	137
Figure 6.18	Experimental setup for MEMS force sensor	138

LIST OF TABLES

TABLE NO.	TITLE	PAGE
Table 3.1	Deflection findings by Analytical method for Steel transducer	57
Table 3.2	Deflection findings by Analytical method for MEMS transducer	60
Table 4.1	Deflection of a Steel force transducer at different forces [106]	69
Table 4.2	Deflection of a Silicon force sensor at different forces [106]	78
Table 5.1	Nominal dimensions of the force transducers	82
Table 5.2	Relative components of error and their contribution for Measurement Uncertainty as per ISO 376-2004/2011	88
Table 5.3	Relative components of error and their contribution for Measurement Uncertainty as per IS 4169-88 (reaffirmed 2003)	90
Table 5.4	Difference between ISO - 376 and IS - 4169	94
Table 5.5	Relative uncertainty measurement of force devise as per IS 4169 with factors discussing the metrological characterization	95
Table 5.6	Sample calculation of measurement uncertainty for 0.5 kN force step	95
Table 5.7	Relative uncertainty measurement of force devise as per ISO 376 with factors discussing the metrological characterization	96
Table 5.8	Uncertainty Budget at higher value at 1.0 kN force step	98
Table 5.9	Relative uncertainty measurement of force devise with improved sensitivity as per ISO-376 with factors discussing the metrological characterization	100
Table 6.1	Device Parameters	103

Table 6.2	Different Material Layers	106
Table 6.3	Material Processing Techniques	107
Table 6.4	Material Layers for the device	109
Table 6.5	Mask details	110
Table 6.6	Development process of MEMS sensor	111-113
Table 6.7	Wafer Specifications	115
Table 6.8	Oxidation process Schedule	121
Table 6.9	Optimized Process for LPCVD Low Stress Polysilicon	124
Table 6.10	Process Parameters for P-Diffusion	125
Table 6.11	HER Process Recipe	132
Table 6.12	Process Results	132
Table 6.13	HAR Process Recipe	133
Table 6.14	Process Results	133
Table 6.15	Associated uncertainty components along with their relative (%) contribution	138
Table 6.16	Different factors pertaining to metrological characterization with uncertainty of measurement of MEMS force sensor	139
Table 6.17	Maximum Measurement Uncertainty budget (%) of MEMS silicon force sensor at 10 N	140

SYMBOLS

SYMBOL	STANDS FOR	UNIT
m	mass	kg
g	acceleration due to gravity	$m.s^{-2}$
ρ_a	density of air	$kg.m^{-3}$
ρ_m	density of material of weight	$kg.m^{-3}$
F	Force applied	N
μ	Poisson's ratio	--
ρ	Resistivity	Ohm/m
R	Resistance	ohm
L	Length of wire	mm
Di	Diameter of wire	mm
σ	Stress	$N.m^{-2}$
E_a	Axial Strain	mm/mm
E_t	Transverse strain	mm/mm
I	moment of inertia	mm^4
E	modulus of elasticity	GPa
δ	deflection	mm
w_{rep}	relative uncertainty due to repeatability	%
w_{rpr}	relative uncertainty due to reproducibility	%
w_{res}	relative uncertainty due to resolution	%
w_{zer}	relative uncertainty due to zero offset	%
w_{int}	relative uncertainty due to interpolation	%

w_{hys}	relative uncertainty due to hysteresis / % reversibility	
$w_{\text{c (tra)}}$	combined uncertainty of the force % transducer	
$W_{\text{(tra)}}$	expanded uncertainty of the force transducer	%
W_{bmc}	best measurement capability of the force % transducer	
W	uncertainty of measurement of force % transducer	
k	Coverage factor	--
U_j	Signal voltage	mV
U_i	Supply voltage	V
C	Sensitivity of Wheatstone bridge	mV/V
F_n	Nominal load capacity	N
D	Flexure rigidity	N.mm
h	Thickness of plate	mm
r	Radius of plate	mm
w	Deflection of plate	mm
Q	Shear force	N
A	Area of plate	mm ²
a	Distance from the centre of sensor	mm

LIST OF PUBLICATIONS

Publications in Journals

1. R Kumar and S. Maji (2016), Force transducers- A review of design and metrological issues, *Engineering Solid Mechanics*, **4**, 81-90.
2. R Kumar, B. D. Pant and S Maji (2016) Design, Development and Metrological Characterization of a Force Transducer, *Journal of Scientific and Industrial Research*, **75**, 320-321.
3. R Kumar, B. D. Pant and S. Maji (2017), Development and Characterization of a Diaphragm-Shaped Force Transducer for Static Force Measurement, *MAPAN-Journal of Metrology Society of India*, **32(3)**, 167–174.
4. R Kumar, Shanay Rab , B. D. Pant and S Maji (2018), Design, development and characterization of MEMS Silicon diaphragm force sensor, *Vacuum*, **153**, 211-216.
5. R Kumar, Shanay Rab , B. D. Pant, S Maji and R. S. Mishra (2018), FEA based design studies for development of diaphragm force transducers, *MAPAN-Journal of Metrology Society of India*, **Accepted**.

Publications in Conferences

1. R Kumar, B. D. Pant, S Maji and S S K Titus (2017), Testing and characterization of a MEMS Silicon Diaphragm based load cell, *In Proceedings of 5th National Conference on Advances in Metrology, (Admet-2017)*, March 23-25, 2017, The North Cap University, Sec-23A, Gurugram-122017, Haryana, India.
2. R Kumar, Shanay Rab Hayat, B.D. Pant and S Maji (2017), Design and Development of a MEMS Silicon Diaphragm Load Cell, *In the Proceedings of the 17th International Conference on Thin Films*, November 13-17, 2017, CSIR-National Physical Laboratory, New Delhi, India.

Chapter 1

Introduction

1.1 Force Introduction

Force is one of the most important physical entity, and hence its measurement is quite significant since time immemorial. If we look at the history of civilization, the significance of force measurement can be realized for a very long time. History of old civilization shows that people of ancient times used to apply their muscular force with the help of levers and rollers to generate large forces to accomplish the heavier jobs like pushing, pulling & lifting of heavier objects at that time. The concept of force measurement in the modern era was given by Sir Isaac Newton, who led the way for precise measurement of force and formulated laws related to its measurement. Modern research is still based on these certain analytical expressions developed by him. [1].

Force measurement is very important now a days for most of engineering applications, for desired accuracy and precision measurement with the day by day increasing demand for improved accuracy in measuring compressive & tensile forces in various testing machines of all kinds, used further at shop floor to evaluate the strength of the materials to have confidence in accessing about the optimum serving life of the components. Thus it makes a mandate for the National Metrological Institute (NMI) to pay attention to work upon to ascertain the accuracy of force measurement. Accurate / Precise measurements of forces have become important for the applications e.g.

i) Evaluating the strength of materials & engineering components by periodic verification of material testing machines as per standard like IS-1828-2005(part-1)/ISO7500-1:2004.

- ii) Controlling production process (achieving quality control of products) by way of monitoring cutting force measurement during different machining processes (e.g. turning, slotting, milling, drilling or shaping etc.),
- iii) Various grade steel producing rolling mills.
- iv) Designing safe buildings, infrastructures, installation of big machinery
- v) Measuring thrust of, rocket aircraft, gas turbine engines and jet engines
- vi) Load cell weighing bridges and electronic weighing apparatus
- vii) Weighing of aircraft (calibration of aircraft weighing kit) and other items of commercial, industrial and strategic applications
- viii) In the field of automobiles (footbrake, air bag, suspension and transmission system, speed control system.)
- ix) Hardness block calibration for verification of hardness scales like Rockwell scale, Vickers scale including their micro-hardness scale and Brinell scales
- x) Medical research (bone joints, bite force of tooth of human body)

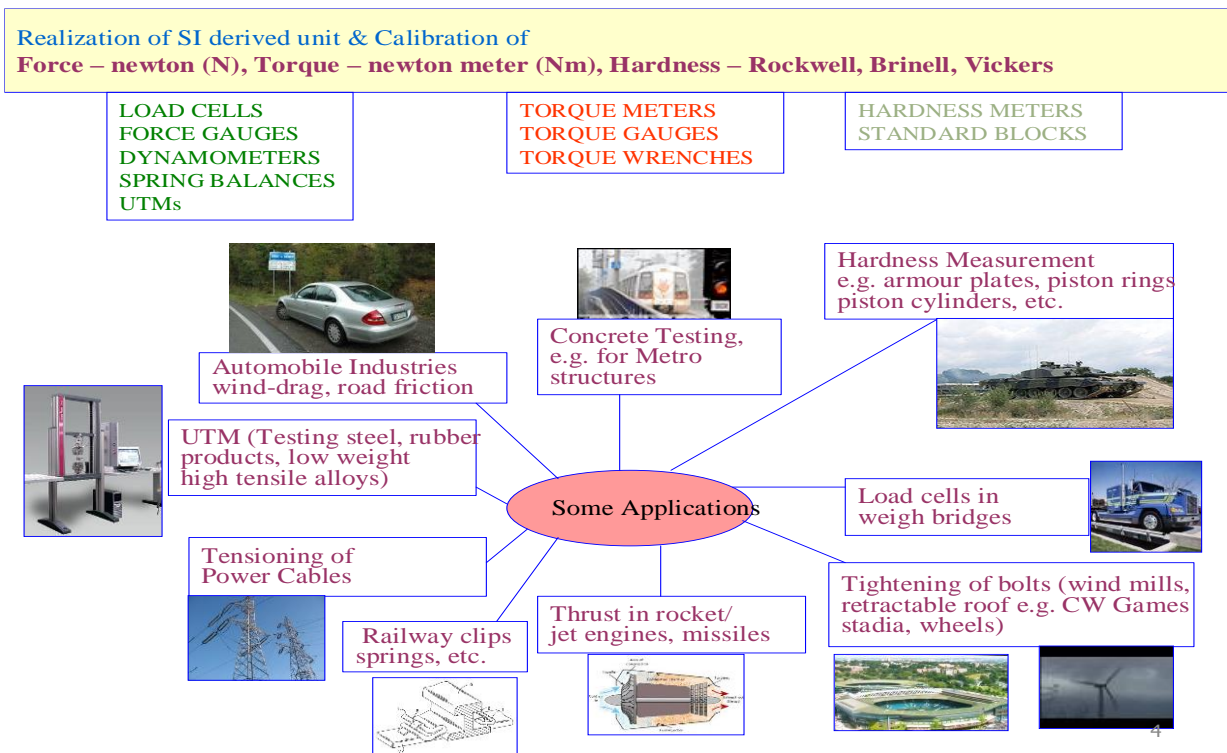


Fig. 1.1 Different applications of force transducers

1.1(A) Role in Standardization Indian industries have started recognizing the importance of qualities for long term survival in the growing global competitive market through consistency in their operation. Consistency cannot be ensured unless test and measuring equipment are of appropriate measuring capability and are traceable to the national measurement system with an unbroken chain of calibration. The fundamental of standardization are based on scientific research involving the establishments of standards and improvement in the measurement and calibration of instruments. The accurate measurement of force helps in quality control of the product development and to optimize different material synthesis processes. Some of their favourable features make the force transducer indispensable in the fields like

- Process control and complex automation
- Industrial and agricultural production processes
- Material handling and labour safety devices
- Civil engineering practice,
- Mining industry, medical biology and therapy

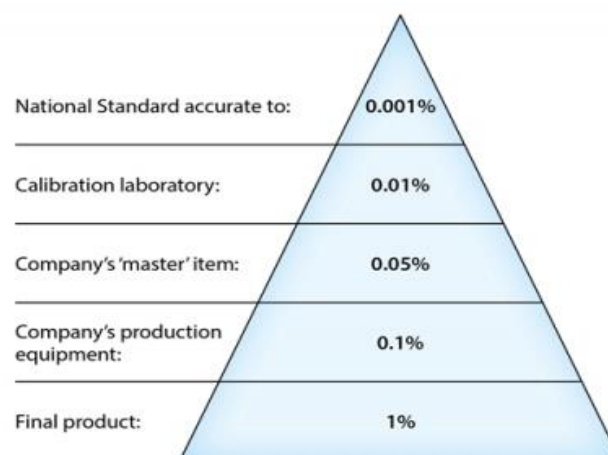


Fig. 1.2 Unbroken chain of traceability of force measurement

Therefore, force measurement is important in engineering applications as mentioned above, thus insisting accurate / precise measurement in meeting the multiple objectives of quality assurance, consumer protection, export promotion and safety norms. There is a great demand from the users that goods and services they wish to use have to be certified by organizations operating the quality system as per international standards like ISO 9000 & 14000 and ISO/IEC17025. The fundamental of all these standardization is based on the scientific research involving the establishment of measurement standards and improvement in the measurement and calibration of measuring instruments used by industries. The static force has been realized by a variety of force measuring machines /force sensors. The ranges of force varies from μN to MN [2-4], depending upon the use of force for different usage and may vary as given in the sections to follow.

1.1(B) Realization of force The generation and realization of the SI unit of Force has traditionally been performed through the first principal of dead weight, is the force because of gravitational force on the masses, minus the air buoyancy effect. Thus the exerted force by a dead / stationary mass on its supports in air is by the equation below.

$$F = mg (1 - \rho_a / \rho_m) \quad (1.1)$$

F is the force in Newton (N), m is the mass in kilogram (kg), g is the local value of gravity (m/sec^2), ρ_a is density of air (kg/m^3) and ρ_m is the density of mass (kg/m^3).

1.2 Force proving device Basically a force proving device is made up of a force transducer (spring element made of some elastic material) and combined with some associated indicating instrument (like dial gauge or digital electronic indicator etc.). The force transducer is loaded to the force to be measured, and the associated indicating instrument measures some deflection unit (analogue reading or electrical output like mV/V) which is

known as a resultant change in the element due to applied force on it. Force transducers are based on the elastic properties of a mass or a structure. This property enables to measure the magnitude of any force in terms of a change in dimension produced in a body or structure subjected to the unknown force.

The various type of force transducers along with their associated indicating device like analogue force proving ring & bow dynamometers/elliptical rings fitted with dial gauge, mercury based standardizing box columns, amsler loop dynamometers, dial gauge dynamometer of make A. Macklow-Smith and resistive strain gauged based load cells etc.[5-6], act as a bridge in disseminating the national standard of force (apex level) maintained at the NMI (National Measurement Institute) to the actual point of use at shop floor level i.e. various material testing machines installed at productions hubs. These are also act as the heart of the material testing machines, whenever these are used as an integral part of the material testing machines to indicate the real time load position during a particular material test. Spring scales were most commonly used for measurement of force since early 19th century, and the actual advancement of the force transducers started at NIST, USA [7-8] in 1927 by two scientists, Petrenko and Whittemore. These type of force mechanical systems were used for measurement of static forces, metrological applications and precise force measurement applications. Various types of force transducers / devices, such as integral force proving rings, bow dynamometers, load cells, etc., which are based on measurement of the elastic deformations, have been developed over the years and have been in use for force measurement with varying degree of performance. These are described in the following section.

1.2 (A) Category of dial gauge based force measuring devices



(a)



(b)



(c)



(d)

Fig. 1.3 Dial Gauged Instruments (a) Analogue Ring Shaped Force Proving Instrument (b) Bow Dynamometer (c) Amsler loop dynamometer (d) Dynamometer of make (A. Macklow-Smith Ltd.)

Force proving rings & various types of dynamometers make use of dial gauge as indicating device to measure the deformation. Like are commonly used as force sensors and sometimes as a strain sensor in various engineering applications. This consists of an elastic element ring or elliptical shaped made of high-grade steel and machined in such a way to provide two self aligning compression loading pads in either compression mode or with self aligning tension shackles in tensile mode or in both the modes (Figure 1.3). The elastic deformation of the force-proving device when subjected a standardized force can be measured along the axis of

force application by means of a dial gauge, vibrating reed or micrometer screw mounted inside the force transducer along the vertical axis. The proving ring is loaded in a force standard machine along its axis and the elastic deformation is recorded against various incremental forces applied. The output of the proving ring is recorded in either divisions or mm units.

In Indian scenario, it has also been found through survey that around 60-70% Indian customers are using analogue force proving rings/bow dynamometers at site of material testing labs of different manufacturing hubs and productions units of Indian goods, to verify different force scale ranges of material testing machines as per the Indian Std. IS-1828-2005(part-1)/ISO7500-1:2004 due to easy availability and cheaper cost of force proving rings only, in spite of various inherited disadvantages associated with analogue instruments, like it can be use for specific forces points only, non linear, require temperature corrections and unable to realize the low forces accurately [9]. They cannot to be used for automated processes and many proving rings are required to realize the forces over large range and to maintain a strict temperature control and subjected to the operator's capabilities. Moreover the dial gauge fitted with the proving ring gets sticky after a few months of use due to atmospheric pollution, thus increasing the repeatability error and lowering down the accuracy of the force measured. These are further cannot be used as transfer force standard either to have proficiency testing within accredited laboratories or to establish the compatibility of the national standard with the standard established in different countries.

1.2 (B) Standardizing Box



Fig. 1.4 A mercury based Standardizing Box

The standardizing box has been used prior to the proving ring. It consists of steel hollow cylinder with rigid ends. The force is applied to the ends in axial direction. A micrometer attached to a small plunger is fitted on the wall of the hollow cylinder and a small glass capillary ending in a bulb is fitted diametrically opposite to the micrometer. The hollow cylindrical space is filled with mercury. Before the calibration or using this box for force measurement, mercury level in the capillary is brought to a datum level with the help of a zero adjusting screw and micrometer is also brought to zero position. When force is applied the volume of the hollow cylindrical space changes and the level of the mercury shifts from the prefixed datum level. It is brought back to the datum level by manipulating the micrometer screw which is the corresponding micrometer output reading against the standard force applied.

Standardizing boxes are presently in a very limited use due to basic disadvantages e.g. difficult to use, problem of leakage of mercury, used for selected forces only, temperature sensitive and low forces measurement with inaccuracy, may not be used for automating the processes, subjected to the operator's technical competency, cannot be used as transfer force

standard either to have proficiency testing within accredited laboratories or to establish the compatibility of the national standard with the standard established in different countries.

Due to all these shortcomings associated with analogue force proving ring/ bow dynamometer and standardizing box makes it difficult to be used them as a force transfer standards, therefore the best alternative is to use the strain gauge force transducer as the strain gauge force transducer are more accurate, user friendly, and can be used over a wide range and in different environments in comparison to the existing elastic proving rings/bow dynamometers and standardizing boxes, thus makes them most suitable to use them as force transfer standards for participating in proficiency testing and inter comparisons to establish the measurement compatibility among the national standards maintained globally at different locations of other NMI's [10-11].

1.2 (C) Development of Force Transducers based on Hall Effect & Tuning Fork type)

Researchers have recently developed ring shaped force transducers based on Hall Effect sensors for field applications related to static and dynamic force measurements. Higher bandwidth force transducers in a wider range can be manufactured at a low cost in comparison to the commercially available strain gauge force transducers. But, this developmental work are still in a very preliminary phase and are yet to be proved over a large scale to find their suitability for various applications. [12-13].

Non-conventional methods are also tried for force measurements recently some years back on a tuning fork based force transducer mechanism, which converts force into resonance frequency, and also not sensitive to the elastic bodies characteristics. A 50 N force transducer has been developed by means of a (DETF) double-ended tuning fork for investigated preliminary studies. The results were found interested in contrast to conventional strain gauged based force devices in terms of Standard ISO 376. The relative error components like

reproducibility, repeatability, zero, interpolation, and reversibility were considered for comparison study between the two. The metrological suitability is yet to be established for tuning fork load cell in terms of its use as a travel standard for inter comparison work among different force standards. Although preliminary investigations are excellent, but further rigorous verifications of metrological capabilities of such force transducers are to be established. (Figure 1.5) [14].

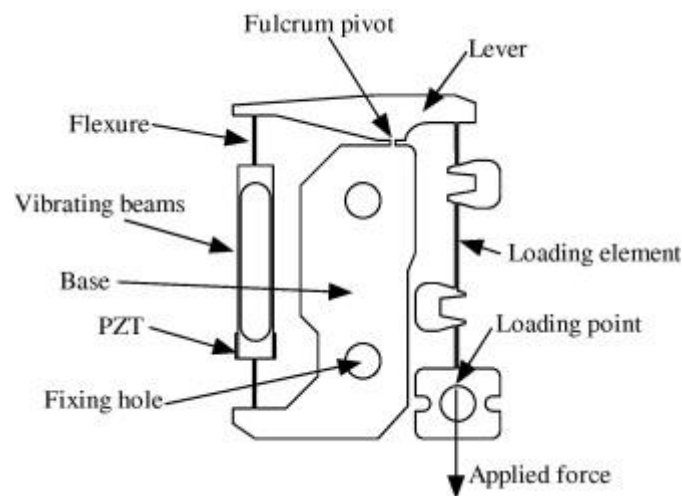


Fig. 1.5 A Tuning Fork type Force Transducer [14]

1.2 (D) Strain gauged force transducers

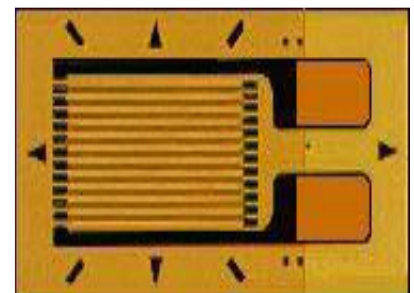


Fig. 1.6 A typical strain gauged force transducer with Wheatstone bridge and a typical strain gauge [11]

A limited accuracy of analogue force measuring device has led thrust over the development of strain gauged force transducers for last few decades, which are free from the errors as in case of analogue proving rings/bow dynamometers. With the high growing demand of industrialization and higher accuracies in force measurements 1960's onwards, strain gauges have been started using for many applications. The strain gauged force devices have been able to perform very well over the years and some researchers studied aspects of design and performance. The strain gauged force devices are based on measurement of the device strain proportional to change in resistance of metallic foils (strain gauges) fixed on device spring elements and are being used for force measurement. This change in resistance of strain gauges are measured by connecting four strain gauges in a Wheatstone bridge configuration and suitably placed on the elastic element and powered by an external excitation voltage. The voltage difference generated in the bridge is observed in a digital indicator as an electrical output signal equivalent to the corresponding strain in the elastic body due to force applied. Suitable data acquisition system helps in amplification and display of voltage in either mV/V or division or units like N, kN, kgf etc.

Principle of operation: A strain gauge force transducer consists of elastic spring member, defined as a load sensing member, and strain gauges are applied on it. The elastic spring member absorbs the force applied and produces a corresponding strain. The resistors of the strain gauge glued to proper locations of the measuring body will change the resistance. It follows from the principle of strain gauges, that the change of resistance due to deformation of the measuring element is very small, in the range of 0.1 to 0.4 Ohm depending on the type of the strain gauge. This small change can be measured through bridge connection of the strain gauges, which also eliminates other disturbing effects due to its symmetrical arrangement.

The principle of the strain gauge is quite simple. Due to a load applied to a wire piece results in change in length and diameter of the wire, which correspondingly changes the electrical resistance of the wire. The resistance R of wire of length L and diameter D_i with resistivity ρ is,

$$R = \rho \left(\frac{4L}{\pi D_i^2} \right) \quad (1.2)$$

Differentiating the expression with variable terms, we obtain,

$$\frac{\frac{dR}{R}}{\frac{dL}{L}} = \left(1 - \frac{2dD_i}{dL} + \frac{\frac{d\rho}{\rho}}{\frac{dL}{L}} \right) \quad (1.3)$$

The gauge factor F indicates the change in the resistance to the corresponding change in length of wire. The Poisson's ratio ν , is the ratio of the transverse strain E_t (decrease in diameter) and axial strain E_a (increase in length) and the last term denotes the change of resistivity to the axial strain. By rewriting equation and considering the transverse and axial strain have reverse signs, we obtain,

$$F = 1 + 2\nu + \frac{\frac{d\rho}{\rho}}{E_a} \quad (1.4)$$

This equation is be derived for any cross section and gives the resistance change. The very last term in above equation is the effect due to piezo-resistivity and may be positive /negative. The Poisson's ratio has a value in range of 0 to 0.5 for most materials. The strain gauge is an ideal secondary transducer in a strain gauge type force transducer. Change in resistance is found by arranging the strain gauges to Wheatstone bridge configuration and measuring the electrical signal (mV) produced. The signal voltage of the force transducer is proportional to the supply voltage, the load and the sensitivity of the force transducer. Thus the output voltage of the force transducer can be obtained from the following formula.

$$U_j = CF \frac{U_i}{F_n} \quad (1.5)$$

Where U_j is Signal Voltage(mV) ; U_i is Supply Voltage(V) ; C is the Sensitivity of the cell(mV/V) and F is the Load(N) ; F_n is the nominal load capacity(N)

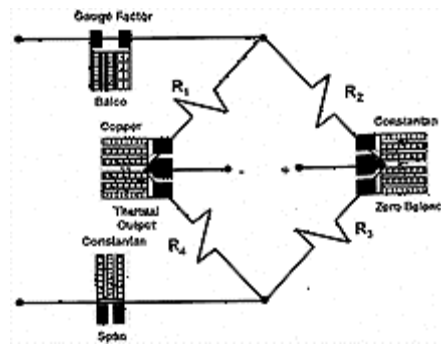


Fig. 1.7 Bridge Circuit with compensation resistors

1.3 Limitations of Present Industrial Force Proving Instruments

1.3.1 Motivation

The exhaustive literature review of the subject and the practical experience gained in laboratory measurements as well as during laboratory assessments for conformity as per ISO/IEC 17025 has revealed that 60-70% laboratories in India follow the conventional analogue technology for dissemination of force measurement traceability throughout the nation; despite of many pros and cons associated with the analogue technology. Moreover in the Indian scenario, the analogue type force proving rings/ bow dynamometers are widely used despite of being many inherited demerits over the digital strain gauged transducers. Also, the majority of Indian customer's are bound to use the analogue instruments as the imported strain gauged force transducers are very costly. These high cost precision digital force transducers are available worldwide through many manufacturers are of very complex shape, design and instrumentation, which are not easy to fabricate and are difficult to strain gauging to such intricate shaped force transducers [10-11]. Indian market is still looking towards the R&D institutions for low cost and reliable solutions in order to replace the existing analogue force proving ring transducers by digital load cells of higher accuracies.

Although the analogue force measuring devices i.e. force proving rings/ bow dynamometers are cheaper in cost and are easily available at affordable prize, but on the other hand having many inherited problems like [7-9].

- Non linearity & localized error of the dial gauges due to rack - pinion gear arrangement
- The standard force steps output is for specific use only
- One cannot interpolate the intermediate force steps required in-between calibration points
- Temperature correction needs to be applied occasionally
- Therefore being mechanical systems employed for deflection measurement and having substantial losses due to mechanical components and mechanisms.
- These force proving instruments were unable to measure force precisely to cope the continuous technological development hence cannot be employed for automation purpose

While on the other hand the strain gauged force transducers have more advantages over analogue type of force transducers as follows:

- These are more linear due to electrical output thus very high accuracy is achieved
- Output results can be fitted either in two or three degree a best-fit least-squares line to give the best fit curve line to interpolate the any desired output between the standard calibration points
- Can be easily adopted anywhere for automation purpose due to electrical output
- The electrical signals are free of the losses that are inherited in the measurements systems like frictional losses in dial gauges and offer results with improved resolutions
- Temperature compensation is possible, hence does not require temperature correction.

The objective of the thesis is to design and develop a low cost force transducer, with simple design element like diaphragm, using indigenous material like metals and strain gauges easily available in the Indian market which are easy to machine and fabricate in the moderate load range using conventional strain gauging technology. Also an attempt to make a new class of MEMS based silicon diaphragm force transducer in low range, this has also been the topic of active research for quite sometime, but they have yet to be widely accepted in commercial application segment. Here we describe some of the salient features of Silicon Force Transducers.

1.3.2 Salient features of Silicon Force Transducers

Silicon force transducers possess almost all kind of advantages possessed by the strain gauged force transducers. The additional features possessed by this class of transducers are:

- Very high sensitivity
- Accuracy and precision
- Reliability
- Small size and weight

In Indian scenario, silicon load cells are almost absent; therefore it is high time to pursue the research in this direction. Therefore the work has been focused keeping in view two main objectives as follows:

- 1) Focus on design/ development of conventional force transducers.
- 2) Design/development of MEMS based force transducers and analysis of sensitivity and its repeatability at varied loading conditions ranging 10 N to 50 N.

1.4 Research Objectives

The following research objectives are framed through present research work:

- The objective of the proposed research is to investigate and analyze metrological characteristics of low cost, ingenious shaped diaphragm force transducers to optimize their design for static force measurement applications.
- To design & develop low cost, reliable, accurate and portable force transducers which could be used as transfer standards for different industrial segments.
- To provide a guided method for improvement of force transducers for static force measurements for their sensitivity and accuracy.
- To develop Strain gauged based force transducers and conduct metrological characterization as per ISO 376-2004 (now, 2011) and IS 4169-1988 (reaffirmed 2003) standards.
- To develop MEMS based sensor for industrial applications in the entire measurement range of 10 to 50 N.
- To ascertain the performance characteristics of developed MEMS sensors.

1.5 Specific Research Objectives

- To study the various types of force measuring methods and force transducers.
- To study the literature related to design process for the diaphragm force transducers based on the classical plate theory and deflection theory of MEMS based diaphragm devices.
- To investigate the computational methods for the above design studies
- On the basis of the findings of the computational methods, and to compare the findings with the analytical expressions of literature available.
- To fabricate force transducers as per the design studies of rated capacities in steel and silicon material respectively.
- To carry out metrological characterization of the force transducers developed against

the force standard / calibration machines and different standard procedures.

1.6 Research Methodology

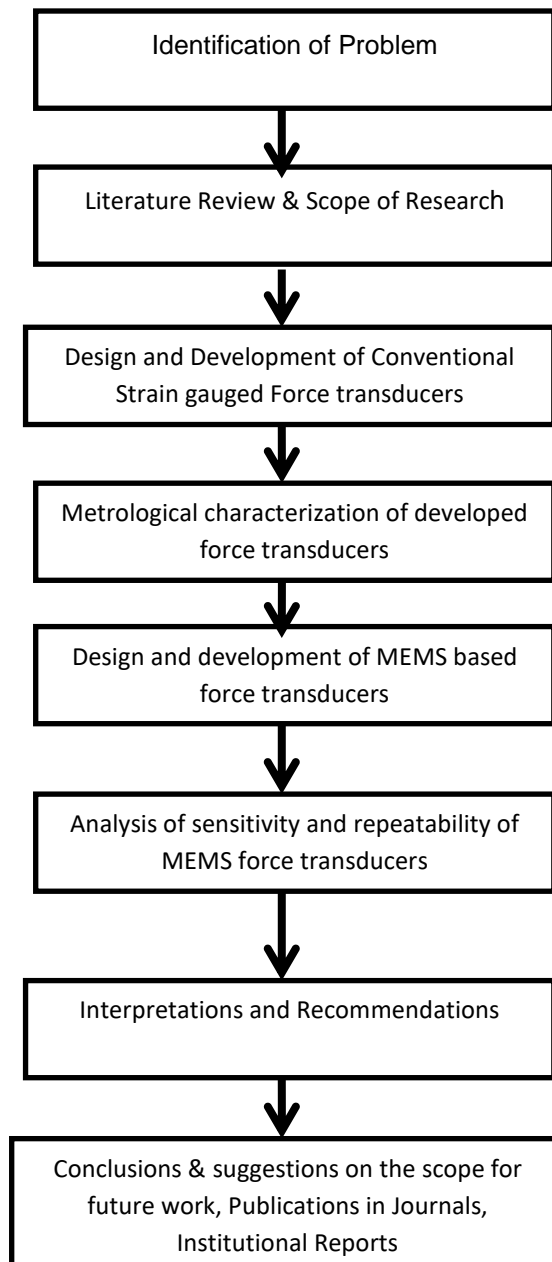


Fig. 1.8 Research Methodology Flowchart

1.7 Thesis Organization

The thesis comprises of seven chapters with brief description given below:

Chapter 1 Introduction

First Chapter discusses the various applications of force, realization of force by first principal method and other secondary force measurement methods. The chapter briefly discusses the salient features of different force measurement methods and their limitations. The dissemination of SI unit of force maintained from the apex level to the shop floor is discussed and demonstrated. Various types of force transducers like dial gauge force proving rings, bow dynamometers, standardizing box, tuning fork force transducer, and strain gauged force transducers are discussed briefly also. The brief introduction has led to the present research and the objectives of the research are mentioned in the chapter.

Chapter 2 Literature Review

Second Chapter discusses about the literature review regarding the research done in past and present time in the field of force measurement. Many research articles have been tried to search out for studying and reviewing past research work. The research area covers different force measurement methods and various force measuring instruments which are used for different field applications. The literature review helped in identifying the scope, objectives and suitable solutions to the research problem identified.

Chapter 3 Design of diaphragm based Force Transducers through analytical approach

Third Chapter discusses about the classical plate theory of bending of circular plates and deflection theory for very small MEMS based devices available from literature reviewed for design studies of diaphragm based force transducers. The theory of bending of diaphragm and analytical expressions has been discussed. The usefulness of these theorems has been discussed further for designing of diaphragm based elastic loading elements.

Chapter 4 Computational studies of diaphragm based force transducers

Fourth Chapter After design studies of diaphragm based spring element for force transducer through analytical approach, the results obtained with these expressions are further compared by finite element analysis to validate the design studies of force transducers. The adopted procedure for finite element analysis has been discussed and results are reported. The application and benefits of finite element analysis in optimal location of strain gauges is demonstrated.

Chapter 5 Fabrication and metrological investigation of the EN 24 steel grade based diaphragm force transducer

Fifth Chapter The chapter describes about the complete fabrication process of strain gauged force transducer and also presents the different aspects of metrological investigations of the force transducers. Calibration procedures based on standards ISO 376-2004 (now, 2011) / IS 4169-1988 (reaffirmed 2003) have been discussed. Different factors lead to the overall uncertainty of force transducers and uncertainty evaluation has been discussed.

Chapter 6 Fabrication and performance evaluation of MEMS based diaphragm force sensor

Sixth Chapter discusses the complete fabrication process of MEMS based silicon diaphragm force sensor. The designed and developed MEMS sensors are further investigated for their metrological performance evaluation in accordance to standard procedures. Uncertainty evaluation has been discussed as per the different applicable uncertainty components of calibration procedure.

Chapter 7 Conclusion and future scope of work

Seventh Chapter summarizes the present research. The chapter attempts to discuss the future scope of the work presented and shortcomings observed by the researcher during the course of investigations.

The last section of the thesis includes the **References** and **Appendices**.

1.8 Summary

The chapter discusses the fundamentals related to force realization systems and force measurement instruments. The force measuring systems have been discussed briefly along with their salient features. The force measurement instruments (force transducers) have been given a broad overview starting from their history to the present developments. Briefly, many force transducers developed so far have also been discussed. In addition, the research objectives are identified and the research methodology to be adopted for accomplishing the goals has also been discussed.

Chapter 2

Literature Review

2.1 Introduction

Previous chapter highlighted to describe the significance of force measurement since old civilization days and developments of force measurements with modern era by formulation of measurement laws based on analytical expressions. The importance of realization and standardization of precise measurements related to various force applications have been highlighted. An overview of different technique force transducers and measuring systems have been highlighted. Now there is need of an exhaustive literature review to discuss the past and present research for related to different aspects of force transducers. This chapter aims to provide a rationalized review for retrospective investigations of past & present research and to highlight limitations. Attempts are also to be done to discuss the factors which forced to investigate in the objectives as discussed in previous chapter.

2.2 Analogue Force Transducers (Dial Gauged)

- Dial gauged force proving ring which are ‘O’ shaped force measuring devices were first invented in 1927 at National Institute of Standards and Technology, USA (NIST, USA). It consists of a sensing body e.g. circular elastic ring equipped with a deflection measuring tool like dial gauge, micrometer /vibrating reed etc. [7-8], the circular ring force devices have been studied since 1927, still now a lot of researchers have also studied different investigative aspects of circular ring force devices. Efforts have been done for low range circular ring force devices for research, teaching and experimental purpose related to fluid mechanics applications in the laboratory, but limited for specified

range of forces up to 20N. [15].

- Dial gauged force devices employ dial gauge as a deflection indicator. The applied force to the circular proving ring gets standardized in terms of the deflection of the elastic sensing element (circular elastic ring) of the dial gauged force transducer. This physical deflection is standardized by readout of dial gauge reading. This deflection may be linear in a particular range of dial gauge spindle travel or may not be linear during sensing of deflection in terms of the dial gauge spindle travel, as the dial gauge itself having localized linearity errors. The ring shaped dial gauge force transducers have served as transfer force standard for a longer period of time due to cheaper cost, simple design and ease to make and handling due to robustness. Such force transducers may be of limited use only e.g. for calibrated specific points and may not be used for any in-between intermediate points by use of interpolation curve as in case of digital force devices. Studies related to investigation of long term stability of dial gauged force devices have found that there are considerable variations related to deflection of the ring dial gauged force devices with time as shown by dial gauge, micrometer /vibrating reed. The calibration records have been analyzed with reference to calibration certificates and the deviation is found up to 0.5 - 1 % [16].

2.3 Digital Strain Gauged Force Transducers

- Strain gauged force transducers came into existence since 1977 which started the era for development of modern force transducers. Although other measuring instruments like circular proving rings, elliptical bow dynamometers, standardizing box etc. are also developed for force measurement, still strain gauged force devices are dominantly used

on a very wide scale. Strain gauged force transducers are able to produce results of very good stability with lower measurement uncertainty. This type of force devices are most widely used and are available commercially, throughout the globe of various make. The force transducers may have different metrological characteristics as per intent use and precision required with wide range of capacities [17].

- Some researchers have developed small size strain gauged force transducers with measuring springs sensing element diameters and heights ranging between 1mm to 20 mm. It is found from the studies that at a thickness < 0.3 mm, the measuring errors of the measuring springs sensing elements are strongly influence due to strain gauges. Further it was investigated that if the curvature radii of the measuring springs sensing elements are small or varying then the relative humidity should be maintained constant at low values, [18].
- In this work the researcher has developed a new strain gauge device to measure gripping forces for functional biomechanical models. The strain gauge device capable to detect radial force with an accuracy of 1 %, further can be differentiate into six components per segment of maximum 250 Newton can be measured which are further practically used for biomechanical models to generate valuable input data [19].
- Modeling related issues of sensing elastic spring elements like geometrical and parametric modeling have been discussed by the researchers earlier. In these work investigations on elastic elements of N type was done for development of strain force transducers. Further investigation on issues related to design of axis symmetric force devices helps in understanding the designing criteria. [20]
- Efforts are always being made time to time to develop low capacities precision strain

gauged force devices of many shapes and sizes throughout the world and their preliminary outcomes are being discussed. The design, development and characterization have been reported of artifacts of 1 and 2 Newton capacities and the measurement uncertainty is also discussed [21].

- Studies on quality of transfer force transducers have been conducted many times for investigating their longer period behavior so that they may be used as reliable transfer force standard to disseminate the measurement traceability chain of the standard force machine (Dead weight, Lever or Hydraulic amplified force machine) to the industrial calibration force machines (Universal testing machines) maintained at user industries sites. Such comparisons are very helpful in understanding the role of quality of transfer force transducers in terms of their long term sensitivity stability say in ten or more years because the quality cannot be judge until several measurements done over a longer time period. The various systematic component errors should be considered for studying data which are quite helpful in understanding the properties of force transducers and the need of corrective action required, if the deviations are found away from allowable limits. The study has been done by considering the data of many different types of precision force transducers of different range and capacities. [22-24].
- Innovative design of force transducer has been discussed for suppressing of various parasitic components factors like eccentric load, rotation and overlapping effects, temperature variations for minimizing the uncertainty of force transfer transducers. Work related to applied compensation techniques to nullify parasitic force components has been discussed earlier by other researchers also [25].

2.4 Force Transducers (Tuning Fork Type)

- Many efforts have been put in past to build precision force devices using mechanical resonators to convert the applied force in a form of resonator vibration. These resonators developed in a form of tuning fork double ended through which the applied force is further converted in terms of frequency of the resonator. The advantage of these transducers is that they require a very less time for thermal stabilization. The tuning fork is derived by an electric current. Tuning fork double ended transducers of nominal capacity 50 N has been fabricated at (NMIJ) National Institute of Metrology Japan and further calibrated by using 500 N force standard machines. The results are found encouraging and as good as equal to the strain gauged force transducers. The force transducer showed a low value of creep, hysteresis and temperature coefficient. The force transducer also qualified longer term stability verification. But, having some demerits also like inferior resolution in terms of time and large sizes which lead to insist on further improvements and modifications of tuning fork force devices so that they may use as force transfer standard to participate in international comparisons and the proficiency testing between the calibration labs and may also be calibrate force standard machines / force calibration machines [26-27].
- Research has been done related to static force measurement in terms of frequency as an output against the force applied by a newly developed quartz tuning fork resonator frequency force transducer. A high resolution quartz resonator force transducers have significant advantages over conventional strain gauges force transducers. Force is directly applied to resonant force transducer's diaphragm, which directly converts the applied force into linearly varied resonant frequency [28-30].

- The tuning fork double-ended resonators as force devices have low creep, high stability, and output in digital form. A resonator force device of 50 N has been designed, fabricated and investigated. The performance evaluation of the resonator is evaluated with the help of a high accuracy dead weight force machine. The outcome verifies the better performance of the resonator more than the strain force transducers. Such force transducers may utilize an integrated support structure with a low capacity DETF. Double-ended tuning fork resonators are excited through piezo-electric effect which generates resonance frequency corresponding to the applied axial force, thus the force has been standardized in form of frequency. Design, development and performance evaluation of DETF-based force transducer of capacity 20 kN with a 0.02 % repeatability in the whole range has been reported [31-32].

2.5 Silicon based Force Transducers

A new class of silicon force transducers has come up during the last one and half decade also has been the topic of active research for quite some time, but they have yet to be widely accepted in commercial application segment. Silicon force transducers possess almost all kind of advantages possessed by the strain gauged force transducers. The additional features possessed by this class of transducers are very high sensitivity, accuracy, reliability and small size and weight.

This kind of load cells use the mechanical characteristics of a single crystal silicon Fig. 2.1 [33-35] as load sensing elastic element and piezoresistive characteristics of monocrystalline or that of polycrystalline silicon for the sensing of the generated stress during the applied load. The major advantage of this type of load cells is the gauge

factor of Silicon piezoresistors is more (almost a couple of hundred times of that of the metallic strain gauges) leading to very high sensitivity [36-38]. Disadvantages being the high cost and lower fracture strength of the material. These limitations could be overcome through indigenous design, custom packaging and batch fabrication of the sensor. With the evolution of Micro Electro Mechanical Systems (MEMS) technology [39-41], Si load cells can be scaled down and batch fabricated with custom designs. Silicon load cells have extremely significant applications in biomedical [42-45] and industrial segments [46] requiring precise and reliable force measurements. Several kinds of Si load cells based on MEMS technology have been developed while a lot more to come for a variety of application segments [47]. Different kind of designs is possible with the advent of micromachining technology of the silicon. Hybrid load cells using SS as sensing element and poly silicon strain gauges as transduction elements have also been tried out [48]. One such kind of load cell is shown in the [49-50]. The size of the force transducer is reduced to a great extent, bringing the total cost down. Another kind of Si load cells make use of the mechanical characteristics of a single crystal Silicon as the mechanical sensing elastic element as well, in which a Si membrane or cantilever [51-52] is directly subjected to the load to be measured and the stress generated is measured through the embedded piezoresistors configured in Wheatstone bridge or in a potential divider configuration. In the present work we propose a new kind of Si load cell to be developed entirely on a silicon substrate. The extremely minute size and low mass with more sensitivity would guarantee its portability, thus opening new opportunities for different application segments. Our emphasis would be to come out with cost effective designs to enhance its marketability [53].

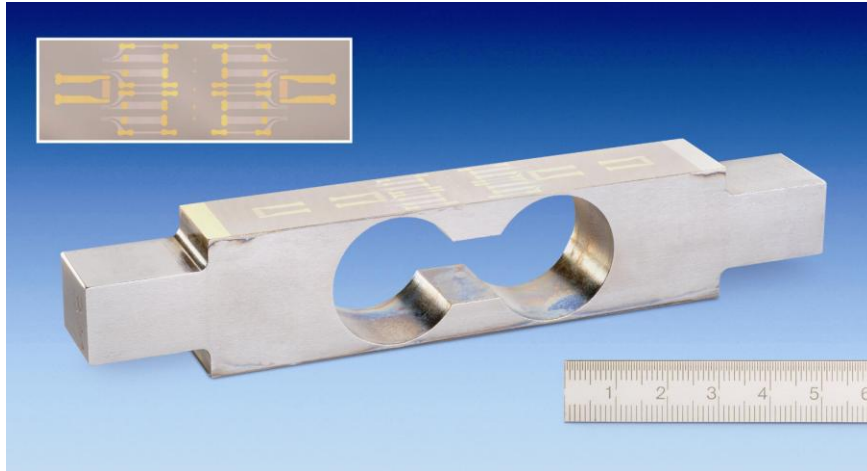


Fig. 2.1 A silicon load cell with thin-film strain gauges [33]

2.6 Modified Ring shaped Analogue Force Transducers

- Various modifications, related to design of circular ring force device with different cross sectional area; shape and uniform strength have been done in past. The whole purpose of such modifications is for saving the material and manufacturing cost significantly and to make a continuous profile due to large variable cross section as a result of which the net deflection and sensitivity is improved of analogue force transducers [54].
- For measuring and monitoring forces during cutting under various processes of machining like drilling, milling and turning, etc., modifications have been done in limited capacities of the circular ring force devices to an extended form of octagonal ring force devices. An octagonal ring force device attached with a dynamometer has been used with the measuring equipment for greater stability, to stop the rotation of top section of the device and also to make the force measurement free from transverse and vertical sensitivities.
- The present study investigates the changing of microstructure through different heat

treatment process techniques for AISI 4340 steel and also evaluating performance evaluation of AISI 4340 spring steel based force dynamometers. The different heat treatment processes led to different microstructure and corresponding hardness value at Rockwell hardness ‘C’ scale like 35, 45 and 55. A set of force transducers are being fabricated with different hardness value materials and then metro logically studied. The results indicated that the reversibility characteristics of force transducers with hot quenched and tempered processed materials have been better with enhanced hardness value [55].

- The researchers have studied the role of different heat treatment methods over the elastic sensing elements of force transducers and the following measurement of the reversibility performance of force devices which significantly contributes to uncertainty of force transducers. It has been a very effectual method for achieving good performance in measurement of force during calibration and other applications. The heat treatment methods caused different hardness values of the sensing elastic material of force transducer. The microstructure of the material changes by heat treatment of the sensing element whose characteristics are deciding factor for change in performance of force transducers majorly relative uncertainty due to hysteresis [56].
- Electro-mechanical cutting force measurement dynamometers have been discussed by the researchers regarding different design criteria and machining operations. Suitable elastic material and their designing properties have been analyzed for making of force dynamometers. Locations for pasting of strain gauges have also been analyzed for detecting the strains generated on the dynamometers due to cutting forces. Fixing and mounting positions of the force transducers have also been discussed for different

machining processes [57].

- Different types of cutting force dynamometers have been analyzed for measurement of generated forces during various cutting and machining operations like metal chipping during drilling and allied operations. In many cases octagonal ring shape force transducers are being used widely and these have been designed to monitor the cross sensitivity, torque and thrust generated at the tool post and which may be found within few Newton. Natural frequencies were also analyzed for ensuring of rigidity of the force transducers. [58].
- Researchers have also developed a combination of multiple octagonal rings arranged in such a way to measure three forces simultaneously during a metal cutting process e.g. main cutting force on tool, cutting tool feed force and cutting tool thrust force. This combination works like a three component force dynamometer. The strain gauges mounted on these multiple octagonal dynamometers connected in form of Wheatstone bridge. The whole fabrication process of this development including its static and dynamics characteristics has also been reported. It is interested to note here that most of the researchers have used the octagonal ring type force transducers for studying the cutting processes. [59-60].
- In the same manner the cutting force dynamometers are developed for turning process also. The study reveals that the criteria of orientation of dynamometers and the strain gauges locations have been optimized to achieve maximum output sensitivity and to reduce the cross sensitivity to the least minimum. These cutting force transducers are further subjected to rigorous static and dynamic tests during their performance evaluation for ensuring reliability for static and dynamic cutting forces measurement [61-62].

- Empirical equation for designing dynamometers for drilling operations has been established. This derived equation quite useful in fabricated dynamometers which were quite capable in measuring torque and drill thrust during a drilling operation. Several drilling tests were performed by this fabricated dynamometer, and on the basis of test results of drilling operation force measurements. Empirical equations for estimation of values related to torque and thrust during a drill operation were established, after that calculating cut forces using the empirical formulas for torque and thrust have been compared with the data results of previous work done by other authors by plotted graphs for verifying about relation between them. Thus, dynamometer designing assurance criteria along with its reliability of usage of the dynamometer in drilling and related processes has been established and have been approved with the help of these derive expression for measuring cutting forces for conventional and newly developed materials [63].
- Researchers have discussed about the different procedures for ensuring the performance of indicators used in multi-component force dynamometers. Some guidelines and methods are developed for indicators related to procedures and performances are developed for multi-component dynamometers for evaluating self-consistency tests of the measurement results as a performance indicator. It has also been proved how these proposed indicators can become very authentic tools for self-diagnosing the class of the force devices, in normal operations and even in some other cases also [64].

2.7 Force Transducer based on Agriculture need

- Researchers have done various modifications to ring shaped force transducer for finding solutions related to agriculture like tillage which is a very important agricultural operation for representing used energy which is a significant part of the total energy utilized in crop production. It was found that the portion of draft force of field cultivator and mold board plow and was about 1.8 and 2.14 times as much of the disk harrow and chisel plow. This large difference of implement draft indicates that the significant energy savings can be achieved by properly selection of energy-efficient tillage implements and suitable changes could be made for further efficient implementation [65].
- In the same manner, a dynamometer of draft capacity 180 kN was developed with an 2-Dimensional drawbar designed as a double extended octagonal ring (DEOR). It is made of 2 extended octagonal rings, vertically oriented on both area of the tractor drawbar. Strain distributions were best matched with the help of using finite element method for the extended octagonal rings investigated to find out optimum strain gauge locations to keep the cross sensitivity minimum between these two e.g. vertical force measurements and draft of dynamometer. The calibrations related to Vertical and draft of 2-DEOR dynamometer was performed in a laboratory using a uniaxial testing machine. Results of calibration indicated that 2- DEOR dynamometer had a negligible cross sensitivity with a linearity of about 0.99. An injector of sweep-type liquid manure was also successfully tested for the draft and vertical force with the help of 2-DEOR dynamometer in a field without any mechanical problems [66].

2.8 Force Transducers based on Special Purpose / Need

- Several attempts have been done to make different type of force transducers to fulfill special some need, purpose or objective. A few of them were made by converting structures into load sensing transducers using strain gauges technology so that they could measure the loads with the required accuracy depending upon the structure, loading conditions, accuracy requirement or calibration methods used and placement/number of strain gauges. The study further discusses the use of statistical methods for determining the magnitude of the force shared by the structures [67].
- Specific application based attempts have been done time to time for design and fabrication of the force devices to measure axial / shear forces with bending moment at the end of a structural beam. The force transducer developed could also be used for knee braced frames investigations. Such developments are very widely used for investigating experiments of large scale structures [68].
- Developments regarding force transducer compensation system has been done, which is very critical and prevalent during dynamic conditions use of force transducer. The compensation system helps in minimizing the inertia error which is very dominate for different frequency range of the force transducer. The investigation case of a material testing machine used for dynamically testing. It is found that the real time force indication was quite different e.g. indicated force of the force transducer may differ from the real force absorbed by the specimen during dynamic test. On root cause analysis it is found it is due to the load string mass. The equations for dynamic motion for the testing machine are developed. The compensation system developed on the basis of errors identified and it is found further that the errors are compensated and is minimized

significantly [69].

- Misalignment sensitivity test for load cells have been experimentally investigated through a relatively very simple test procedure in which the eccentric forces are applied to load cell by using an angular block and results are reported. The methodology for misalignment test of load cell is discussed and the variation in eccentric load sensitivity along with the variation of the loading button radius has been reported. The methodology reported has the advantages of being applied directly to universal or compression type load cells without any special threaded eccentric fixtures etc. [70].
- Researchers have developed less expensive force transducers for concrete bridge girders applications with easy installation procedures. The C and Square shaped force transducers were fabricated and implanted with the structures to be investigated. Stress – strain could be measured in the concrete bridges and other concrete structures with the help of these developed force transducers. Even some special requirements like measuring micro strains could be done during the experimental investigations of concrete structures [71].
- Piezoresistive three axial micro force / torque sensors in ring shaped developed by the researchers for a nominal capacity of 5 N. The desired working range of the force was from 2 N to -2 N. The force transducer element was modelled using three dimensional finite element techniques to check the suitability of dimensions for pasting 16 strain gauges over the hollow structure of the force transducer sensing element [72].
- Many different type of force devices have been developed in past by a number of researchers keeping in view the intent use and applications in various fields. Some of them are multi component force transducers (three components and six components) for

measurement of different three or six axial component forces simultaneously; others were ring shaped force / torque transducers for measurement at micro level along with their uncertainty evaluation. Another class of force transducers for measurement of very low forces in micro and pico range was micro electro mechanical system (MEMS) based force transducers for micro-robotic applications etc., low cost fiber optic force sensors were also developed by researchers for measurements of minute invasive forces of soft tissue also the system proved useful in many different measurements of biomechanical like tendon forces. The devise was proved to be reliable and sensitive method for measurements related to biomechanical applications [73-76].

- Uncertainty evaluation for multi component force transducers related issues have been addressed by some researchers. They have discussed the methodology and uncertainty factors to be considered which affects the overall measurement results [77].
- The use of piezoelectric sensors for commercial weighing in static applications considering different accuracies classes have been investigated by researchers. Firstly it was investigated for low accuracy requirements like class D for ordinary accuracy weighing instruments. Secondly with suitable compensation methods along with adjustment in sensors, they were able to meet the higher accuracy requirements of medium accuracy requirements of class C for commercial scales. Especially for static precision measurements of high nominal loads the piezoelectric sensors offered unused potentials in this field [78]. With the highly advancement in electronic instrumentation techniques, a novel attempt has been done by re modifying a junk electronic balance into a force devise for performing physical experiments. By converting this junk balance into a force devise was an economical way of receiving precious laboratory instrument, but

also very constructive exemplary work of instrumentation [79].

- Researchers have designed, developed and experimented ultra-low height, hollow cylinder force transducers for applications related to heavy duty machinery and heavy constructive engineering works. These force transducers are of low height to measure high magnitude forces. The ratio of the height to the diameter of hollow cylinder force transducer is limited to less than $7/4$ [80].
- Researchers have discussed and addressed the various factors which affect the output of implantable force transducers, used for patellar tendon graft force measurement. The study further suggests that the implantable force probe should always be used with the graft and should not be calibrated in any case without the graft [81].

2.9 Computational Studies of Force Transducers

- Ring strain sensor has been studied through computational method like (FEA) finite element analysis method to discuss proper positions for placing the strain gauges. The Abaqus software has been used for studies and suitable boundary conditions have been applied to the 3D model developed of the ring sensor. The finite element analysis has been done first for a complete proving ring and then for quarter of the ring and results is discussed. A comparison has been made for different possibilities for locating strain gauges for measurement of strain more precisely [82]. Similar studies were done by researchers to evaluate and compare deflection of a ring strain sensor by using analytical, computational and experimental techniques. Previously, deflection related studies of ring sensor were not done, but deflection is the primary issue for dial gauged proving ring force transducers, and force is directly converted in terms of the axial deflection of

proving ring [83-84].

- Criterion for the design of the elastic elements for very large forces has been discussed by the researchers. Different types of elements like columns, bending lamina, cantilever, sphere, hollow cylinder, including other axis symmetric elastic elements. Literature related to analytical formula for calculating stress and strains including deflection, of different shapes as available have been discussed [85]. Further, CAD based parametrical model and method for finite element analysis of different shaped strain gauge force and pressure devices have been discussed. The force devices are designed fabricated and calibrated according to standard method and force standard machines [86].
- For development of precision force transducers, investigations have been conducted for understanding the nonlinearity issues of output in electrical form with an incremental applied loading, which should be exceptionally minimum. It is further concluded that the error is due to the root cause of geometric nonlinearity changes of the transducer structure formation. A finite element analysis was applied to the structure to detect the nonlinear geometrical behavior of a force device due to an incremental applied force. The results of finite element results were further verified with experimental results [87].

2.10 Procedures of calibration

- The force proving devices are calibrated for metrological parameters as per well defined standard method guidelines as mentioned in ISO 376-2004 / 2011/ IS 4169-88 (reaffirmed in 2003). The metrological results of force proving devices predict the uncertainty of measurement of the force proving devices. The measurement of uncertainty is comprised of different relative uncertainty components like reproducibility,

repeatability, zero deviation, resolution, reversibility, interpolation, and certified measurement capability of the standard force machine, as per the calibration method used. For dial gauge analogue force devices, factors of relative uncertainty due to interpolation and reversibility are not taken into considerations due to some restrictions of the dial gauges. On the completion of the measurement series according to specified calibration method adopted, corresponding respective uncertainty contribution factors are considered as mentioned in the standard guidelines for measurement of uncertainty [88-89]. For the case of dial gauge analogue force devices, the measurement uncertainty of force devices is limited of relative components as discussed over. The force devices are further classified individually on the base of the limits of uncertainty component like repeatability in addition to the total expanded uncertainty of the force device at ($k=2$) to qualified class 00, class 0.5, class 1 and class 2 in case of ISO 376-2004 / 2011 and class 0, class1 and class 2 in case of IS 4169-1988 (reaffirmed 2003).

- Researchers have always tried hard to investigate into uncertainty related issues of force transducers. On the basis of findings it is found that among all the factors, rotational effects are the most dominating factors in evaluating the uncertainty of force transducers. The individual studies have been carried out on various force dynamometers as well as individual load cells of force build-up system. The experimental work on parallelism study of the force build-up system along with the compensation technique for bending moment of all the force transducers of the force build-up system were measured during the investigations. Through experiments it was found that output of build-up system is strongly affected by the individual positions of force transducers whereas it is hardly affected by base platen of the build-up system. A novel test method for force build-up

system was formulated to minimize the orderly errors by the calibration indirectly for the force build-up system. The calibration outcome of force build-up system by the new test procedure designed was found in excellent agreement by indirect calibrations [90].

- A new model has been proposed by the researchers which allow interpretation of the individual rotational effect based on the elastic interaction, as an end effect. The model is validated by a number of experimental cases data of dynamometers of different types, and ranges whose certificates of several year calibrations carried out at regular intervals are available [91].

2.11 Force Calibration Methods

- The various analogue and digital force devices are calibrated by various standard force machines. The standard force machines apply the load on the force devices by a convenient means, which converted into deflection of elastic loading element of the force, devise and suitably measured or recorded by the indicator device. The standard force is converted into standardized deflection of the force transducer, thus the force devise gets calibrated with the help of standard force machine / comparator calibration machines. Thereafter the calibrated force devices are further accustomed to validate the onsite material testing machines, monitoring the measurement of cutting force, measurement of thrust etc. The standard force machine / comparator calibration machines may be founded on any one of the scientific principles like purely dead weight, dead weight lever multiplication, dead weight hydraulic multiplication, build up systems etc. [92].

- **Dead weight force standard machine** provides easy way to first select the precisely known standardized dead weight force and secondly apply these selected dead weights on to the force proving device directly which are under calibration test. The manufacturing and handling of dead weight force machines are become not convenient at higher capacity, due to requirement of big sizes of weights for generation of large forces which leads to very high cost. The dead weight standard force machines are normally manufactured maximum up to 2 MN, and exceptionally of up to 4.5 MN in NIST, USA. The weight masses and value of g can be measured up to few parts in million, the measurement uncertainty in force realization may be as small as 0.002%. (Figure 2.2) [93-99].



Fig. 2.2 Dead Weight Force Machine (2 MN) at PTB, Germany [95]

- **Dead weight cum lever multiplication force standard machine** are comfortably designed for force generation equal to 1 MN, but exceptionally in some National Metrological Institute, up to 5 MN, by multiplying the dead weights force through a

single or a set of multiple levers in a ratio of 10 to 20, depending on the ratios of the lever lengths from the lever fulcrum. This type of force machines may have measurement uncertainty of about 0.009 % (Figure 2.3) [100].



**Fig. 2.3 Dead Weight cum Lever Multiplication Force Standard Machine
(1 MN) at NPL, India [100]**

- **Dead weight cum Hydraulic multiplication force standard machine** is a method based on Pascal's Law for generating forces of higher capacity like 10 MN by multiplying dead weight force through a set of small and big hydraulic piston-cylinder assembly connected hydraulically in series. The dead weight force loaded on small piston cylinder assembly is multiplied by the ratios of area of these two piston cylinder assemblies. The uncertainties of measurement of this kind of force standard machines are usually as low as 0.025 %. High capacity hydraulic force machines fitted with standard force transducer in series are also used as comparator machine, depending on the capacity of the standard force transducer are extensively used for realization of forces in the range of 200 kilo Newton – 100 Mega Newton. These types of force calibrating machines

directly compare the standard force transducer output with the force transducer output under calibration. The force transducers may be single or multi-component and standard build up system (a three load cells set up). The measurement uncertainty may be up to 0.05 % (Figures 2.4) [101-102].



Fig. 2.4 Hydraulic Multiplication Force Machine (3 MN)

(Courtesy M/s GTM, Germany)

- **Low force machines** also developed in recent years for measuring micro and milli Newton forces. This low force machine is principally founded on the electromagnetic force compensation technique in the range of 100 micro newton–100 milli newton has been design and fabricated at PTB, Germany. Electromagnetic compensation balance output is the direct output evaluation of a force transducer. The force standard machine developed for a nominal range of 200 N capacities at PTB, Germany (Figure 2.5) [103]. Another facility for measuring the low force in the range from 1 milli Newton to 10 Newton is made up of a unit of piezoelectric adjustment along with a balance for

precision compensation has been established. A report on metrology characterization of device by using this measuring facility along with results of the examined force transducers has been reported [104].

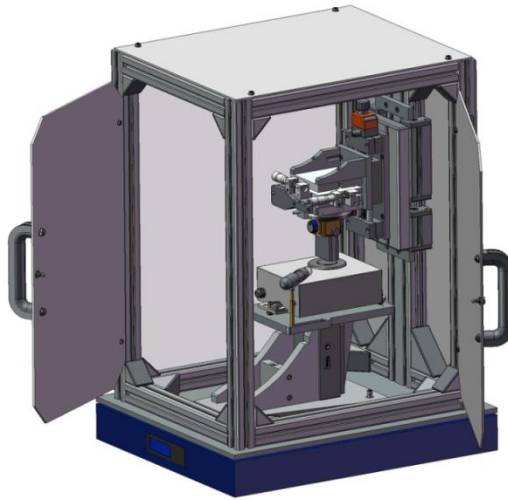


Fig. 2.5 Low force measurement machine, PTB, Germany [95]

2.12 National Measurement Facilities of force in India at NPL, New Delhi

- By act of parliament of India, National Physical Laboratory is maintaining the SI base units and derived units in the country and also the caretaker of standards at national level in India. NPL maintains the SI base units /derived unit's at apex level and also disseminates the maintained measurement standards to the consumer industries and accredited calibration labs by way of calibrating their master standards. The Force and Hardness metrology group at NPL maintains national standards of force, torque and hardness. The standard of force maintained ranging from 1 N to 3 MN, consisting of many force standard machines over and above standardized comparator calibration machines. The national force standard machines such as dead weight force machine or

dead weight cum lever multiplication force machine calibrate the precision transfer force standards, which are used for standardizing force calibration machines. By this way, the force calibration machines are standardized and traceable to the national standard of force through a set of accurate transfer force standards.

- The national standard force machines provide calibration traceability from 1 N to 3 MN. The following dead weight standard force machines are existing at NPL e.g. indigenously developed 50 N dead weight standard force machine, 50 kilo Newton Morehouse dead weight standard force machine and 1 MN GTM dead weight cum lever multiplication standard force machine.
- Dead weight standard force machines are more accurate static force generating machines. NPL has a smallest in-house developed 50 N dead weight force machine (Figure 2.6) and 50 kilo Newton Morehouse dead weight standard force machine (Figure 2.7) in addition to this another 1 kN and 5 kN dead weight standard force machines, used in calibration of force devises of the industries user and testing laboratories. The 50 Newton dead weight standard force machine is an indigenously developed force standard machine to do force measurements in the range of 1 Newton to 50 Newton. This force standard machine can apply dead weights of precise nominal values of 1 N, 2 N and 5 N in different combinations to calibrate force transducers of 10 N, 20 N and 50 N capacities. The force standard machine is operated by computer controlled software which is suitably interfaced and the sequence of the forces can be selected and applied accordingly. The observations obtained against applied force can be taken from a precision digital indicator and are directly stored in MS Excel sheet [97].



Fig. 2.6 Dead Weight Standard Force Machine (50 N) NPL

- A 50 kN dead weight standard force machine of make More House, USA has been established according to the requirements of National Physical Laboratory, Delhi, India (Figure 2.7). This machine consists of weights of different nominal values as per the local 'g' value of the force laboratory with an appropriate buoyancy correction for the densities of air and weight material e.g. steel. Dead weight standard force machine consists of first load as loading hanger, dead weights of different denominations depending upon the capacity of the machine, a solid rigid structure supporting all these components, a pneumatic system for gentle engaging and disengaging of the dead weights with less oscillations with the intention that the forces could be stabilized in a minimum possible time during loading or unloading of weights. The minimum first applied load is through loading hanger generates an applied force of 500 N on the force transducer. This first hanger force is transferred through the upper beam of hanger deposited on top of the force transducer while the lower beam of the hanger is connected to the weight stack. All dead weights are connected one by one directly to the weight stack during loading and

unloading. The machine has total 18 stainless steel weights which can generate forces by various permutations and combinations, ranging from 500 N to 5000 N. Dead weights are in the denominations of 500 N, 1000 N, 2000 N and 5000 N. The machine can easily apply dead weights in any sequence or combinations to generate a maximum applied force on the force transducer up to 50000N [96, 98].



Fig. 2.7 Dead weight Force Machine (50 kN) at NPL [98]

- NPL has also recently established a new 1 MN dead weight cum lever multiplication standard force machine, serving as 1 MN primary dead weight standard force machine (Figure 2.8). The machine has been metrological characterized by way of its calibration and evaluating best measurement capability as per EURAMET standard guidelines through bilateral inter-comparison with PTB, Germany. The expanded measurement uncertainty associated with the dead weight side for force up to 100 kN is found to be 0.002% ($k=2$) whereas 0.009% ($k=2$) for forces above 100 kN and up to 1 MN at lever side. The lever side multiplies the force by 10 times of dead weights side [99].



Fig. 2.8 Force Standard Machine (1 MN) at NPL

- The main objective of the force standard machines maintained at NMI like NPLI is to disseminate the realized SI unit of force to the user industries for providing a continuous chain of measurement traceability at the apex level for a very precision measurement. NPLI has been maintaining force calibration machines of capacity 50 kN, 200 kN, 1 MN and 3 MN. The 1 MN dead weight cum hydraulic multiplication force calibration machine (Figure 2.9) applies the technique of multiplication of static weights hydraulically to generate force in large capacity e.g. 100 to 500 times. The dead weights attached to a small hanger which is further loaded at the top of the small diameter piston-cylinder assemblage. The small dia piston-cylinder assemblage is hydraulically joined through a commonly hydraulic oil line to a larger dia piston-cylinder assemblage. Force generated in the larger dia piston cylinder assemblage is equivalent to dead weight force

on the smaller dia piston cylinder assemblage multiplied by the effectual ratios of area for both the consider assemblies. The force calibration machines are in use for calibration of the force devices upto 1 MN of the calibration laboratories/ user industries [100].



Fig. 2.9 Hydraulic Multiplication Force Machine (1 MN) at NPL

2.13 Commercially available Force Transducers

- It has been noticed that a good number of manufacturers are manufacturing various types of customized force transducers on commercial basis in India over and above across the global market. Some of them are Adi-Artech-Mumbai, J Ragrau Instruments –Delhi, Star Embedded Systems Pvt. Ltd., New Delhi, Sensotech-Chennai, Sushma Industries - Bangalore, GTM and HBM from Germany, Interface Inc. – USA etc.
- Application/requirement based force transducers have been developed of different designs and capacities falling under different accuracy class as per the required intended

use. The various force devices are available to cover up the different force range range from 1 N to 10 MN or even large capacity. The expanded uncertainty of the force transducers may vary from 0.05 to 0.1% for normal applications.

- The force transducers developed for ultra-precision applications may have expanded uncertainty may be as low as 0.005 % is of very complex design and shape and along with issues related to instrumentation. Strain gauging of such intricate shapes are quite difficult task and is an individual propriety secret and barrier to trade about knowing the design secret of such precision force devises.
- Shortcomings are found in the past research as attention has not been emphasized on simple design and shape force transducers, with ease manufacturing considerations including raw materials, machining considerations, heat treatment and strain gauging etc. In addition, the strain gauging of simple shapes is not that difficult job in contrast to shapes of complex design. The force transducers of simpler design and shape are to be designed and fabricated on the basis of literature available.

2.14 Shortcomings of the Past Research

- Although force transducers of different varieties are more widely used for different purposes and applications, but studies related to design criteria and process are not found in organized forms and therefore, the available literature reviewed reveals that this may lacks coherence with the methodologies of design and development of commercially available force transducers.
- From the available literature reviewed like various papers, monographs and technical reports, it has been noticed that most of the researchers have been discussed development

of force transducers to meet some specific measurement requirement only. Most of them are related to dynamic force measurement and a very few related to development of static force measurement transducers. Design of force transducer for intended specific use are done by presuming certain assumptions in computing expression analytically for further computing deflection, stress and strain and of the sensing element which has not been discussed and correlated with computational and experimental methods.

- After reviewing the available literature, it is further concluded that the literature is not very well organized regarding systematic procedures and rationalized designing of the force transducers for static force measurement purposes [105]. The present study aims to comprehensive investigation related to this issue of the metrological characteristics of a force transducer in terms of repeatability, deformation, stress and strain etc. of force transducers, on the basis of analytical expressions available from literature and validated through FEM computation. The simple shaped force transducers such as diaphragm of different materials would be investigated.
- Hence, in this proposed work, an effort is being made towards the development of uncomplicated shape force transducers similar to diaphragm shape force transducer of different materials like steel and silicon, which may be used for measurement of static forces precisely and accurately as required by applications related to metrological investigations. The force transducers are to be developed on the theoretical basis and thereafter the validation of the analytical designs by means of computational tools like finite element analysis (FEM). The designed and developed force transducer to be verified and tested for its rated designed strength and other important parameters like aesthetics (shape and form), ergonomics, efficiency, purpose, cost etc., to know about its

suitability for the proposed intended use. The force transducers developed are to be metrologically investigated as per the standard calibration methods based on ISO 376-2004 / 2011 and IS 4169-88 (reaffirmed 2003) [106].

- Suitability of the force measuring transducer is very well proven by measure of its overall uncertainty by considering the different uncertainty components all together of a force transducer. The force transducer's overall uncertainty consisting of relative component uncertainty contribution by various factors as discussed in the GUM documents (Guide to measurement uncertainty) standards. The uncertainty of measurement of force transducer should be within allowable limits of different categories of classification depending upon the individual relative uncertainty component as well as total expanded uncertainty of force transducer. Therefore, attention has been given to discuss the issues related to metrological characterization of force transducers as per the procedure adopted.

2.15 Summary

The present chapter addresses the important features of the past research work carried out by various researchers related to development of force transducers. The different aspects and phases have been discussed regarding development of force transducers. The review study of literature available has helped to provide an organized and systematic summary of researchers past research work. The literature review study also find out the shortcomings of the previous past research work on force transducers, and helps in deciding future course of action.

Chapter 3

Design of diaphragm based Force Transducers through analytical approach

3.1 Introduction

The force transducers are basically made of an elastic spring element of any shape, size and material subjected to some external forces and associated with some suitable indication system to convert the force applied in terms of deflection, stress – strain etc. The applied force is converted into an equivalent reaction by virtue of elastic spring element's deflection. These force elastic spring elements work under some strain field like bending stress, direct stress or shear stress. Different forms of these types have been used in the force transducer practice, however the most variety is found in the bending elements. Diaphragm based transducers consists of some spring element which works under bending strain field due to bending stress. The force transducers are consists of circular shaped elements and for their analytical investigations, classical plate theory of bending of circular plates and deflection theory for very small MEMS silicon devices are taken into account. With the help these theories available, design parameters like stress – strain and deflection could be computed and an analytical investigation of the force transducer is possible.

3.2 Analytical Approaches

3.2.1 Classical Plate Theory

Plate is an even plain surface element having significantly big proportions in comparisons to its thickness. Generally thickness of plate is kept constant but it could be variable also and is measured perpendicular to its plain surface and normally at the central facade of plate. In the plate theory; plates subjected only to in-plane loading can be solved using two-dimensional

plane stress theory. On the other hand, plate theory is concerned mainly with lateral loading. Cartesian coordinates are mentioned in fig 3.1

3.2.1. A Types of Plate Theories

The following theories that are obtainable from the literature available for the plates analysis are;

- a) Small deflections related to thin plates.
- b) Large deflections related to thin plates
- c) Thick plates.

3.2.1. B Assumptions of Thin Plate Theory.

The theory is applicable suitably for the plates with a depth up to 1/20th or less than that of plate's tangential dimension and having corresponding deflection up to 1/5th or less than that of plate's depth. The theory of thin plate is based on these three assumptions acknowledged as Kirchhoff's hypothesis as summarized below which reduces the 3 dimensional coordinated plate problems into 2 dimensional coordinates. Therefore only two stresses e.g. normal and shear stresses would exist in plate. These 2 dimensional coordinates would further converted into cylindrical coordinate system representing the above two normal and shear stresses in terms of r and θ function.



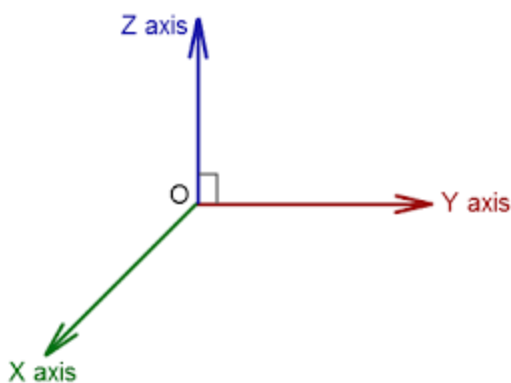
Fig. 3.1 Cartesian axes with plate

Assumptions:

(i) The Centre-plane is neutral plane: The central plane of a plate acts as a neutral plane which is neither compressed nor stretched free of all in plane stress and strain whereas the bending deform the plate over and under this central- plane and the material would compressed above neutral plane while stretched below neutral plane. Therefore the central-plane of the beam would behave in the same manner as per the beam theory.

(ii) Longitudinal line elements of bending force remain perpendicular to the central-plane: Longitudinal vertical line elements of bending force remain normal to the central plane surface area of plate and would stay normal to the central surface area even before and after deformation due to bending force.

(iii) Vertical strain is ignored: Longitudinal vertical line elements length due to bending force normal to the middle-surface area remains the same even before and after deformation.



The diaphragm shaped force transducer has been considered as an axis symmetric circular plate shaped force transducers (figure3.2) have been developed according to the suitable analytical expression obtained by researchers for axial deflection. For Steel (EN24 grade) based diaphragm force transducer, Classical plate

theory used with suitable assumptions and boundary conditions.

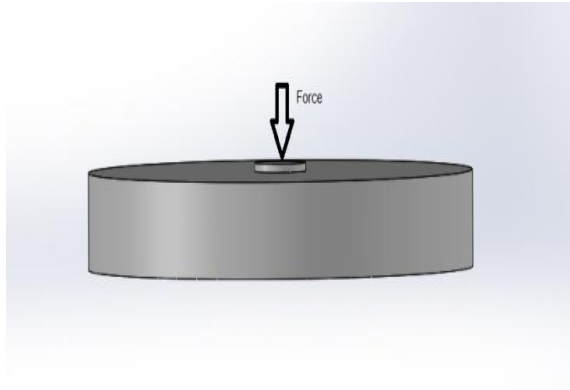


Fig. 3.2 Diagram view of Steel force transducer

Nomenclature

F force applied (N)

r radius of plate

E Young's modulus of elasticity (N/m²)

w deflection of plate

μ Poisson's ratio

Q shear force

δ axial deflection of the diaphragm (mm)

A area of the plate

D flexure rigidity

a distance from the centre of sensor

h thickness of plate

D is the flexure rigidity and defined as the measurement of stiffness or the resistance offered by structure while undergoing bending. The mathematical expression for flexure rigidity is defined as

$$D = \frac{Eh^3}{12(1-\mu^2)} \quad (3.1)$$

3.3 Analytical model for Steel Force Transducer

Theory of Classical Plate (CPT) is widely accepted to evaluate parameters of flexural rigidity for circular plate of isotropic material with different boundary conditions. In the present case; we have consider steel (EN24) circular plate with concentrated central load and clamped edge at $r = a$, as a boundary condition. The diaphragm size, thickness and the depth of the cavity under the diaphragm have been initially optimized analytically for deflection. The sensor further is modeled through of modern computer modeling tools. After a number of permutations and combinations, the final diameter size including thickness of diaphragm has been optimized to achieve a large sensitivity against the applied load on chosen diaphragm. The mathematical expressions for maximum deflection calculation have been taken from available literatures [107-108].

$$Q_r = -\frac{F}{2\pi r} \quad (3.2)$$

Substituting the Q_r value in CPT equation

$$\frac{d}{dr} \left[\frac{1}{r} \frac{d}{dr} \left(r \frac{dw}{dr} \right) \right] = -\frac{Q_r}{D} \quad (3.3)$$

After Integration, above expression becomes

$$w = \frac{F}{8\pi r} (r^2 \ln r - r^2) + \frac{c_1 r^2}{4} + c_2 \ln r + c_3 \quad (3.4)$$

The three constants can be evaluate after applying suitable boundary conditions in equation 4

At $r = 0$, $w \neq 0$ So we must have $c_2 = 0$

At $r = a$, $\frac{dw}{dr} = 0$, so $c_1 = \frac{F}{4\pi D} (1 - 2 \ln a)$

At $r = a$, $w = 0$, so $c_3 = \frac{F a^2}{16\pi D}$

Finally equation 4 becomes

$$w = \frac{F}{16\pi D} \left(2\pi^2 \ln \frac{r}{a} + a^2 - r^2 \right) \quad (3.5)$$

The deflection is depends on coordinates 'r', the maximum deflection is

$$w_{max} = \frac{Fa^2}{16\pi D} \quad (3.6)$$

Now on the basis of the above equation the deflection values are calculated and found as per the table given below:

Table 3.1 Deflection findings by Analytical method for Steel transducer

Force (kN)	Theoretical Deflection (mm)
1	0.1339
2	0.2798
3	0.4197
4	0.5597
5	0.6996

The value of maximum deflection is found 0.6996 mm for Steel force transducer under maximum design loading condition. It is obvious from figure 3.3 that the highest deflection takes place in middle of diaphragm transducer and tends to reduce along the outer periphery radius.

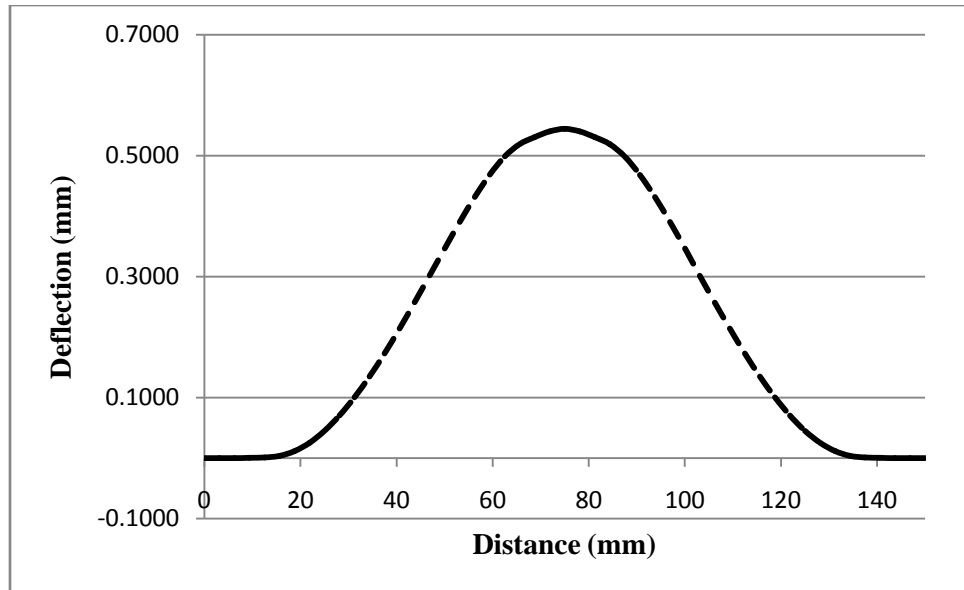


Fig. 3.3 Maximum deflection simulation plot for Steel transducer

3.4 Analytical model for MEMS Silicon Force transducer

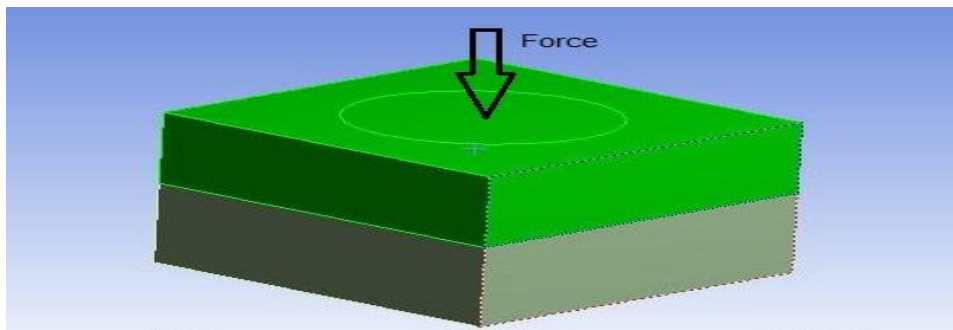


Fig.3.4 Schematic view of MEMS silicon force transducer

In the present design, a diaphragm has been designed, developed and fabricated from a single thin silicon crystal used as an elastic sensing loading element. The diaphragm size, thickness and the depth of the cavity under the diaphragm have been initially optimized analytically for deflection to have a high sensitivity. The sensor has been further modeled by a computer modeling CAD tools. Thereafter a number of permutations and combinations, the final diameter size

including thickness of diaphragm has been optimized within the designed range to achieve a large sensitivity against the applied load on the chosen diaphragm force transducer.

Mathematical expressions for calculation of important design parameters of MEMS diaphragm have been disused in various literatures [109-110]. In case of circular diaphragm along with a clamped edge at $r = a$, the displacement in case of the diaphragm by a force, F may be evaluated by solving the differential equation. As the displacement is axis-symmetric, it is easy to use a polar coordinate system instead of Cartesian coordinates system with its origin at the center of the diaphragm.

$$D \left(\frac{\partial^2}{\partial x^2} + \frac{\partial^2}{\partial y^2} \right) \left(\frac{\partial^2}{\partial x^2} + \frac{\partial^2}{\partial y^2} \right) w(x, y) = F \quad (3.7)$$

Above expression can be written into polar coordinate system

$$\frac{1}{r} \frac{d}{dr} r \frac{d}{dr} \left[\frac{1}{r} \frac{d}{dr} r \frac{d}{dr} w(r) \right] = \frac{F}{D} \quad (3.8)$$

After applying required boundary conditions the deflection found to be

$$w(r) = \frac{Fa^4}{64D} \left(1 - \frac{r^2}{a^2} \right)^2 \quad (3.9)$$

The maximum deflection can be written as

$$w_{max} = \frac{Fa^4}{64D} \quad (3.10)$$

Now on the basis of the above equation the deflection values are calculated and found as per the table given below.

Table 3.2 Deflection findings by Analytical method for MEMS transducer

Force (N)	Theoretical Deflection (mm)
10	0.0038
20	0.0075
30	0.0113
40	0.0150
50	0.0188

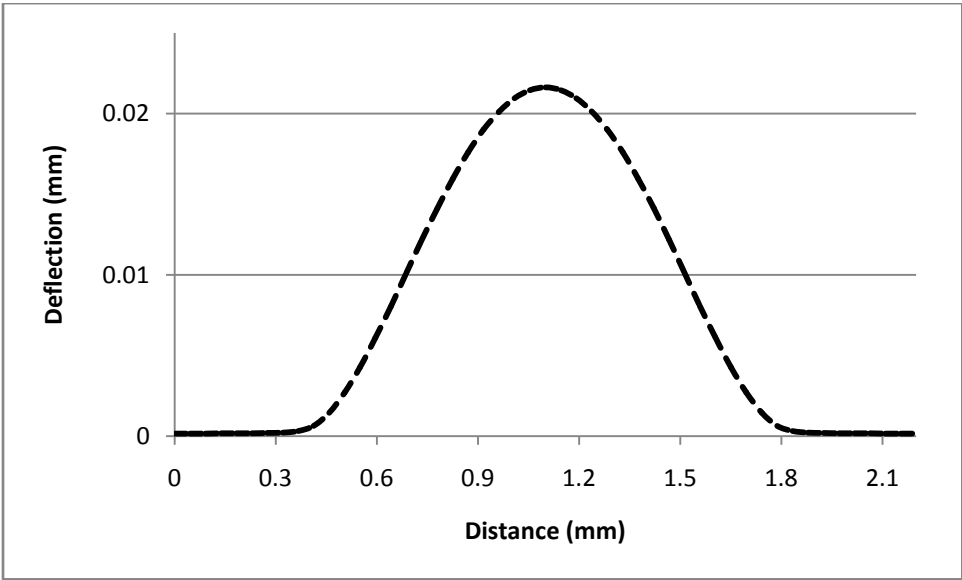


Fig. 3.5 Maximum deflection simulation plot for MEMS transducer

The value of maximum deflection is found 0.0188 for MEMS force transducer under maximum design loading condition. It is obvious from figure 3.5 that the highest deflection achieved in the middle of the sensor and tends to decrease along the outer periphery radius of the sensor.

3.5 Summary

The chapter reports the analytical approach for design studies of circular shaped diaphragm force transducers. The theories like classical plate theory and small deflection theories have been discussed for the design of diaphragms of materials like steel and silicon in the medium and low force range. The different parameters like diaphragm size, thickness, and cavity can be optimized in reference to the analytical deflection value obtained by these theories to get the maximum sensitivity in the designed range. Thus the analytical approaches helped in correlating the different factors affecting the design of force transducers. The analytical approaches also helps in defining the dimensions and nominal capacity of the circular diaphragm shaped force transducers.

Chapter 4

Computational studies of diaphragm based Force Transducers

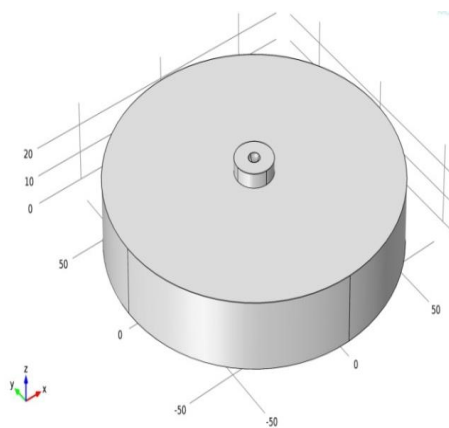
4.1 Introduction

The FE method (FEM) is the formulation of the problem results in a systematic set of algebraic equations. It subdivides a bigger set / problem into small parts / subsets called FEs. The simple equations to model such FEs are assembled to form a large system of equations to model the complete mechanical system. FEM is a numerical framework to solve boundary value problems. Industrial Engineers as well as academic researchers both extensively use FEM to solve complex engineering problems. FEM is utilized in solving multi-physics problems. There are several commercially available FEM software such as ABAQUS, ANSYS, COMSOL, NASTRAN etc that provide Multi-physics solvers. However, the underlying theory of the method is now well understood by practicing engineers and researchers. Most of the people applying the method through softwares available commercially or in-house codes don't understand the methodology as applied to problems. Thus, applications of this approach along with theoretical and experimental investigations can be very helpful in design and performance analysis of mechanical systems particularly the force transducers. Thus, the application of this approach shall be very helpful in design of force transducers best suited for particular load bearing capacities especially when the conventional theories fail to do so.

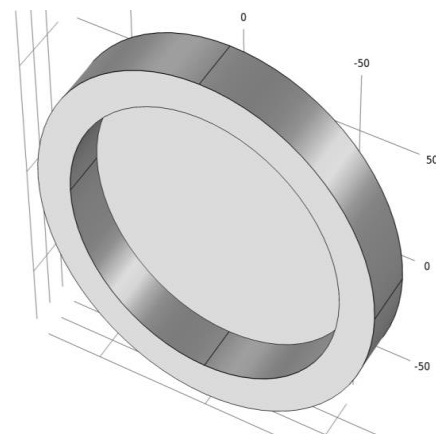
4.2 FE Model of the Steel Force Transducer

A 3-D model of the force transducer, conceptualized as circular plate diaphragm in bending has been designed using software ANSYSTM (Fig 4.1).The whole circular plate diaphragm has been taken for FE analysis. The force transducer of circular plate diaphragm

shape has been investigated to take the advantage of geometrical symmetry of the circular structure. The suitable boundary conditions are defined according to the analytical approaches, while processing the various steps for FE analysis. A 3-D solid continuum with 24936 nodes and 13706 elements is adopted and an analysis of linear type is selected. The selected material is assumed to be isotropic and homogenous in nature also the assumed material is considered to be EN 24 steel, and value of poisson ratio and Young's modulus of elasticity are assumed 0.30 and 210 GPa respectively. The axial compressive force is applied at the centre of the diaphragm. Suitable procedure for FE analysis has been defined. The diaphragm stress/strain and deflection values are evaluated. The findings of the FE analysis are summarized through of stress - strain and axial deflection [106].



Topside view of the EN 24 steel diaphragm



Backside view of the EN 24 steel diaphragm

Fig. 4.1 3-D CAD model of the Steel force transducer

The FE analysis has been done by meshing the full diaphragm as shown in the fig. 4.2, as the whole diaphragm as a single unit carved out from a single steel plate is axis symmetric design, therefore, the FE analysis has been done for full steel diaphragm force transducer, as it has symmetry to either of axis. By this way, the whole steel diaphragm has

been investigated by applying full nominal force at the centre of the diaphragm. The outcome of the FE analysis is in strong correlation to the earlier findings as done by researchers.

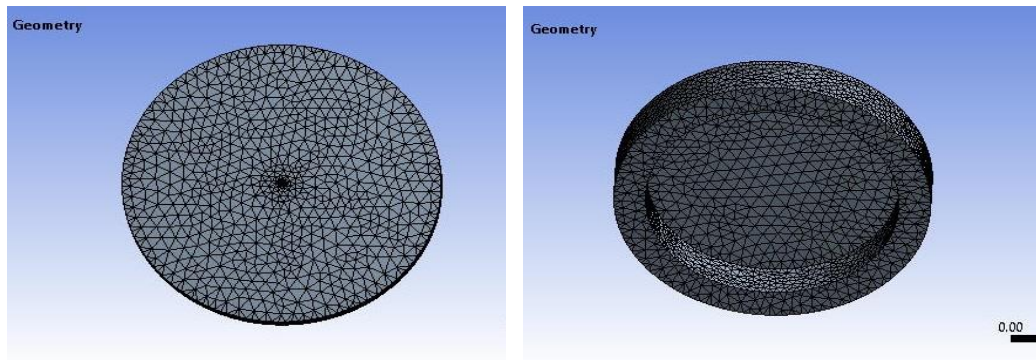


Fig.4.2 Meshing of steel diaphragm

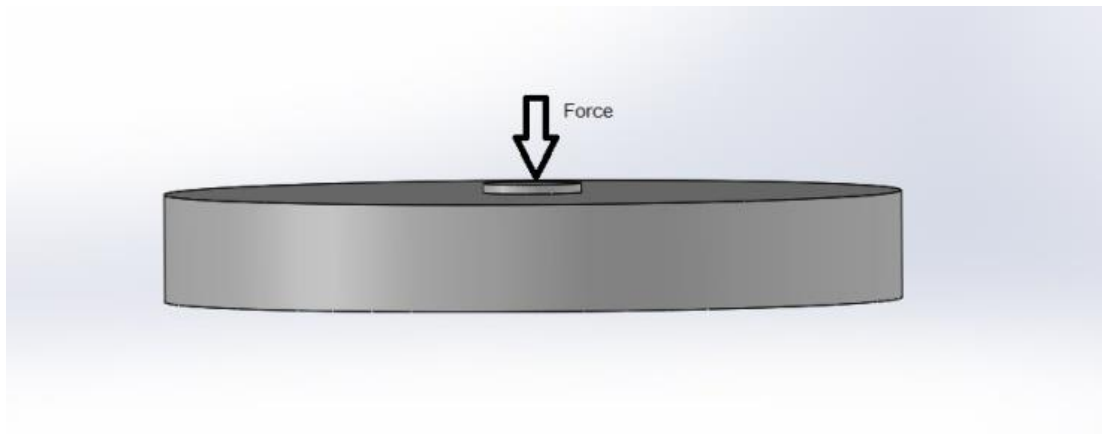


Fig. 4.3 Force application at the centre of the diaphragm

4.3 Key Outcomes of FE Analysis of Steel Force Transducer

- The stress distribution for the whole steel diaphragm force transducer when the axial compressive force is applied is shown in Figures 4.3. The location of maximum stress is found to be close at the top upper point position from where the axial force is applied (force applied is assumed as concentrated force). This applied axial force is assumed to be a point load / force. From the point of application of axial force and its effect around the outer periphery of diaphragm, the stress tends to reduce up to the

extreme end. The stress at the middle section of the diaphragm is sufficiently large, but not as much of as that at the top upper point position Figure 4.4 & 4.5. Since the applied force is believed to be concentrated and pointed tip force, however in actual practice, it might or might not be possible. The force applied may have line contact instead of point contact as assumed. Hence, the few higher values of stress may be ignored, which are shown at the point of application of force (St. Venant's principle). It is well clear from the stress distribution that the values of stress vary abruptly at locations near to point of application of axial force.

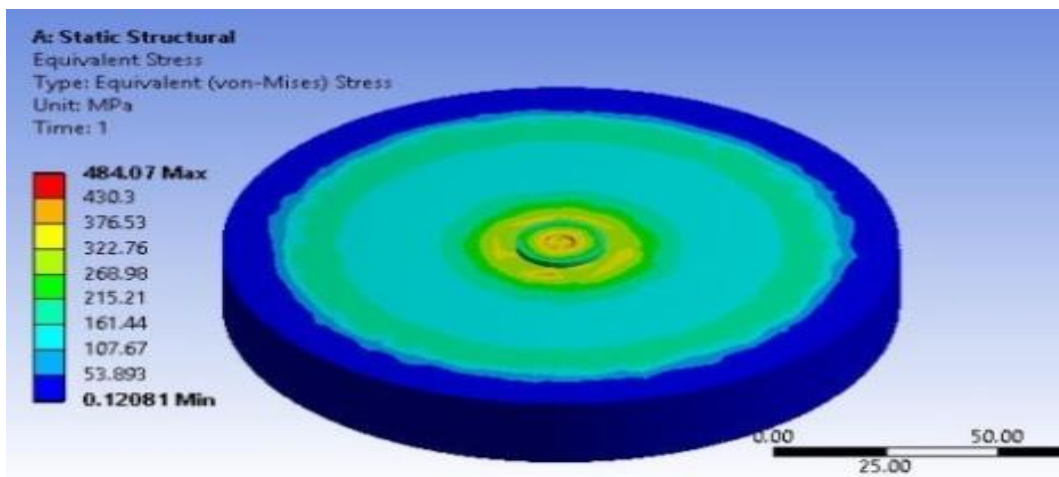


Fig.4.4 Stress for steel force transducer at 5 kN load

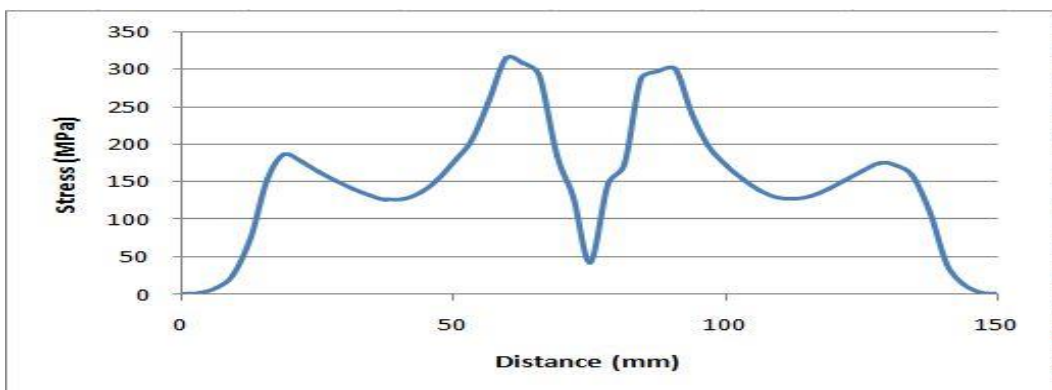


Fig. 4.5 Stress distribution for steel force transducer

- The strain distribution for the whole diaphragm of the steel transducer of force

subjected to axially applied compressive force follow the alike trend similar to the stress distribution as shown in Figures 4.6 & 4.7. The minimum strain is found to be at the outer periphery of the diaphragm and then tends to increase from outwards to the inner part of the diaphragm and maximum near middle of diaphragm, where the axial force is applied. Similarly, some of the higher values of strain are ignored and suitable values are considered. The strain follows the identical trend as in case of the stress and both are well correlated by Young's modulus of elasticity.

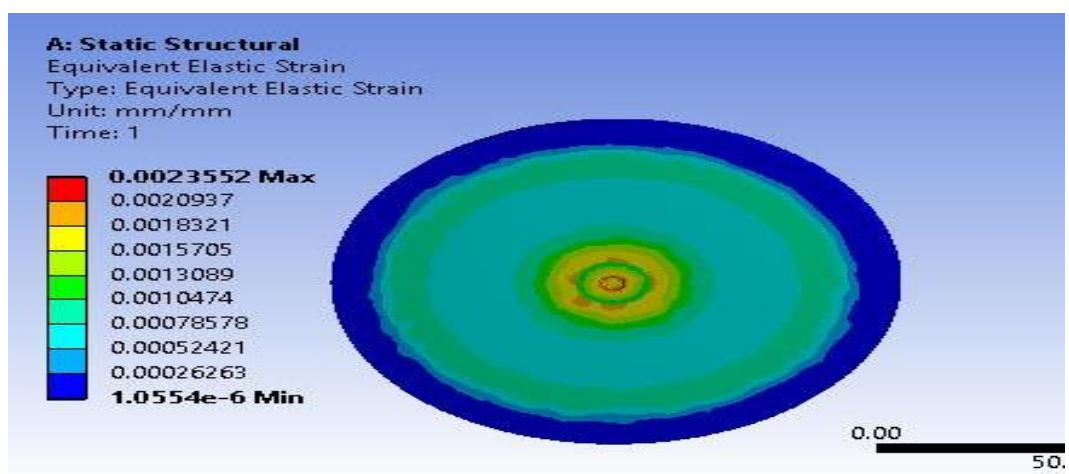


Fig.4.6 Strain for steel force transducer at 5 kN load

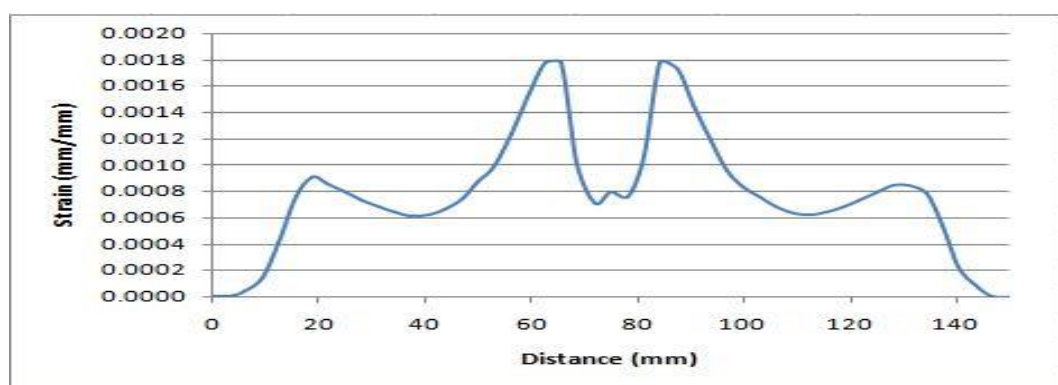


Fig.4.7 Strain distribution for steel force transducer

- The axial deflection for the whole diaphragm of the steel force transducer when it is subjected to the axial compression force is shown in Figures 4.8. The maximum

perpendicular deflection is found at point of application of axial force but this keeps on decreasing along the periphery diaphragm and is almost negligible at the end of outer diaphragm.

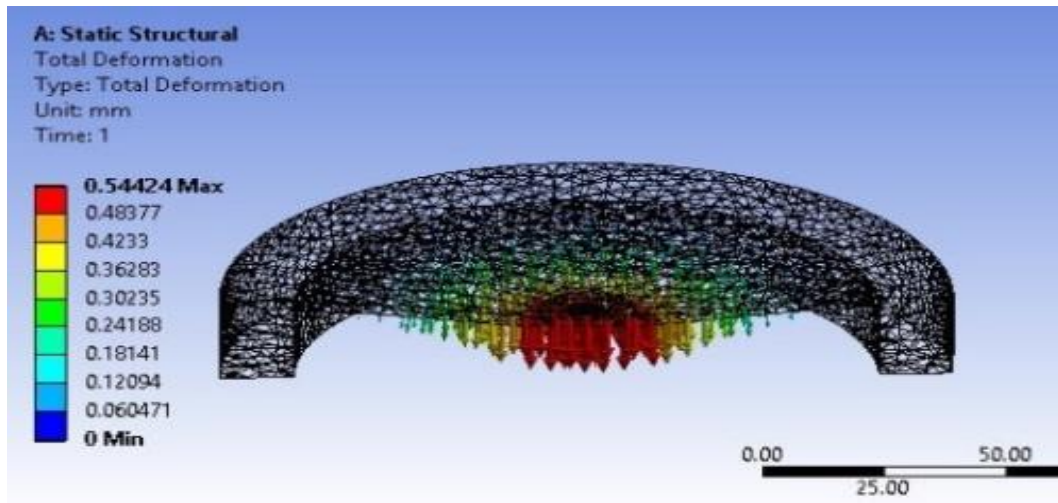


Fig. 4.8 Deflection plot for steel transducer

- For more rigorous investigation, the force transducer is subjected to computational investigations at different five force steps i.e. at (1, 2, 3, 4, 5) kN. The computational procedure is adopted as discussed above to have the (stress-strain- deflection) pattern of different forces. All plots shows similar pattern for (stress-strain- deflection) except magnitude of (stress-strain- deflection). The trend of (stress-strain- deflection) is observed to very similar for all the nominal axial forces and there is proportionally change in the magnitude of the (stress-strain- deflection) values.
- Location of sensing element always plays a vital role for the design of diaphragm based force sensor. The stress and strain distribution plots give the most appropriate location of strain measuring sensor. Therefore stress – strain plots could be very helpful in designing and locating the suitable places over the surface of force transducers, where strain gauges could be applied. Now here as per the plots it is

found that stress – strain values are minimum at outer periphery and maximum at the point of application of concentrated forces. It is clearly evident from figure (4.4 to 4.7) the maximum stress and strain occurs 15.7 mm far from centre of Steel transducer. So, this is most promising location for the strain gauges for better sensitivity. At this location, the highest stress value of 484.07 MPa is found which is less than the yield strength of material used. Similarly, strain is found to be 0.002355 mm/mm also under permissible limit.

- It is important to mention that no effect of top end loading boss has been taken into account as there are no expressions available to discuss the role of end bosses to the deflection of the force transducer. Hence, for FE analysis of the circular diaphragm shaped force transducers, end bosses have not been considered.
- The deflection computed by analytic approach, and FE analysis has been summarized in Table 4.1. The comparison gives an overall comparison by different methods.

Table 4.1 Deflection of a Steel force transducer at different forces [106]

Force (kN)	Deflection (δ) by different methods (mm)	
	Analytical	FE Analysis
1	0.1339	0.1088
2	0.2798	0.2177
3	0.4197	0.3265
4	0.5597	0.4354
5	0.6996	0.5442

- The study reveals that there is significant variation in the finding of analytic process, and computational method. The deviation of values by analytical process to FE analysis is about 22 %.
- The above findings have hinted that the findings in terms of deflection, which is very important for such type of force transducers as the force is harmonized by the deflection values of the force transducer, whereas the output deflection by the expressions for analytical and FEM are not similar.

4.4 FE Model of the MEMS Silicon Force Sensor

A 3-D model of a (2.2x2.2) mm² silicon square shaped MEMS force transducer, idealized in central portion as a circular silicon diaphragm in bending has been designed and modelled by means of the assist of contemporary CAD tool software SolidWorksTM. In this design, a single silicon crystal thin diaphragm over a cavity in vacuum, carved out of a single crystal monolithic <100> Si is used like a mechanical elastic sensing loading element bonded with 0.7mm thick Pyrex glass. The diaphragm size, thickness and the depth of the cavity

under the diaphragm has been optimized to achieve higher output sensitivity against an applied force for nominal intended range of 50 Newton. Following a number of permutations and combinations on diaphragm depth, the most suitable optimized diaphragm element was selected (Fig. 4.9).

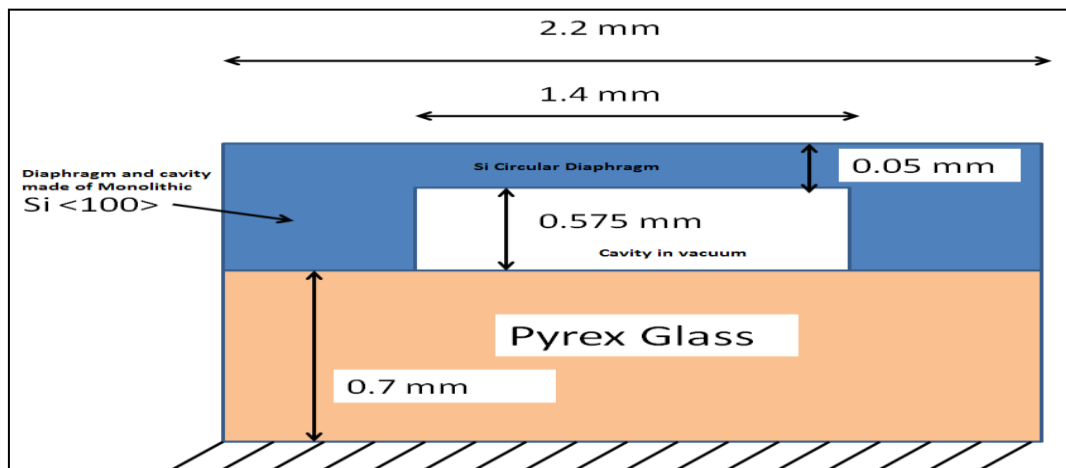


Fig. 4.9 Dimensional cross-section view of diaphragm force sensing element

An extensive 3 Dimensional model has been developed by means of the support of a software tool in the first stage (Fig. 4.10), after that in subsequently step (Fig. 4.11) meshing was done on the designed model so that a drastic assessment of force sensor could be done for evaluating its structure analysis behaviour under the action of the applied force.

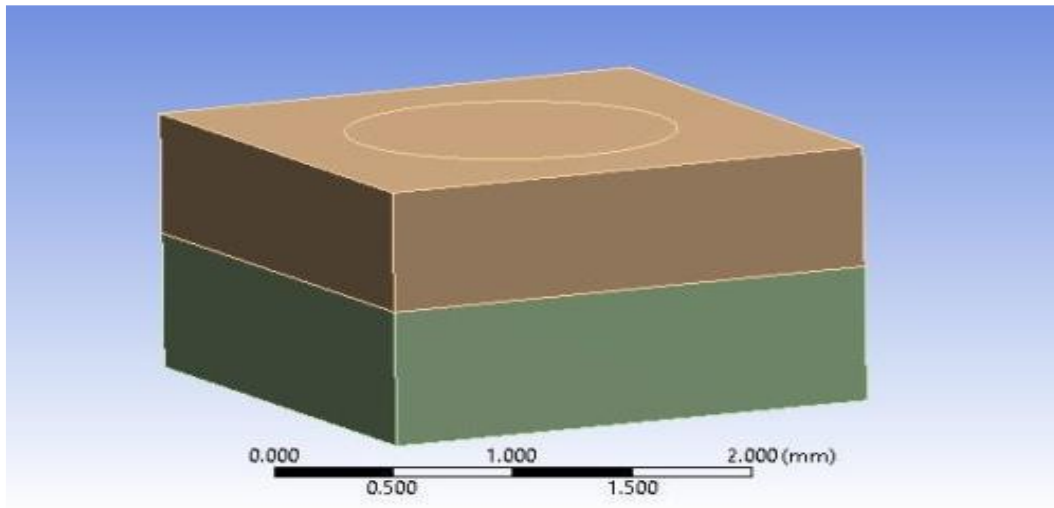


Fig. 4.10 3-D Silicon force sensor CAD model

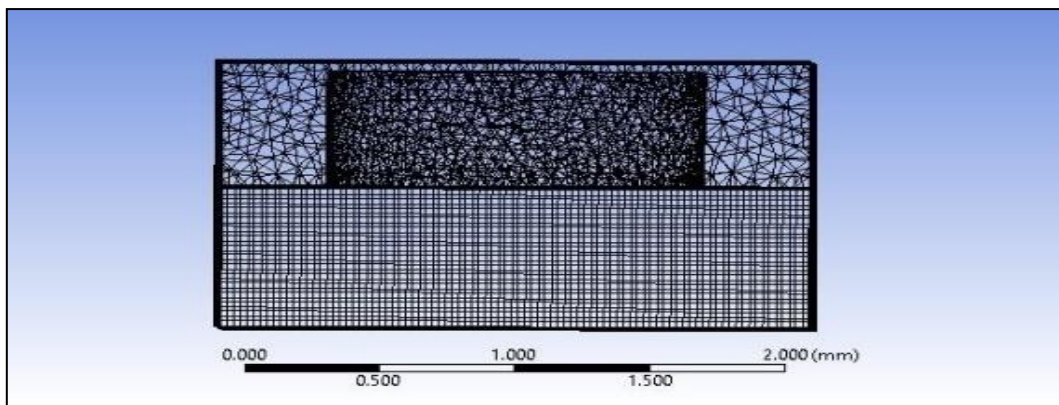


Fig. 4.11 Meshing of the Silicon force sensor

The whole silicon square model with central circular cavity diaphragm has been selected for FE analysis. The circular silicon diaphragm force sensor has been investigated to take the advantage of geometrical symmetry of the structure. The boundary conditions have been defined according to the analytical approaches, while processing the various steps for FE analysis. A 3-D solid continuum with 160701 nodes and 46925 element size in meshing has been adopted. The material is assumed to be isotropic in nature. The material is assumed to be silicon. The value of yield point and elasticity modulus has been chosen for Silicon as

7000 MPa and 190 GPa respectively. Poisson ratio selected as 0.23. The force applied axially in a mode of compression at the centre of the silicon diaphragm (Fig. 4.12). Suitable procedure for FE analysis has been taken and the (stress - strain - axial deflection) are assessed. The summary of the FE analysis have been presented through stress - strain and axial deflection [53].

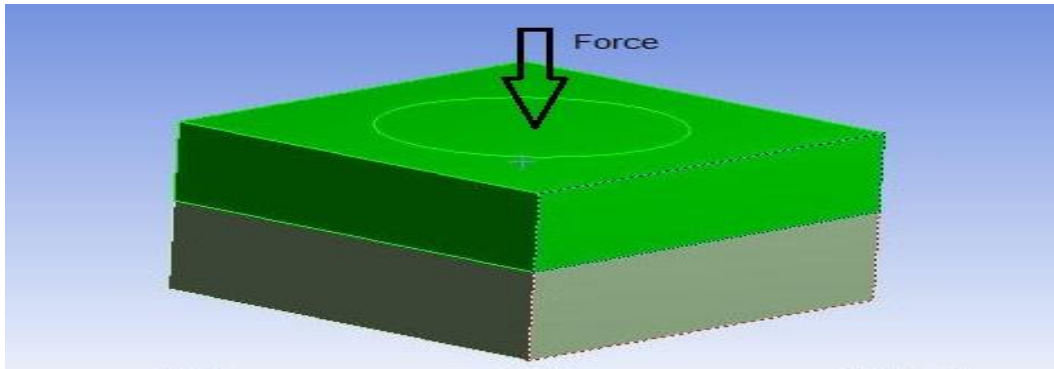


Fig. 4.12 Force application at the centre of the silicon diaphragm

4.5 Key Outcomes of FE Analysis of Silicon Force Sensor

- The computational (simulation) study has been very constructive for locating the utmost suitable position of the piezoresistors. For achieving the highest sensitivity for MEMS sensor, the precise location of piezoresistors performs the crucial job [111-112].
- The stress distribution for the silicon diaphragm sensor while subjected in the direction of the axial compressive load, highest stress takes place on the top upper point from where the axial load is transmitted (force applied is concentrated force) since the axial load applied is assumed to be tip force or concentrated force (Fig.4.13 and 4.14). From the tip of axially applied load application point towards the outer edge of the diaphragm, the stress tends to reduce to the extreme end. The stress at the middle section of the diaphragm is sufficiently large, but less than that at the upper

top point. Since the load applied is believed to be concentrated and tip force, however in actual practice, it might not be possible. The force applied may have line contact instead of point contact as assumed. Hence, the few higher values of stress may be ignored, which are shown at the point of application of force (St. Venant's principle). It is well clear from the stress distribution that the values of stress vary abruptly at locations near to point of application of axial force.

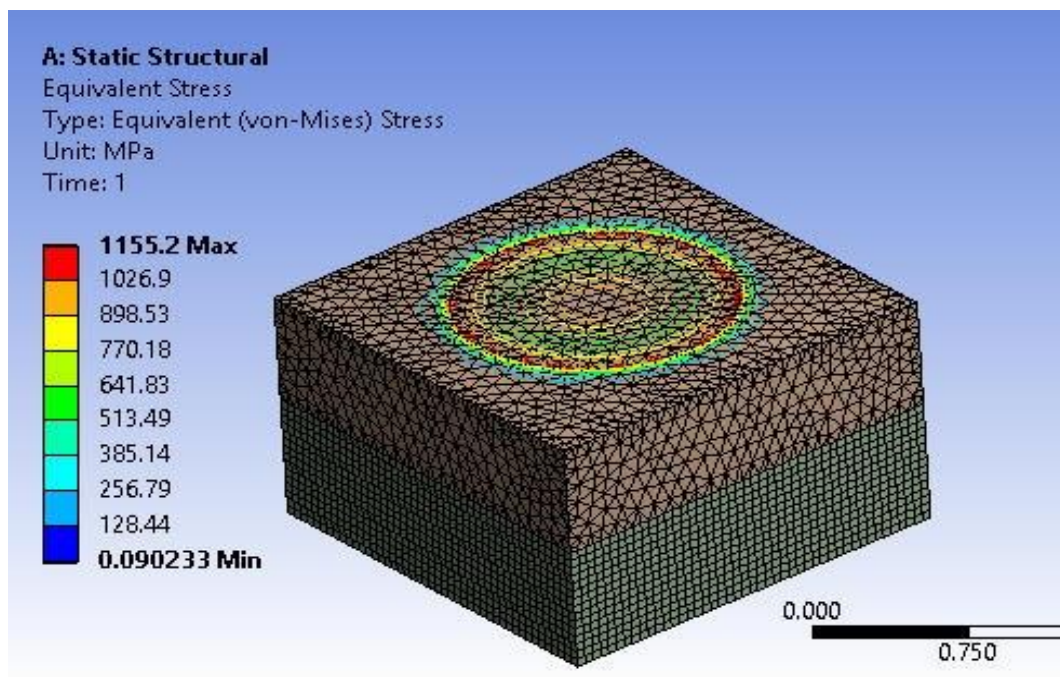


Fig. 4.13 Stress of MEMS force sensor

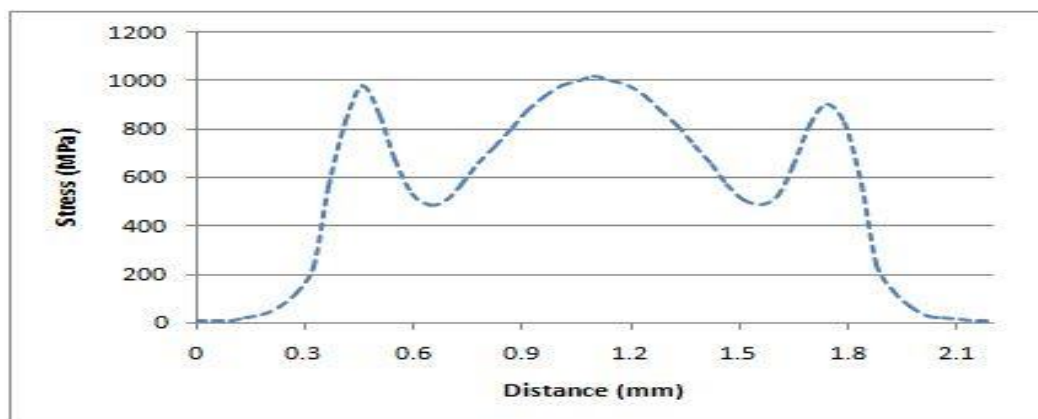


Fig. 4.14 Stress distribution of silicon sensor

- For MEMS sensor the most feasible position of strain resistors is 0.618 mm away from midpoint of the transducer. The highest generated stress is 1155.20 MPa, which is less than the yield strength of silicon matter.
- The strain distribution for the whole diaphragm of the silicon force sensor under axially applied compressive loads follow the alike trend similar to the stress distribution pattern seeing that in Figures 4.15 & 4.16. The strain is minimum at the outer periphery of the diaphragm and then tends to increase from outwards to the inner part of the diaphragm and maximum at the middle of the diaphragm where the axially load be applied. Similarly, some of higher values of strain are ignored and suitable values are taken into account. The strain follows the identical trend as in case of the stress and both are well correlated by Young's modulus of elasticity.

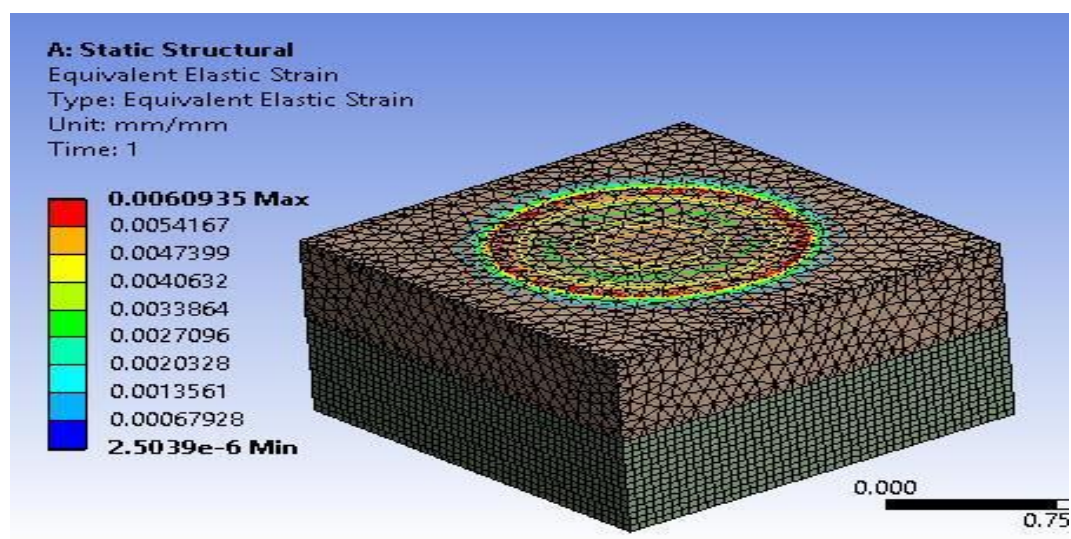


Fig. 4.15 Strain of MEMS sensor

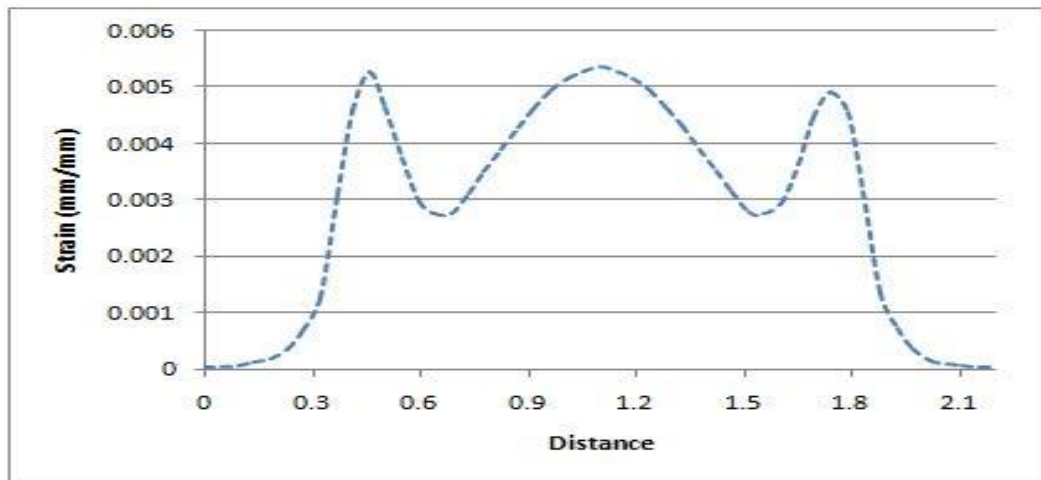


Fig. 4.16 Strain distribution of MEMS force Sensor

- The axial deflection for the whole diaphragm of the silicon force sensor when it is subjected to the axial compression force is shown in Figures 4.17. The axial deflection is maximum on the tip of the point application of axially load since the load be considered like concentrated force, however tends to reduce all along the outer periphery of the diaphragm as well as is nearly insignificant on the outer ending of the diaphragm (this outer end is considered fixed as per the analytic derived expressions as discussed earlier).

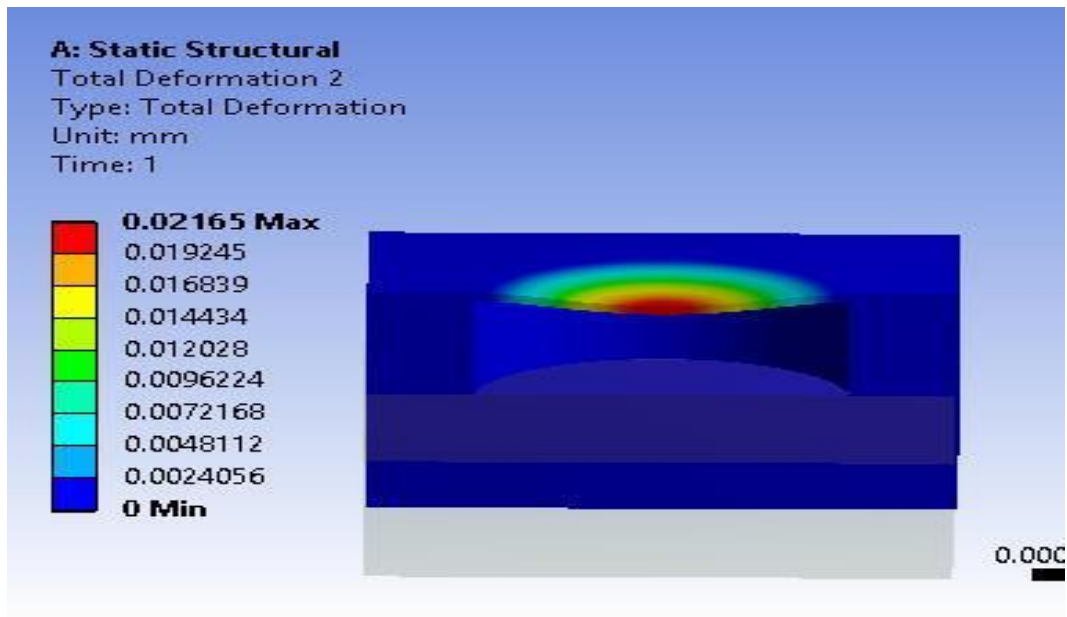


Fig. 4.17 Deflection plot for silicon force sensor

- The deflection is the mainly significant factor during diaphragm based sensor design. On unlike loading situation obtained computational deflection values by simulation are shown in figure 4.18. The highest deflection on the midpoint of the sensor, however it tends to reduce all along the radius as well as nearly insignificant on outside edge of the sensor. Due to the alike deflection tendency only one side deflection from the centre point has been considered in the fig. below.

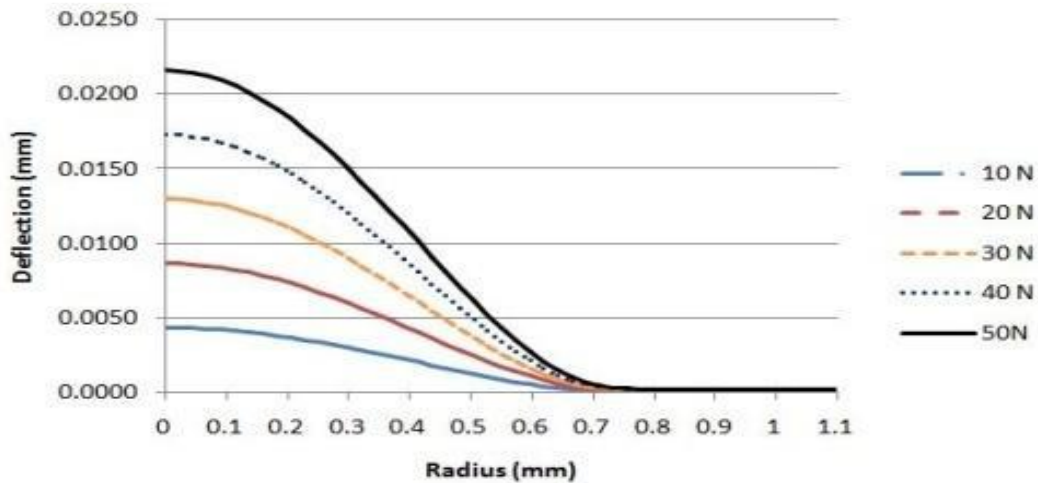


Fig.4.18 Computational deflection data of silicon force sensor

- For more rigorous investigation, the silicon force transducer is subjected to computational investigations at different force steps i.e. at (10, 20, 30, 40, 50) Newton's. The computational procedure is adopted as discussed above to have the (stress – strain – deflection) pattern used for different forces. Plots shows similar pattern for (stress – strain – deflection) except magnitude of (stress – strain – deflection). The trend of (stress – strain – deflection) is found very similar for all the nominal axial forces and there is proportionally change in the magnitude of the values of (stress – strain – deflection).
- Location of sensing element always plays a vital role for the design of diaphragm based force sensor. The stress and strain distribution plots give the most appropriate location of strain measuring sensor. Therefore stress – strain plots could be very helpful in designing and locating the suitable places over the surface of force transducers, where piezoresistors could be formed. Now here as per the plots it is found that stress – strain values are minimum at outer periphery and maximum at the point of application of concentrated forces. It is clearly evident from figure (4.13 to 4.16) the maximum stress and strain occurs 0.61875 mm far from the middle of the

silicon sensor. So, this is most promising location for the strain gauges for better sensitivity. The highest stress is found to be 1155.2 MPa which is less than the yield point strength of the matter used. Similarly, strain is found to be 0.00538 mm/mm also under permissible limit.

- The deflection computed by analytic approach, and FE analysis has been summarized in Table 4.2. The comparison gives an overall comparison by different methods. The computational deflection data plotted in figure (4.17 and 4.18) by means of changed load situation showing the highest deflection occurs in the middle of plate. The highest hypothetical value of deflection is found 18 micron at 50 Newton load. The hypothetical deflection numbers obtain by using analytic equation and computational data deflection obtained by Ansys MultiphysicsTM simulation tool are revealed in figure 4.19 follow the like tendency.

Table 4.2 Deflection of a Silicon force sensor at different forces [106]

Force (N)	Deflection (δ) by different methods (mm)	
	Analytical	FE Analysis
10	0.00376	0.00433
20	0.00752	0.00866
30	0.01128	0.01299
40	0.01504	0.01732
50	0.01880	0.02165

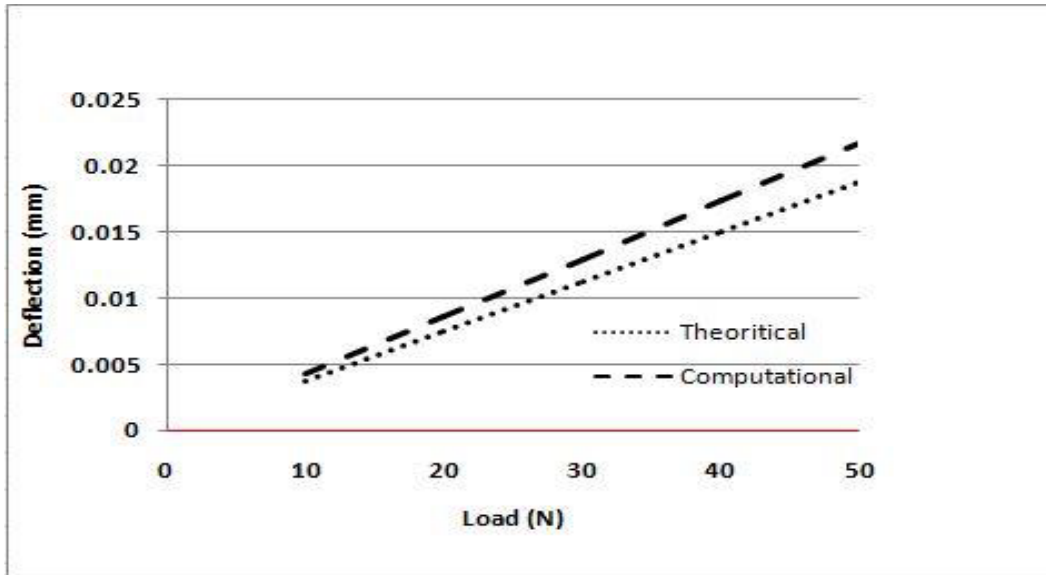


Fig. 4.19 Comparison between computational and theoretical results of silicon force sensor

- The study reveals that there is significant variation in the finding of analytical method, and FE analysis. The deviation in the values of analytical method to FE analysis is about 13 %.
- The above findings have hinted that the findings in terms of deflection, which is very important for such type of force transducers as the force is harmonized by the deflection values of the force transducer, whereas the output deflection by the expressions for analytical and FEM are not similar.

4.6 Summary

The chapter discusses FE analysis of circular shaped steel diaphragm force transducer and MEMS based silicon diaphragm force sensor. The FE analysis has been done with the help of software Ansys Multiphysics™. The idealized full diaphragm for both the cases of steel and silicon diaphragm force transducers have been subjected to similar boundary conditions as in the case of analytical approaches. Stress - strain pattern is helpful in locating

the strain gauges. Deflection, which is very important in case of optimization of diaphragm size, diaphragm thickness and depth of cavity under the diaphragm for both the force transducers, have been measured by FE analysis and analytical approach. The proposed parameters all along by means of size and choice of the material have been validating by means of FE analysis. The FE analysis (FEA) has been conceded out for computational investigations (simulation) to have a fairly accurate assessment in view of mechanical design and features. The significant parameters like (stress – strain – deflection) have been established within acceptable restrictions. A comparison has been made for deflection by different methods and it is observed that there is significant variation in the findings of analytical approach to the results of FE analysis. The deflection obtained by FE analysis is about 22 % of the analytically computed deflection in case of steel force transducer and 13% in case of MEMS silicon force sensor.

Therefore FEM based analysis that gives a quick and reliable estimation of deflection and stress-strain distribution in force transducers. The FEM based simulation can give relatively closed results as compared with the mathematical model obtained. The sensitivity of the transducer is related to the most promising location of piezoresistors and strain gauges.

Chapter 5

Fabrication and Metrological Investigation of the EN 24 steel grade based Diaphragm Force Transducer

5.1 Introduction

Analytical and computational investigations are completed about the spring elastic element design of steel (EN-24) diaphragm shaped force transducers in the previous chapter 3 & 4. Now the force transducer is to be fabricated as per optimized designed dimensions according to suitable machining processes and thereafter strain gauges are to be pasted at the selected optimized locations. The strain gauges are to be configured in a Wheatstone bridge and then the data is to be collected through suitable data acquisition system DK-38 (a high resolution digital indicator) for their metrological investigations.

5.2 Fabrication of Steel Diaphragm Force Transducer

The sensing spring elastic element of the EN24 steel diaphragm force transducer is machined on a CNC lathe machine as per the specified dimensions. The dimensions of the spring elastic element have been calculated according to the analytical as well as computational analysis has confirmed that the stress – strain are in within safe limits. The material EN 24 steel has been selected due to its good elastic properties. The force transducer is fabricated for nominal capacity of 5000 N for the measurement of the medium range of forces which is quite useful for Indian industry. MEMS based silicon diaphragm force sensor of nominal capacity 50 N is also fabricated through Micro electro mechanical systems techniques to facilitate the measurement of force in the lower range also in good demand for Indian industry (fabrication details of MEMS sensor discussed in chapter 6). The nominal optimized dimensions of these two types of diaphragm force transducers are given in Table

5.1. After the fabrication of the sensing spring element through machining process, it is further subjected to heat treatment using the salt bath to achieve the required targeted hardness value (HRC Scale) in the range of 40-45 HRC. After achieving hardness of requisite range, the elastic element is finished and the surface roughness throughout the sensing element is restricted to few microns. Thereafter the elastic element is electroplated for better aesthetic look.

Table 5.1 Nominal dimensions of the force transducers

Sl. No.	Capacity (N)	Diaphragm size (mm)	Thickness (mm)	Width, <i>b</i> (mm)
1	5000	120	3	20
2	50	1.4	0.05	0.625

The elastic element is now to be strain gauged and the strain gauges are to be bonded at a predetermined specified place identified with the help of computational and analytical investigations. The surface requiring pasting of strain gauges has to be cleaned properly and need to locate the places of strain gauge. The surface is further cleaned with the help of solvents like benzene or acetone and surface roughness to be improved to very high level of the order less than 1 micron with the help of very fine emery paper. The locations of the strain gauges are to be defined carefully and then suitably marked by means of marker pen etc.

5.3 Bonding of Strain Gauges

On the basis of finite element (FEM) findings the strain gauges are being pasted on top of the identified marked positions. The machined spring element (e.g. circular steel diaphragm force element without strain gauges) has been applied to an preload overloading

of around 10 to 20% above on the rated full capacity for two to three times for normalizing the elastic membrane, followed by two to three full load up to the full capacity, as a result of which the stress of sensing membrane brought in working range. The pre-located gauged surface area of elastic membrane are marked at the specified locations for application of strain gauges have been prepared carefully along with the surface irregularity is controlled near to less than one micron for proper bonding of strain gauges. Poor surface finish may lead to improper pasting of strain gauges which leads to improper metrological evaluations of force devices. Hot curing epoxy resin is used for pasting of strain gauges. Appropriate pre and post curing intended for pasting of strain gauges along with connections are made according to the Wheatstone bridge. Strain gauges of nominal resistance value of $350 \pm 0.3 \Omega$ have been connected now in form of a Wheatstone bridge configuration (Figure 5.1). According to the early research findings and computational analysis of selected geometrical model, the area of moderate stresses are preferred for pasting of strain gauges on defined marked locations i.e. in between the centre and the outer periphery of the circular diaphragm. A set of 4 strain gauges are applied from vertical axis at an angle of 90^0 , 180^0 , 270^0 , 360^0 respectively on the elastic element's outer flat surface area as per (Figure 5.2). Initially the Wheatstone bridge is null balanced as the resistance value of all strain gauges are same at no load condition of the force device, as soon as some load is applied to the force device, resulted in change in the values of the strain gauges makes the Wheatstone bridge unstable and the output generated in the form of an voltage electrical unit is generated equivalent to force applied. It may also be well understood that the electrical output is proportional to the stress - strain, which in turn is proportional to the load applied. The electrical yield could be indicated by means of a proper data acquiring method like a digital meter in volts i.e. mV/V. A typical strain gauged force device has been revealed in Figure 5.3. A high resolution precision digitized indicator Dk-38 of 0.00001 mV/V resolution or

better has been used for recording observations of the force device.

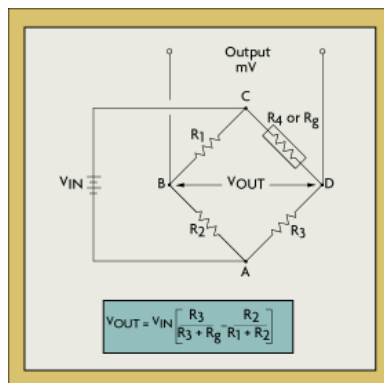


Fig. 5.1 A typical Wheatstone bridge [10]

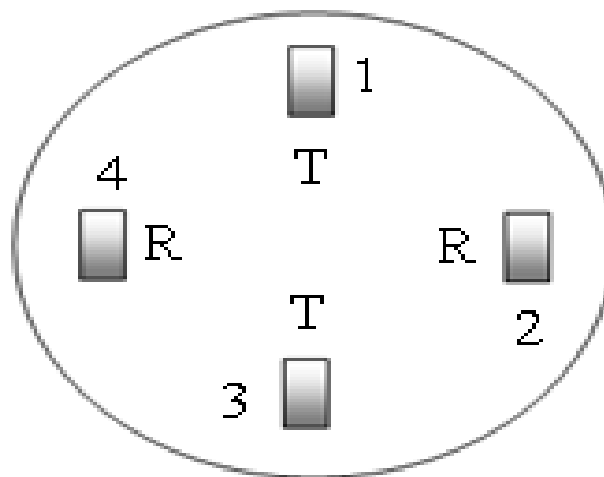


Fig. 5.2 Arrangements of Strain Gauges



Fig. 5.3 Strain Gauged Force Transducer



Fig. 5.4 Experimental setup for steel diaphragm force transducer at force machine of 50 kN dead weight at NPL, New Delhi.

5.4 Investigations of a of Steel diaphragm for Metrological characteristics

The Steel diaphragm is investigated metro logically for its characteristics as per the calibration procedures on the basis of ISO 376-2004-2011 and IS 4169-88 (2003, reaffirmed). A 50000 N force dead weight machine was used for precise application of forces for the force devise of 5 kN nominal capacity (Figure 5.4). The calibration has been done at 10 points for the forces from 0 to 5 kN at the intervals of 0.5 kN. The best measurement capability of realized force by this 50000 N force dead weight machine is 0.003 % at ($k = 2$) [98]. For metrological characterization of 50 N MEMS diaphragm force transducer, an experimental set up is designed and fabricated (details are discussed in chapter 6), whose uncertainty of measurement for realized force is 0.01 % at ($k = 2$). The 50000 N force dead weight machine used for metro logically characterization of force devise are computerized control and operated through software. The machine employs a total of 18 stainless steel static masses ranged from 500 N to 5000 N pneumatically operated to generate pre determined known force accurately up to a maximum capacity of 50000 N. The 50000 N force dead weight machine is capable to carry out calibrations as per the standard method IS 4169-88 and ISO 376-11. The force standard machines are instructed as per the sequence of calibration force applied depending upon the capacity of force transducer. The observations after waiting for

specified time (like 30 seconds, 45 seconds etc.) are recorded in automatic mode. The readings are automatically stored in MS excel sheets format and used for further calculations. The Metro logically characterization reveals the uncertainty measurement of force device. Uncertainty measurement of force device depends upon relative components uncertainty of errors like repeatability error, reproducibility error, resolution error, interpolation error, zero offset error, reversibility error etc. The relative measurement uncertainty depending upon calibration procedure adopted helps in classification of the force transducer like 0.0 class, 0.5 class, 1 class or 2 class as in case of ISO 376 – 2004 / 2011 and while class 0, class 1 or class 2 in case of IS 4169-1988 (reaffirmed 2003). For classification, emphasis is given over the individual component of the uncertainty of force transducer at the same time to the force device expanded uncertainty [88-89].

5.4.1 Calibration method according to Standard ISO 376 -2004 / 2011

The metrological evaluation involves findings of relative component of uncertainty because of reproducibility error, repeatability error, zero offset error, interpolation error, resolution error and reversibility error. Procedure adopted for calibration has been discussed below:

- a. Digital display is switched on for about 30 minutes for thermal stabilization of the indicator at zero load output prior to start off the actual calibration, zero load output is recorded (prior to tarring) and corresponding calibration signal is noted. Suitable time for thermal stabilization to be provided also.
- b. Before actual starting series of calibration forces, force device is preloaded at least three times to its highest nominal capacity and maintain the total load not less than 90 seconds. This will help in checking the stability of the output of the force transducer over full load.

- c. Calibration of force device has been completed in compressive direction as required. Suitable accessories are used like compression pads intended for apply of compressive force to the force device in respective mode.
- d. Initially at 0° position, calibration was performed by applying 2 sequence of calibrating forces in rising order starting from 10% to 100% in a interval of 10% The reading of no load after removal of nominal force is also noted. The two sets of observations will help in estimation of relative uncertainty component due to repeatability.
- e. 2 sequence of calibration forces also in rising order have been carried out at two rotational positions 120° and 240° . Similarly, readings at no load are also taken after removal of nominal force. One series at 0° , 120° and 240° each helps in estimating relative component of uncertainty because of reproducibility.
- f. The force device is subjected to a full nominal load at least once for not less than 90 seconds every time prior to initiating calibration at a new location. This is to counter the rotation effect up to an extent.
- g. After the end of each calibrations series loading, the residual zero readings output after a wait of at least 30 seconds, related to without load at force device, were noted.
- h. Measurement uncertainty of force transducer includes the relative uncertainty component for errors like zero offset, reproducibility error, repeatability error, reversibility error, resolution error, and interpolation error including uncertainty associated with the best measurement capability of the used force machine.

$$w_{c(tra)} = \sqrt{(w_{rep}^2 + w_{rpr}^2 + w_{int}^2 + w_{rev}^2 + w_{zer}^2 + w_{res}^2)} \quad (5.1)$$

The relative contributions of dissimilar factors pertaining to force device measurement uncertainty as given below in table 5.2:

Table 5.2 Relative components of error and their contribution for Measurement Uncertainty as per ISO 376-2004 /2011

S. No.	Relative error Component	Type of Error/ Distribution	Estimated Variances for input quantity
1	Error due to Repeatability	Type ' B' / Rectangular	$W^2_{(rep)} = a^2 / 3$
2	Error due to Reproducibility	Type ' B' / U shaped	$W^2_{(rpr)} = a^2 / 2$
3	Error due to Interpolation	Type ' B' / Triangular	$W^2_{(int)} = a^2 / 6$
4	Error due to Reversibility	Type ' B' / Rectangular	$W^2_{(rev)} = a^2 / 3$
5	Error due to Zero deviation	Type ' B' / Rectangular	$W^2_{(zer)} = a^2 / 3$
6	Error due to Resolution	Type ' B' / Rectangular	$W^2_{(res)} = a^2 / 3$

5.4.2 Calibration method according to Standard IS : 4169-88, re-affirmed 2003

- a. Digitized indicator is kept on about 30 minutes for thermal stabilization of the indicator at zero load output prior to start off the actual calibration, zero load output is recorded (prior to tarring) and corresponding calibration signal is noted. Suitable time for thermal stabilization to be provided also.
- b. Before actual starting series of calibration forces, force device is preloaded at least three times to its highest nominal capacity and maintain the total load not less than 90 seconds. This will help in checking the stability of the output of the force transducer over full load.
- c. Calibration of force device has been completed in compressive direction as required.

Suitable accessories are used like compression pads intended for apply of compressive force to the force devise in respective mode.

- d. Initially at 0° position, calibration was performed by applying 1 sequence of calibrating forces in rising order starting from 10% to 100% in a interval of 10% The reading of no load after removal of nominal force is also noted.
- e. 2 sequence of calibration forces also in rising order have been carried out at two rotational positions 120° and 240° . Similarly, readings at no load are also taken after removal of nominal force. One series at 0° , 120° and 240° each helps in estimating relative component of uncertainty owing to repeatability error.
- f. Force devise is subjected to a full nominal load at least once for not less than 90 seconds every time prior to initiating calibration at a new location. This is to counter the rotation effect up to an extent.
- g. After the end of each calibrations series loading, the residual zero readings output after a wait of at least 30 seconds, corresponding to no load at force devise, were noted.
- h. Measurement uncertainty of force devise includes the relative uncertainty component error due to for zero offset, resolution, repeatability, reversibility, and interpolation including uncertainty associated with the best measurement capability of the used force machine. (Table 5.3).

**Table 5.3 Relative components of error and their contribution for
Measurement Uncertainty as per IS 4169-88 (reaffirmed 2003)**

S. No.	Relative error Component	Type of Error/ Distribution	Estimated Variances for input quantity
1	Error due to Repeatability	Type ' B' / Rectangular	$W^2_{(rep)} = a^2 / 3$
2	Error due to Interpolation	Type ' B' / Triangular	$W^2_{(int)} = a^2 / 6$
3	Error due to Reversibility	Type ' B' / Rectangular	$W^2_{(rev)} = a^2 / 3$
4	Error due to Zero deviation	Type ' B' / Rectangular	$W^2_{(zer)} = a^2 / 3$
5	Error due to Resolution	Type ' B' / Rectangular	$W^2_{(res)} = a^2 / 3$

Metro logically characterization of the force devise has been reported in Figures [5.4-5.6].

$w_c (tra)$ which is %age combined standard uncertainty, and $W (tra)$ which is %age expanded uncertainty, at $k=2$ (whereas k is known as the coverage factor at 95% confidence level) would be determined by the subsequent equations from 5.1 to 5.3. Whereas the terms denotes the %age variances of component errors of measurement uncertainty, articulated as %age, because of repeatability(rep) error, reversibility(rev) error, zero(zer) deviation error, interpolation (int) error and resolution(res) error. [113-114].

$$w_c (tra) = \sqrt{(w_{rep}^2 + w_{int}^2 + w_{rev}^2 + w_{zer}^2 + w_{res}^2)} \quad (5.2)$$

$$W_{(tra)} = k \cdot w_c (tra)$$

The %age measurement uncertainty, W shall be calculated by Equation (5.3), taking into account the Measurement uncertainty linked with the reference force standard machine [115].

$$W = \sqrt{(W_{tra}^2 + W_{REF}^2)}. \quad (5.3)$$

The unlike factors pertaining to the measurement uncertainty of the force transducer are as follow:

A short explanation of unlike components has been described for good perception and significance of all elements of the measurement uncertainty of force devise.

(a) % age component of error due to Repeatability and its contribution for Measurement Uncertainty (rep)

This component of %age uncertainty contribution of repeatability error is calculated with the help of two repeated calibration sequences of forces in increasing order without disturbing the position of force transducer; at a same position i.e. sequence 1 and 2 at 0° position. For example, if 2 calibration sequences (1,2) are recorded in increasing order at same location say 0° position then the %age measurement uncertainty contribution owing to repeatability error is calculated like so:

$$W_{rep} = \frac{\text{Max (1:2)} - \text{MIn (1:2)}}{\text{Ave (1:2)}} \times 100 \% \quad (5.4)$$

(b) % age components of error due to Reproducibility and its contribution for Measurement Uncertainty (rpr)

This component of %age uncertainty contribution of reproducibility error is calculated with the help of three calibration sequences of forces in increasing order e. g. Sequence 1, Sequence 2, Sequence 3 at three different rotational angular positions at 0°, 120° and 240° respectively. For example, if three calibration sequences (1,2,3) are taken in increasing mode at three different angular position, say 0°, 120° and 240° the %age measurement uncertainty contribution due to reproducibility error is calculated like so:

$$W_{rpr} = \frac{\text{Max (1:2:3)} - \text{MIn (1:2:3)}}{\text{Ave (1:2:3)}} \times 100 \% \quad (5.5)$$

(c) % age components of error due to Zero deviation and its contribution for Measurement Uncertainty (zer)

The component of %age uncertainty contribution of zero deviation error is calculated at the end of each respective force calibration sequences at different angular positions e.g. 0°, 120° and 240° respectively. It is basically from the remaining indicated zero values of the force transducer indicator, when the calibration sequences is over at the end e.g. The force is totally removed from the force transducer, it should be further noted that the %age error of zero deviations will be constant for each force step. For example, if a force devise of nominal capacity of 5 kN capacity is calibrated and subjected to a calibration force sequences up to its maximum capacity during its calibration process, there after complete removal of the force at the end of calibration series, the zero output indicated by the force indicator will become zero deviation error. therefore, if three calibration sequences are undertaken and the remaining of zero deviation at the end of these calibration sequences are 1', 2' and 3' respectively for each sequences, the %age zero deviation error is calculated like so:

$$W_{zer} = \frac{\text{Max (1':2':3')}}{\text{Ave (1:2:3 at full rated capacity of force transducer)}} \times 100 \% \quad (5.6)$$

(d) % age components of error due to Resolution and its contribution for Measurement Uncertainty (res)

The % age component error of resolution is calculated by simply dividing unit of resolution of force indicator with average values of force indicator at any specified force step of calibration sequence. It should be further noted that the %age resolution error keeps on reducing as we shift towards the higher force in ascending mode of calibration. Its value is always higher at the lower step and only this higher value of resolution is considered for estimation of measurement uncertainty at all force steps.

$$W_{res} = \frac{\text{Resolution of indicator}}{\text{Ave value at the particular force step}} \times 100 \% \quad (5.7)$$

(e) % age components of error due to Reversibility and its contribution for Measurement Uncertainty (rev)

The %age component error of reversibility is calculated from difference between two consecutive calibration sequences of force by increasing and decreasing order on all specified force steps of calibration sequence to assess the %age component error caused by reversibility. This type of error is not applicable for analogue force measuring devices, due to large localized error found in dial gauges; hence it is not taken into account. It is applicable only in the case of a digital output force indicator of force transducers. The %age measurement uncertainty contribution due to reversibility is,

$$W_{\text{rev}} = \frac{(\text{Desending}-\text{Ascending})}{\text{Ascending}} \times 100 \% \quad (5.8)$$

(f) % age components of error due to Interpolation and its contribution for Measurement Uncertainty (int)

The %age uncertainty contribution component of interpolation is not applicable for analogue force measuring device due to a very high localized linearity errors associated with dial gauges used in it, whereas it is applicable in case of digit output devices like strain gauged force transducers having outputs in terms of some electrical outputs like mV/V. For the present investigations, we computed the %age uncertainty component error due to interpolation by an internal developed computer program. The software is based on program for polynomial fitting using the second or third degree polynomial, by fitting the least square polynomials in a straight line, thus gives a best fit curve equations for calculating any intermediate point output like force v/s deflection or vice versa. The nominal force data is stored in force units e.g. Newton's (N) and the corresponding output display of the digital indicator in mV/V or digits.

For example, “50, 2023” denotes 50 is the value of force in Newton’s (N), whereas 2023 is corresponding average output value of display against applied force of 50 N. Now this data is stored as a data file with “.dat” extension. This stored file is now accessed by means of this software and runs the program of polynomial fitting of least square to calculate square root mean error. Final outcomes are generated in a file of “out” extension and could be further accessed either in the form of MS word file or MS excel file. The %age measurement uncertainty contribution of interpolation is,

$$W_{\text{int}} = \frac{(\text{Ave value of deflection} - \text{Computed value of deflection})}{\text{Computed value of deflection}} \times 100 \% \quad (5.9)$$

The foremost dissimilarity among ISO- 376:2004 and IS- 4169:88, re-affirmed2003 is that the IS- 4169-88, not consider %age component uncertainty of repeatability error into account at say 0° position, whereas ISO- 376 considers it. Remaining factors are alike for both standard methods.

Table 5.4 Difference between ISO - 376 and IS - 4169

S. no.	Heading	(IS – 4169)	(ISO – 376)
1	No. of Force calibration Sequences	3 One each at 0°, 120° and 240°	4 Two at 0° and one each 120° and 240°
2	Calibration Series at 0° position	1	2

**Table 5.5 Relative uncertainty measurement of force devise as per IS 4169
with factors discussing the metrological characterization**

Force (kN)	%age deviation due to uncertainty component					Relative uncertainty associated with force machine W_{REF}	Measurement Uncertainty at ($k=2$)
	Zero deviation (2 a)	Repeatability (2 a)	Resolution (2 a)	Interpolation (2 a)	Reversibility (2 a)		
0.5	0.007	0.028	0.014	0.016	0.061	0.003	0.042
1.0	0.007	0.050	0.007	0.006	0.069	0.003	0.053
1.5	0.007	0.052	0.005	0.013	0.060	0.003	0.051
2.0	0.007	0.053	0.004	0.008	0.056	0.003	0.050
2.5	0.007	0.040	0.003	0.001	0.065	0.003	0.047
3.0	0.007	0.031	0.002	0.003	0.071	0.003	0.047
3.5	0.007	0.053	0.002	0.002	0.067	0.003	0.054
4.0	0.007	0.041	0.002	0.004	0.073	0.003	0.052
4.5	0.007	0.018	0.002	0.001	0.073	0.003	0.044
5.0	0.007	0.043	0.001	0.002	0.000	0.003	0.031

Table 5.6 Sample calculation of measurement uncertainty for 0.5 kN force step

Force (kN)	%age deviation due to uncertainty component					Relative uncertainty associated with force machine W_{REF}	Measurement Uncertainty at ($k=2$)
	Zero deviation (a^2)/3	Repeatability (a^2)/2	Resolution (a^2)/3	Interpolation (a^2)/6	Reversibility (a^2)/3		
0.5	0.0000041	0.0000653	0.0000163	0.0000094	0.0003101	0.003	0.04

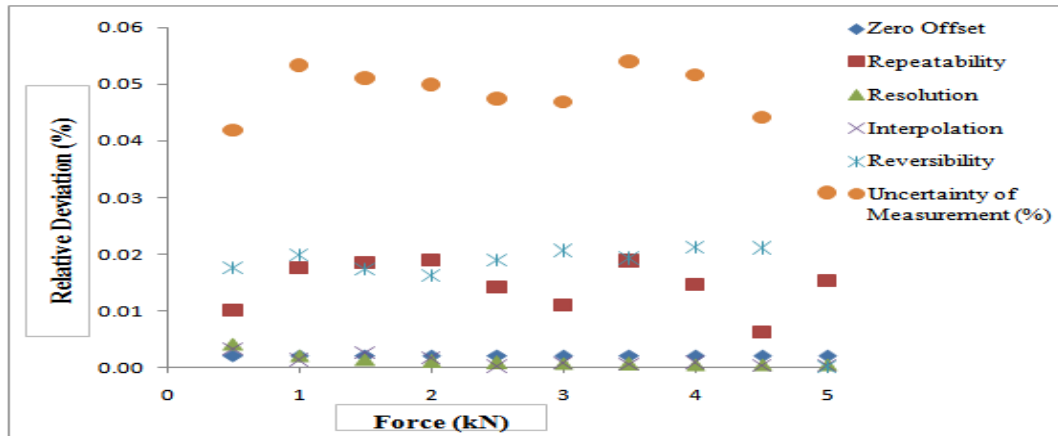


Fig. 5.5 5 kN force transducer metrological characterization according to IS 4169-1988 (reaffirmed 2003) [116]

Table 5.7 Relative uncertainty measurement of force device as per ISO 376 with factors discussing the metrological characterization

Force (kN)	%age deviation due to uncertainty component						Relative uncertainty associated with force machine W_{REF}	Measurement Uncertainty at ($k=2$)
	Zero deviation (2 a)	Repeatability (2 a)	Reproducibility (2 a)	Resolution (2 a)	Interpolation (2 a)	Reversibility (2 a)		
0.5	0.007	0.028	0.042	0.014	0.012	0.063	0.003	0.051
1.0	0.007	0.014	0.057	0.007	0.012	0.070	0.003	0.058
1.5	0.007	0.014	0.047	0.005	0.001	0.059	0.003	0.049
2.0	0.007	0.011	0.057	0.004	0.001	0.051	0.003	0.050
2.5	0.007	0.009	0.046	0.003	0.008	0.065	0.003	0.050
3.0	0.007	0.007	0.031	0.002	0.003	0.074	0.003	0.048
3.5	0.007	0.014	0.053	0.002	0.012	0.053	0.003	0.050
4.0	0.007	0.021	0.043	0.002	0.000	0.071	0.003	0.053
4.5	0.007	0.021	0.027	0.002	0.008	0.071	0.003	0.047
5.0	0.007	0.017	0.043	0.001	0.003	0.000	0.003	0.032

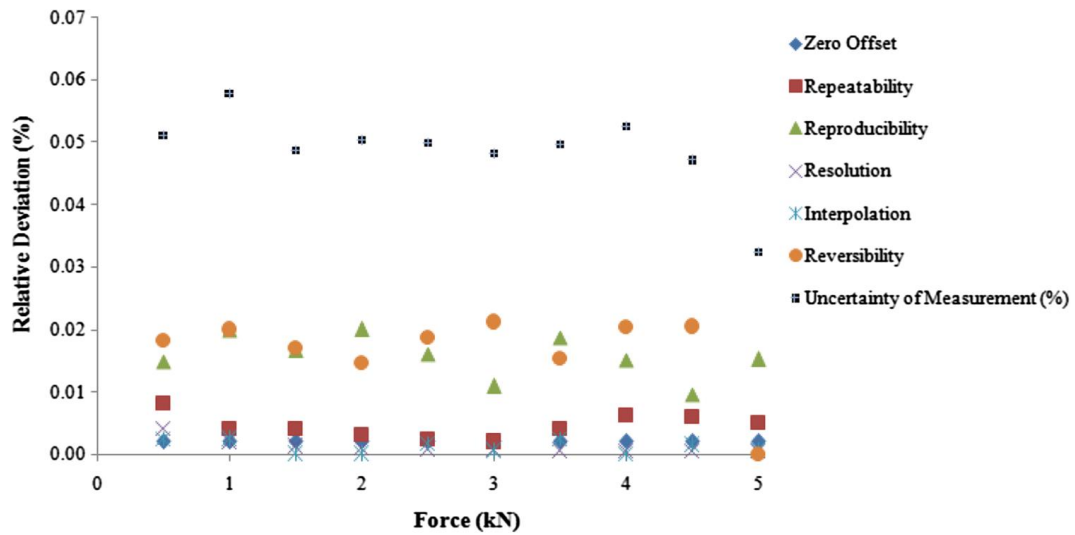


Fig. 5.6 5 kN force transducer metrological characterization according to ISO 376-2004 [116]

The maximum measurement uncertainty is found to be 0.58% at 1.0 kN force step as depicted in table 5.7 and figure 5.6 for which the uncertainty budget is presented in table 5.8, as follows.

Table 5.8: Uncertainty Budget at higher value at 1.0 kN force step

Source of Uncertainty	Estimate X1 (2a)	Limits ± X1 (a)	Probability Distribution /Divisor	Standard Uncertainty	Sensitivity Coefficient (ci)	Uncertainty Contribution	Degree of Freedom
Repeatability	0.014	0.007	Rectangular/√3	0.004	1.0	0.004	∞
Reproducibility	0.057	0.0285	U Shaped/√2	0.02	1.0	0.02	∞
Zero offset	0.007	0.0035	Rectangular/√3	0.002	1.0	0.002	∞
Interpolation	0.012	0.006	Triangular/√6	0.0024	1.0	0.0024	∞
Reversibility	0.07	0.035	Rectangular/√3	0.02	1.0	0.02	∞
Resolution	0.007	0.0035	Rectangular/√3	0.002	1.0	0.002	∞
Relative combined standard Uncertainty)						0.0288	
$w_{c(tr)} = \sqrt{(w_{rep}^2 + w_{rpr}^2 + w_{int}^2 + w_{rev}^2 + w_{zer}^2 + w_{res}^2)}$							
Relative expanded uncertainty, $W_{(tra)} = k \cdot w_{c(tr)}$						0.058	
W_{REF}						0.003	
Relative uncertainty of measurement, $W = \sqrt{(W_{tra}^2 + W_{REF}^2)}$						0.058	

Further analysis has improved the sensitivity of the force devise. This was achieved by adding together 2 strain gauges in series in all the four arms of the Wheatstone bridge. This has improved the sensitivity with no much major change in the uncertainty of measurement of force devise. Diagrammatic arrangement has been depicted in figure 5.7. Rated resistance value of 350 Ω of individual strain gauge has been used. The measurement data are briefed in Table 5.9.

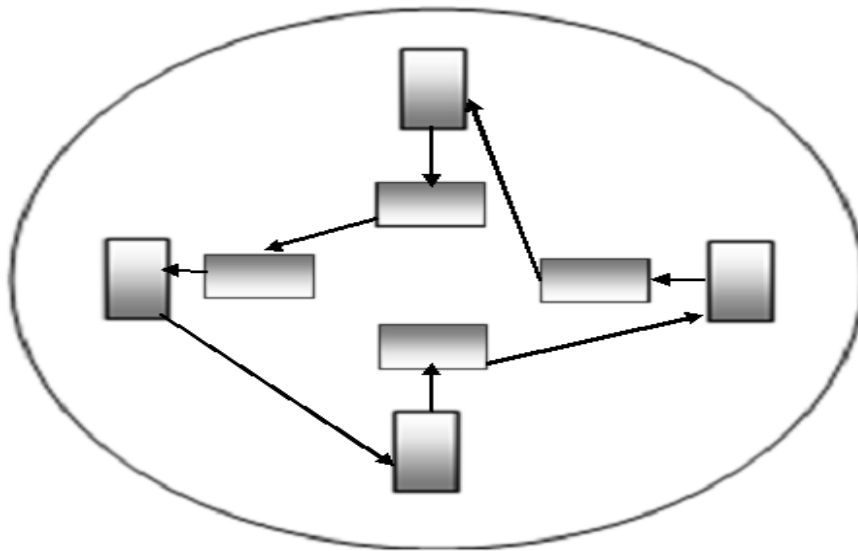
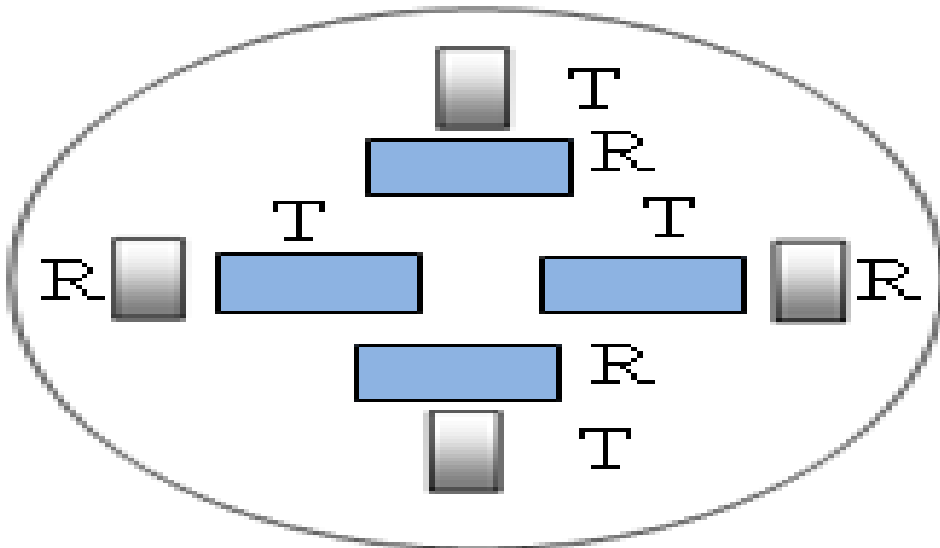


Fig.5.7. Schematic diagram of array of strain gauges (R: Radial; T: Tangential) with connectivity of strain gauges

Table 5.9 Relative uncertainty measurement of force devise with improved sensitivity as per ISO-376 with factors discussing the metrological characterization

Force (kN)	%age deviation due to uncertainty component						Relative uncertainty associated with force machine W_{REF}	Measurement Uncertainty at ($k=2$)
	Zero deviation (2 a)	Repeatability (2 a)	Reproduci- bility (2 a)	Resolution (2 a)	Interpolation (2 a)	Reversibility (2 a)		
0.5	0.003	0.014	0.041	0.007	0.023	0.071	0.003	0.052
1.0	0.003	0.010	0.045	0.003	0.007	0.061	0.003	0.048
1.5	0.003	0.007	0.039	0.002	0.015	0.048	0.003	0.040
2.0	0.003	0.007	0.050	0.002	0.001	0.051	0.003	0.046
2.5	0.003	0.005	0.048	0.001	0.001	0.032	0.003	0.039
3.0	0.003	0.006	0.041	0.001	0.012	0.037	0.003	0.036
3.5	0.003	0.006	0.026	0.001	0.001	0.019	0.003	0.022
4.0	0.003	0.004	0.042	0.001	0.003	0.019	0.003	0.032
4.5	0.003	0.005	0.040	0.001	0.006	0.013	0.003	0.030
5.0	0.003	0.005	0.053	0.001	0.004	0.000	0.003	0.038

On comparison of results summarized from tables 5.7 & 5.9, it is evident that there is barely any influence on the overall uncertainty of measurement of force devises, in spite of improvement in overall output sensitivity. Nevertheless, there is considerable decrease in %age component of measurement uncertainty because of zero and resolution in Table 5.9, while comparing with reported measurements in Table 5.7[116]. Further efforts are underway to improve the measurement uncertainty of the force devise with the purpose of their use as a portable force transfer standards, allowing the establishment of an unbroken chain of measurement traceability from national primary force standard machines to the

secondary level force calibration machines, for allowing the verification of material testing machines at user's site.

5.5. Summary

The chapter describes the procedure for fabrication and fixing of strain gauges to the spring sensing loading element of force devise. The force devise of rated capacity 5 kN, is fabricated. The force transducers are investigated for their metrological characterization as per standard calibration methods based on international/national standards like ISO-376:2004 / 2011 and IS-4169-88 reaffirmed 2003. Different contributing factors towards the measurement uncertainty of the force devises are discussed and method for their calculation has been discussed. The results have also been discussed. Also investigation regarding results of using of two strain gauges at each arm of a Wheatstone bridge, fixed at a location in series to improve the output sensitivity of force devise has also been discussed.

Chapter 6

Fabrication and performance evaluation of MEMS based diaphragm force sensor

6.1 Introduction

After the successful design of the MEMS device as discussed in previous chapters, now, it has to be realized practically through the development of a compatible fabrication technology. Although, several MEMS standard fabrication processes are already available, but they have to be redesigned and optimized to achieve the successful fabrication of the particular device [117]. Sometimes, an entirely new technology has to be evolved as per the requirement of the design. The realization of a device is always limited by technology because of the limitations in the availability of specific materials required for the device and their process ability: growth, deposition and patterning techniques. Therefore, the technology development is as important as the design of the device. The design of the device is always dependent on the technology. The design of the device has to be finalized in coordination with the technology. Most of the times, both, the design and the technology have to be extended beyond their current existing limits resulting into new ideas of design as well as that of the technology. The realization of the device with designed parameters is most important and the technology development acquires completion when device parameters and performance is achieved repeatedly and reliably.

Fabrication of Silicon diaphragm based force sensor requires stringent micromachining techniques in addition to the usual unit processes [118-122]. The device has been designed in chapters 3 and 4 and the device dimensions along with the dimensions of the different layers are summarized in Table 6.1 and further illustrated in figure 6.1.

Table 6.1 Device Parameters

S.No.	Parameter	Value
1	Chip size	2.2X2.2 mm ²
2	Thickness of Si substrate	0.625 mm
3	Thickness of bonded glass	0.7 mm
4	Total Chip thickness	1.325 mm
5	Diaphragm size and shape	1.4 mm Circular
6	Diaphragm thickness	50 micron
7	Depth of the cavity	575 micron

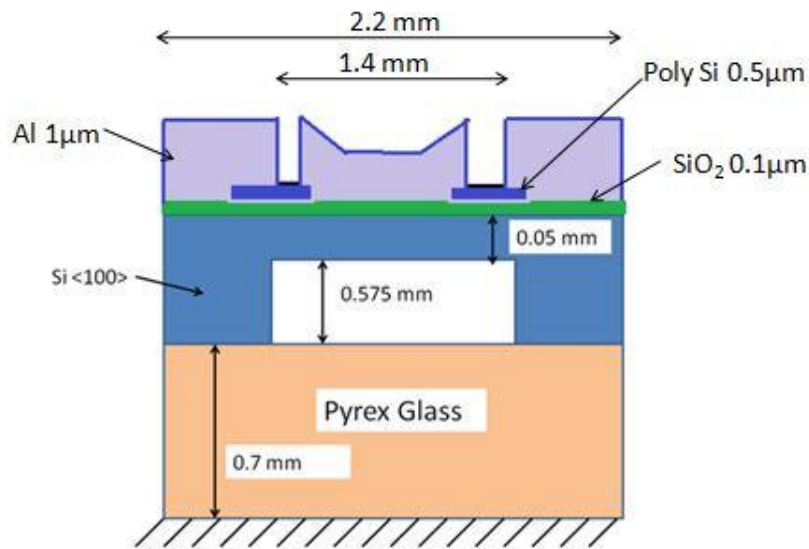


Fig. 6.1 : Block diagram of the cross-section of the device with different dimensions

6.2 Fabrication Approach

The fabrication approach has to be planned meticulously, as both of the MEMS subsystems, mechanical and electrical/electronic sub-systems have to be fabricated simultaneously to realize the device. For the current device, the fabrication technology is different from the general MEMS fabrication processes.

6.2.1 Selection of materials

Selection of materials for the device is very important. It covers the kind of materials [123-125] required for the fabrication of the device. As the force sensor utilizes the mechanical or rather structural properties of the Si diaphragm, it is important to choose the basic structural material for the device very carefully. The Si diaphragm is the basic sensing element which senses the force applied over it; therefore, it should have good elastic properties and simultaneously can be micro-machined using wet or dry etching techniques. For the current device, single crystal silicon (100) wafer was chosen as the substrate as it can be easily bulk micro machined with (111) bounded crystallographic planes in wet ODE (orientation dependent etching) processes based on KOH and TMAH or Dry Bulk Micromachining process[126]. In the current work, for the fabrication of silicon diaphragm we have chosen the dry bulk micromachining of silicon using DRIE technique. Although it is a bit costlier process but provides very precise control on the dimensions of the diaphragm, which is most important to achieve the designed parameters.

6.2.2 MEMS Fabrication Processes

As the Force Sensor is made of two sub systems: (i) Si diaphragm (micromechanical sub-system) and (ii) integrated Piezoresistors at the top of the diaphragm (microelectronic-sub system), one requires to have a fabrication technology which is capable to fabricate both the subsystems using a single substrate. For the fabrication of microelectronic-sub system, the whole VLSI technology is available, well developed and optimized through the last several decades starting with the invention of Integrated circuit by Jack Kilby in 1958 [127]. The micromachining technology to create micromechanical sub system has come up during the last couple of decades and the integration of the two subsystems in a single chip is a new challenge for which new techniques and approaches are taking place day by day. There is always a plenty of room for innovation, new techniques would keep on coming up for the fabrication of MEMS, particularly in the area of micromachining technology incorporating Si as well as non-Si materials. Since MEMS hold a promise to miniaturize the 3D systems and to fabricate multi-disciplinary chips involving biology, chemistry, physics, engineering and medicine, new technologies with combined disciplines is the requirement of the day. Consequently, the design and development of these multidisciplinary devices becomes a complicated task. Moreover, the technology should be able to cope up with the scaling down of the devices, which is a salient feature of MEMS [128]. The miniaturization is, however, limited by the technology. Therefore, development of the new technology compatible with the issues related to the miniaturization is most significant.

Now, the different materials layers required, and the technology to create structures or patterns in them is analyzed for the fabrication of the current device using Silicon-MEMS

technology. The different materials and material-layers can be grouped in the following two categories as given in Table 6.2.

Table 6.2 Different Material Layers

S. No.	Type of material	Details	Variation
1	Substrates	Single Crystal Si	N or P type
		SOI (silicon on insulator)	N or P type device as well as handle wafers
		Pyrex 7740 Glass	In different thickness
2	Materials to be grown or to be deposited	Semiconductors	Single crystal silicon, Polysilicon
		Dielectrics	SiO ₂ , SiN ₄
		Metals	Cr, Al and Au

The different techniques required to work with the above material layers can be grouped into four categories as shown in Table 6.3.

Table 6.3 Material Processing Techniques

S. No.	Type of technique	Details	Variations
1	Material Formation Techniques	PVD	Sputtering
		CVD	LPCVD, PECVD
		Growth	Thermal
		Spin on processes	Spin Coating of photoresists, SU-8
2	Materials Patterning techniques	Lithography	Optical, Laser direct write, E-Beam, X-Ray.
		Etching	Wet and dry etching
3	3D structure formation techniques	Micromachining 3D Printing	Surface Micromachining: Wet and Dry etching(RIE), UV LIGA 3D Printing
			Bulk Micromachining: Wet (KOH, TMAH) and Dry etching (DRIE)
4	Bonding Techniques	Wafer bonding	Anodic, Fusion, Eutectic
		Die bonding	
		Wire bonding	Wedge, Ball

For the successful technology development leading to the fabrication of a device, the basic unit processes have to be optimized to be compatible with the deposition and patterning of the different material layers, so that one can further develop a process compatible to the specific application. In the subsequent section the optimized unit processes for the fabrication of the Si diaphragm force sensor has been presented.

6.3 Materials chosen for the device

The different material layers chosen for the fabrication of the current device are tabulated in table 6.4 along with their salient features.

Table 6.4 Material Layers for the device

Sl. No.	Material layers	Purpose	Salient features
1.	<100> single crystal Si	Substrate	Excellent mechanical strength
2.	-do-	Diaphragm	Excellent elastic material
3.	-do-	Cavity walls	Good mechanical strength, different shapes possible
4.	Pyrex glass	Cavity sealing	Excellent bonding strength with Si
5.	SiO ₂	Masking layer, Electrical insulation, passivation	High quality insulator, mask against etching of Si, high quality passivation layer
6.	Polycrystalline Si	Piezoresisters	Good piezoresistive properties, controllable resistivity
7.	Al	Connecting lines	Highly conducting material

6.4 Mask details and layout

Mask layouts have to be generated for every material layer of the device. This is done with the layout software Tanner Tools LeditTM. The complete fabrication process has been designed to have five levels of masks. Layout for each layer was very precisely verified for the dimensions of every etch layer, alignment and registration marks. The Mask details have been tabulated in

table 6.5. The combined layout for all the layers is illustrated in Fig. 6.2. The fabrication of the masks was carried out on Heidelberg pattern generator tool at CSIR-CEERI, Pilani.

Table 6.5: Mask details

Device: Si Diaphragm Force Sensor					GDS File name:CEERI_FS_SR.gds	
Chip Size: 2.2mmX2.2mm		Grid 0.3mm	Total step and repeated Area: 110mmX110mm		Mask Plate Size: 6" X 6" X 0.09"	
Mask Id	Required Field	Name of the Layer	GDS-II No.	Function of the layer	Grid Open/Closed	Remarks
Mask# 1	Dark Field	Active	43	Poly Resistors	Opened	
Mask# 2	Bright Field	Poly	46	Si Diaphragm by DRIE process	Closed	Mirror Image Round y-axis; Reverse for mask making
Mask# 3	Dark Field	Metal 2	51	Contact Opening	Opened	Reverse for mask making
Mask# 4	Bright Field	Metal 1	49	Metal Interconnect and contact pads	Opened	
Mask# 5	Dark Field	Over-glass	52	Pad opening	Closed	Reverse for mask making

The snapshot of the mask layout of the force sensor showing the diaphragm, the polysilicon piezoresistors in Wheatstone bridge configuration, the connecting metal lines and the contact pads is shown in Fig. 6.2.

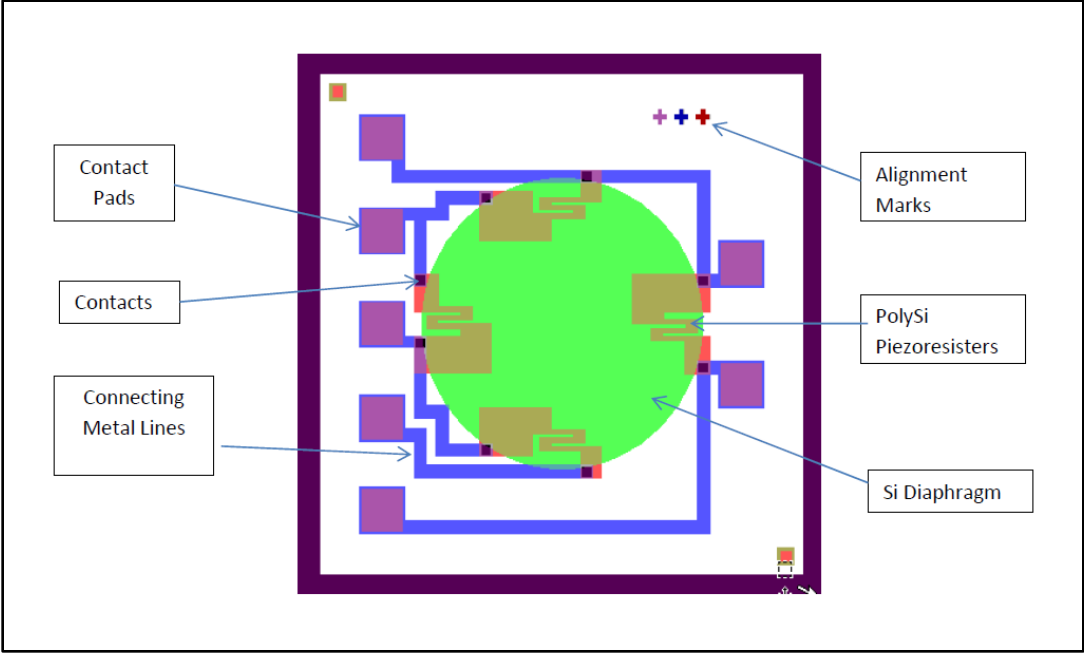


Fig. 6.2 Snapshot of the combined mask layout

6.5 Process flow chart

The process developed for the fabrication of force sensor has been tabulated in table 6.6. This table shows only the major processing steps whereas there are several minor processing steps in between these major steps which will be described appropriately. The illustrated process flow chart is shown in fig. 6.3. This work has been published in Vacuum [53].

Table 6.6 Development process of MEMS sensor

1.	Initial Wafer cleaning
2.	Wet Oxidation : 1µm thick
3.	Oxide etch: Front side

4.	Dry Oxidation 0.1 μ m
5.	Low Stress Polysilicon deposition 1.0 μ m LPCVD
6.	Polysilicon Phosphorous diffusion $R_s= 150 \Omega$
7.	Polysilicon Oxidation 0.1 μ m
8.	PolySi Anneal
9.	Photolithography-01 (Piezo-Resistor patterning) Mask 1
10.	RIE of polysilicon: Front side
11.	RIE of Polysilicon- Backside,blanket removal
12.	Photolithography-02 (diaphragm definition, Backside) Mask 2
13.	Oxide etching from diaphragm (Backside)
14.	Photolithography – 03 (contact) Mask 3
15.	Oxide etch for contact opening
16.	Al Sputtering
17.	Si Bulk Micromachining :DRIE of diaphragm
18.	Plasma cleaning
19.	Photolithography –04 (Interconnect) – Mask 4
20.	Cleaning (Blanket UV exposure +developer)
21.	Al- Sintering 450° C, 30 min, Forming Gas
22.	Deposition PECVD Oxide (Front side) 0.5 μ m
23.	Photolithography 05 (contact pad opening) Mask 5
24.	RIE of PECVD Oxide
25.	Cleaning (Plasma +)

26.	Anodic Bonding, (Silicon-Glass)
27.	Dicing
28.	Die bonding & wire bonding.
29.	Testing



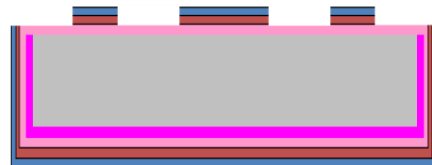
Oxidation (wet) 1.0 µm



Poly oxidation (0.1 µm)



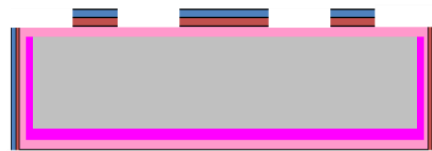
Front Side Oxide Etch (Blanket)



Polysilicon patterning (Mask 1)



Re-oxidation(dry) 0.5 micron



RIE of back side Poly (Blanket)



Low Stress Polysilicon Deposition (LPCVD)
and P diffusion



Oxide etching from back-side

(1)

(2)

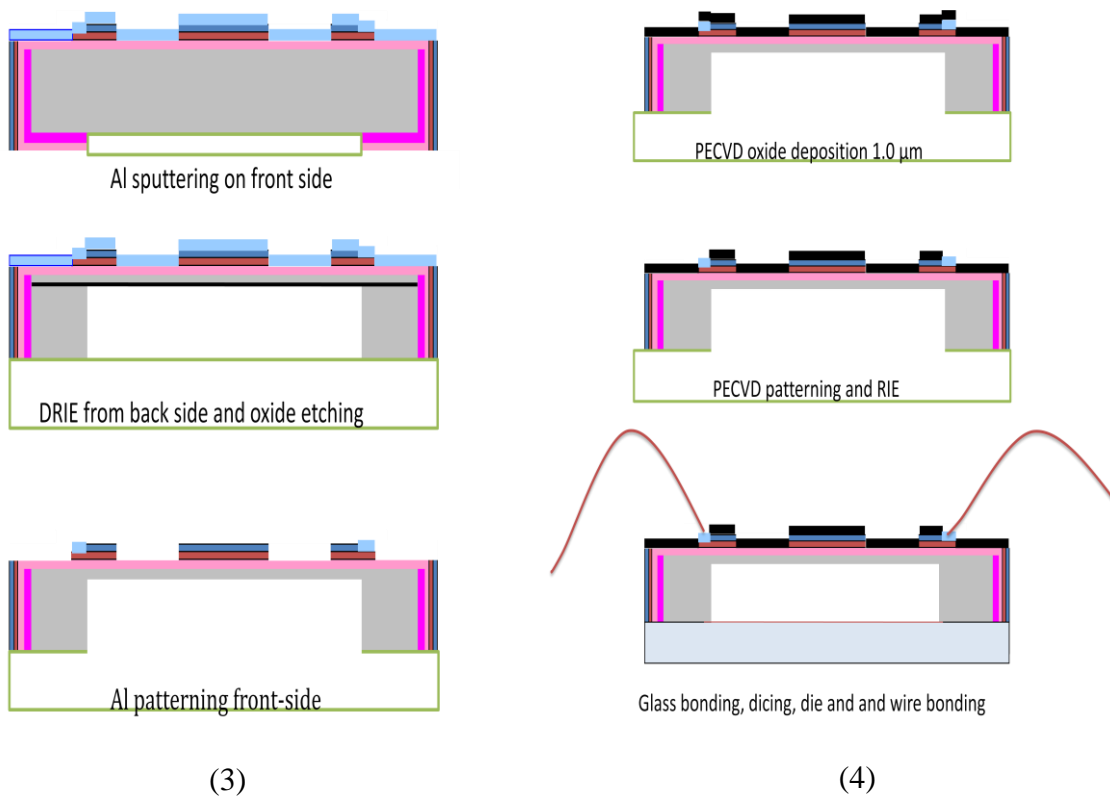


Fig.6.3 Process Flow Chart

6.6 Device fabrication

The fabrication of the device has been covered in the subsequent sections.

6.6.1 Wafer selection

As the fabrication of force sensors involve the fabrication of a Si diaphragm with an enclosed cavity, we need to close the cavity from the bottom side. We have to choose a substrate which could be very precisely etched from back side using DRIE technique. For this, we need

front to back alignment. Therefore, the front to back side alignment has to be taken up and to be implemented very precisely so that the piezoresistors are perfectly placed on the diaphragm.

In view of the above, N-type (100), 150 mm diameter wafer is chosen and we start with a batch of five wafers. The thickness of the wafers varies between 600 to 650 micron, we measure the thickness of a batch of 25 wafers using a dial guage or micrometer having a least count of 1 micron, and select 5 wafers having a thickness either exactly 625 micron or very close to it. The specifications of the wafers are tabulated in Table 6.7

Table 6.7 Wafer Specifications

S. No.	Parameter	Details
1	Type	CZ
2	Orientation	<100>
3	Size	150mm
4	Dopant	N Phos
5	Resistivity	5-7 Ω cm
6	Thickness	625 \pm 25 μ m
7	Flats	Two
8	Polishing	DSP(double side polished)

Device was fabricated starting with a batch of 5 number of 150 mm <100> single crystal silicon DSP prime wafers. The specifications of these wafers have been tabulated in table 6.7. These wafers were thoroughly cleaned using the initial wafer cleaning processes described in the following sections.

6.6.2 Silicon Wafer Cleaning Processes

In the present work a three-step process has been utilized for the cleaning of the silicon wafers in the beginning of the process. At subsequent stages only a couple of them have been utilized as per requirement.

Step 1: Degreasing

Dip the wafers in hot trichloethylene (TCE) for 5 minutes followed by a dip in methyl alcohol and then acetone along with an ultrasonic agitation treatment for 2 minutes each. Wash the wafers thoroughly in deionized (DI) water.

This step removes most of impurities.

Step 2: RCA Cleaning in Solution 1

The wafers are now dipped in an oxidizing solution consisting of:

1:1:5 volumes of NH_4OH : H_2O_2 : H_2O at $70\text{-}80^\circ\text{C}$ for 10 minutes.

It removes almost all of the organic impurities left after the step 1 above, through their oxidation into volatile or soluble compounds. The problem is that it also oxidizes the Si surface. This thin layer of SiO_2 over Si is etched out through a 10-20 second dip in $\text{HF} + \text{H}_2\text{O}$ (1: 50 by volume).

The wafers are now thoroughly rinsed in DI water.

Step 3: RCA Cleaning in Solution 2

The wafers are now dipped in another solution consisting of

5:1:1 volumes of H_2O : H_2O_2 : HCl at 80°C for 10 minutes.

This solution takes care of the inorganic impurities and converts them into soluble chlorides.

We have also used two more cleaning processes which have been utilized either for silicon as well as glass wafer cleaning or cleaning of the photo-masks at different fabrication steps.

1. Piranha cleaning
2. Boiling nitric acid

6.6.3 Piranha and Nitric Acid cleaning

Piranha cleaning is one of the most popular cleaning process. It is a combination of sulphuric acid (H_2SO_4) and hydrogen peroxide (H_2O_2). This solution is heated at temperatures 80°C to 120°C to carry out the cleaning efficiently. The composition varies from 50:1 to about 3:1. At the higher hydrogen peroxide concentrations, the mixture is self heating. The mixture has a short self life, as the hydrogen peroxide, which decomposes very fast. Therefore, it needs to be used shortly after mixing. It is a highly oxidizing solution resulting in the growth of a thin native oxide film over the silicon surface. Therefore, a subsequent dip in dilute HF: H_2O in the ratio of 1:50 is necessary. Photo masks often contain traces of photo resist either at the initial stage after the etching of chrome layer or during the subsequent steps when the traces of photo resist from the wafer during contact printing get onto the mask. The mask plate is cleaned in piranha; a great care has to be taken as there is a possibility of breaking of the mask due to the evolution of heat. For this kind of cleaning of Masks a dilute solution of 5:1 ratio of H_2SO_4 : H_2O_2 was used. Another composition of 3:1 ratio for the cleaning of the wafers at certain steps of fabrication of the two devices has been used.

Another cleaning solution is Nitric Acid (HNO_3). It is heated at 110°C and is a strong oxidizing agent. Therefore, again a dilute HF dip is necessary after the cleaning process. The

wafers are thoroughly washed in DI water and then loaded into a running DI water tank till the resistivity of the DI water approaches 12 M Ohm Cm. The wafers are now perfectly clean and can be transported to the next processing port.

During this cleaning step the following precautions have been observed:

1. All the glass wares used in the cleaning process must be thoroughly cleaned in chromic acid and rinsed in DI water.
2. The inside surfaces of the beakers and the tweezers should never be touched with bare hands.
3. Quartz beakers and wafer carriers should be used.
4. For HF dip, Teflon beakers and wafer carriers should be used.

Chemical cleaning is carried out in a specialty chemical bench having special arrangement of continuous evacuation of the chemical fumes, especially acid fumes, through a powerful exhaust, quartz etch tanks with temperature control, as illustrated in Fig. 6.3.



Fig. 6.4 Specialty Chemical Bench for cleaning (RCA cleaning in progress)

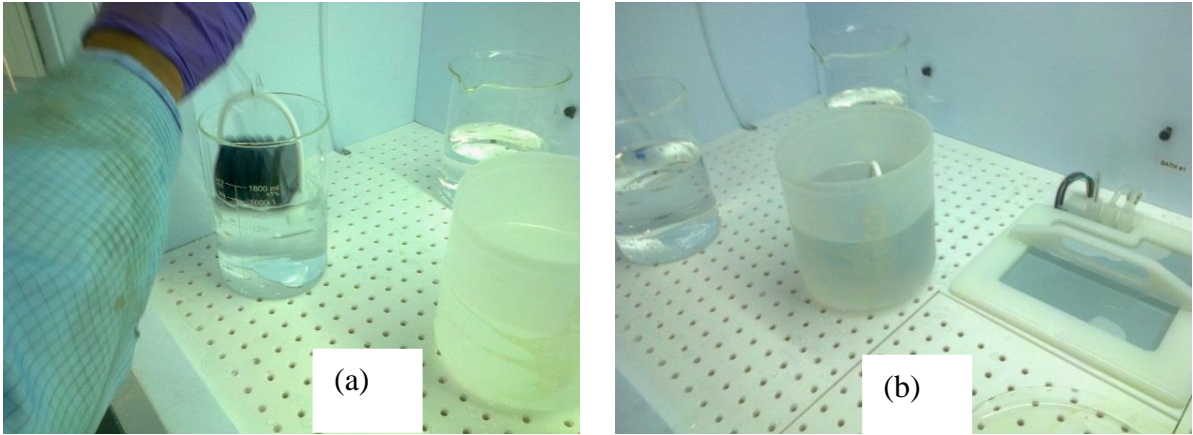


Fig. 6.5 (a) Wafer cleaning in Piranha. (b) Removal of native oxide in dilute HF

After the thorough cleaning of the wafers the next step is the thermal oxidation. It deposits a uniform layer of 1.0 Micron oxide on all surfaces of the wafers. It is described in the next section.

6.6.4 Thermal oxidation

Oxidation of silicon is one of the most significant process in the fabrication of integrated circuits as well as MEMS. It is the oxide of silicon which has made possible the revolutionary development of VLSICs, simply because of its well controlled patterning and growth techniques for repeatable high quality dielectric. This oxide has two important applications in the current device as:

- (i) Masking layer in DRIE of silicon for the fabrication of the Si diaphragm.
- (ii) Dielectric isolation layer between the substrate and the conducting layers in the device, e.g. polysilicon, Al lines and electrodes.

For the above two applications the desired properties of SiO₂ have to be different. For masking purposes, it should be free from the pin holes and should have a high selectivity against the etching medium. For dielectric isolation, it should have a high dielectric constant as well as high break down. The biggest advantage with the oxide is its simplicity of growth technique as well as the patterning. Several techniques for its growth and deposition have been developed and are in use. These techniques are:

- (i) Thermal oxidation (including rapid thermal techniques)
- (ii) Vapour phase technique – CVD (chemical vapour deposition)
- (iii) Plasma enhanced chemical vapour deposition (PECVD).

Although the growth or deposition techniques are well known, still one requires developing and characterising the process for a particular process for specific applications.

For the current work, two types of oxidation processes have been used:

- (i) Dry oxidation
- (ii) Wet oxidation; and

Dry oxidation process provides a better quality oxide which is used as isolation between the piezoresistors and the Si substrate. Wet oxidation provides a fast growth of SiO₂ useful for masking in DRIE process.

The first major fabrication step is that of the growth of the thick oxide 1.0 micron. It was grown through the wet oxidation process. This process is carried out in MRL Bandit Furnace model SBR 1503, Fig. 6.5. The temperature of the furnace is ramped up at a rate of 4⁰C/min. The wafers were loaded in the furnace. A dry-wet-dry oxidation at 1000⁰C was carried out as per the schedule in Table: 6.8.

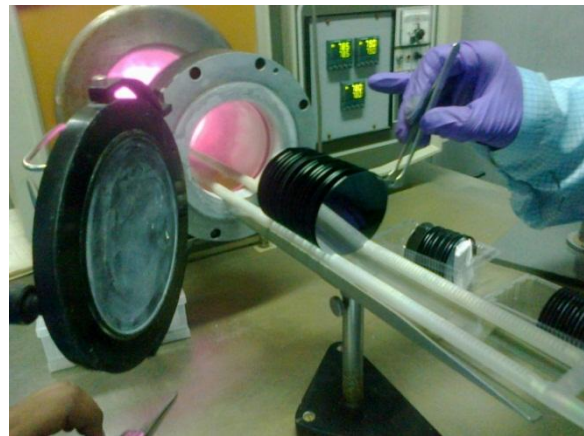
Table: 6.8 Oxidation process Schedule

Parameter	Dry	Wet	Dry
Flow rate of O ₂ (SLPM)	6.5	1.0	6.5
Temperature (°C)	1000	1000	1000
Time (min)	20	520	20
Bubbler Temp. (°C)	95	95	95

After the completion of the oxidation process the temperature of the furnace was ramped down at the rate of 7⁰C/min. With a nitrogen flow of 400 SCCM to a temperature of 400⁰C. Wafers are taken out. We obtain a violet-green colour of the oxide.



(a) Furnace with different tubes



(b) Loading of wafers

Fig.6.6 MRL Oxidation furnace Model SBR 1503 used in this work

Process steps:

- (i) Wafer cleaning: Wafers are thoroughly cleaned (as per cleaning steps in section 1) before loading into the oxidation furnace. There should not be any water sticking to the wafer surface.
- (ii) The oxidation furnace shown in Fig. 6.5 is having a large uniform temperature zone. It is set at a particular desired temperature (say 1000⁰C). The bubbler is also kept ready well before the loading of the wafers. Dry N₂ is made to flow through the furnace for a minimum of half an hour before actual loading.
- (iii) Wafers are now loaded carefully on the carrier boat and kept at the furnace tube end for something around 5 minutes so that the sticking water is completely evaporated.
- (iv) The carrier boat is now pushed in at a very slow speed to avoid thermal stress they are left for sometime at the zone interface and then again slowly pushed to the centre of the furnace, which is also the centre of the quartz tube.
- (v) Now a specified gas flow sequence is utilized.
- (vi) At the end of the process, slow pull-out is a must to avoid thermal stresses.
- (vii) The thickness of the grown oxide is now measured using surface profiler Dektak 6M.

6.6.5 Growth of Quality Oxide for electrical isolation of Piezoresistors

After the thick oxidation of the silicon, the next step is the removal of the oxide from the front side of the wafer. The oxide on the back side of the wafers is retained while the oxide on the front side is removed only to grow a quality oxide on the top surface to isolate the piezoresistors to be fabricated in the coming steps, from the substrate surface. For this, the back side of the wafers is coated with positive photoresist, baked at 120°C for half an hour and then they are dipped in buffer HF (BHF). The oxidelayar from the front side is etched out in BHF.

The wafers are then thoroughly cleaned using the RCA cleaning process described earlier. Oxidation of the wafers was carried out again in MRL oxidation furnace using a dry oxidation process to grow a dry oxide of 0.1 Micron.

6.6.6 Polysilicon Deposition for Piezoresistors

Now, a polysilicon layer was deposited over dry 0.1 micron SiO_2 . This layer is used for piezoresistive sensing. The thickness of thin layer has again taken to be 1.0 micron low-stress layer. This low stress polysilicon deposition process was optimized through the variation in process parameters using an automated LPCVD reactor from M/s SEMCO Engineering, France. The wafers can be directly loaded into LPCVD reactor immediately after unloading them from oxidation furnace. The process details are given in Table 6.9. The thickness of the polysilicon has to be critically controlled to 1.0 micron as the deviation in thickness will change the device characteristics. Thickness monitoring is done through a trial run in which polysilicon is deposited on a dummy wafer. It is characterised for the thickness obtained through the thickness measurement using DEKTEK 6M surface profiler. Polysilicon is deposited on the planar wafers in a subsequent process with necessary correction in time of deposition.

Table 6.9 Optimized Process for LPCVD Low Stress Polysilicon

Type of film : Low-stress Poly Si			
S.No.	Process parameter	Unit	Value
1	Deposition Temperature	^o C	590
2	Deposition Pressure	mTorr	250
3	SiH ₄ flow rate front end	SCCM	80
4	SiH ₄ flow rate back end	SCCM	90
5	Deposition rate	nm/min.	37.7
6	Thickness uniformity	%	~10

6.6.7 Phosphorous Diffusion in Polysilicon

After deposition of low stress polysilicon, we have to go for P diffusion in order to make the polysilicon. As the polysilicon cantilevers have to act as one plate of the capacitor, they have to be more or less conducting. P diffusion is carried out in MRL Bandit Oxidation diffusion furnace Model No.SBR 1503 tube number 4. The details of the process parameters are tabulated in Table 6.10.

Table 6.10 Process Parameters for P-Diffusion

Process Type	P Diffusion
Process Temperature	1000 ⁰ C
Ramp up rate	4 ⁰ C/min. with N ₂ flow
Ramp down rate	7 ⁰ C/min. with N ₂ flow
Actual process time	15 min.
N ₂ flow rate	150 SCCM
O ₂ flow rate	800 SCCM
Sheet resistance obtained	150Ωcm
P Diffusion Source	Liquid Source POCl ₃ at 26 ⁰ C

During phosphorous diffusion an oxide layer is formed which is removed in BHF before the measurement for sheet resistivity using a four point probe.

6.6.8 Polysilicon Oxidation and Annealing

Oxidation of polysilicon is carried out at 1000⁰C for 30 minutes in MRL furnace. It results in the redistribution of the dopant concentration there by a slight decrease in sheet resistance. In this process a thin layer of silicon dioxide grows over the polysilicon which acts as a pad layer for the subsequent silicon nitride. This process anneals out the residual stress to a minimum value.

6.6.9 Polysilicon patterning and formation of piezoresistors

The next step is to pattern the polysilicon and to form the piezoresistors. Lithography using mask number 1 is carried out.

6.6.10 Photolithography: Mask-1

Immediately after the polySi oxidation, we go for lithography. First, a positive resist Microposit™ S1818 from M/s Shipley is coated on the wafer using a DELTA 80BM Spin Coater Model No.AK200 from M/s SussMicrotech Lithography, GmbH, and Fig.6.6. The coating recipe no.7 was used for photoresist coating as it provides an appropriate thickness of the photoresist. After coating the photoresist it was dehydrated (pre-baked) at 90°C for 30 minutes in the bake oven to evaporate the solvent in the resist. After prebake, we go for the exposure using SussMicrotech Mask Aligner, Model MAG, Fig. 6.7 and Mask No.1. The layout of the pattern is shown in the fig.6.2 in red colour. Exposure was optimized on 2 dummy wafers coated with photoresist through the same procedure. After the exposure the photoresist was developed in the developer MF 312 CD-27 Microposit from M/s Shipley followed by fixing in DI water for 60 seconds.

Wafer is thoroughly rinsed with DI water and dried up using a nitrogen gun. Post baking of the photoresist is carried out at 120°C for 30 minutes in the bake oven. After post bake wafers are taken out of the oven and kept in class 100 clean air station to cool down to room temperature. Each wafer is inspected under microscope for any kind of defect in the pattern, if there is any fault like pin holes, shifted patterns, photoresist lumps etc., the cause of the fault is fixed up and corrective action is taken and, if necessary, photoresist is removed from that particular wafer having a fault. It is cleaned and rooted once again to photolithography process.

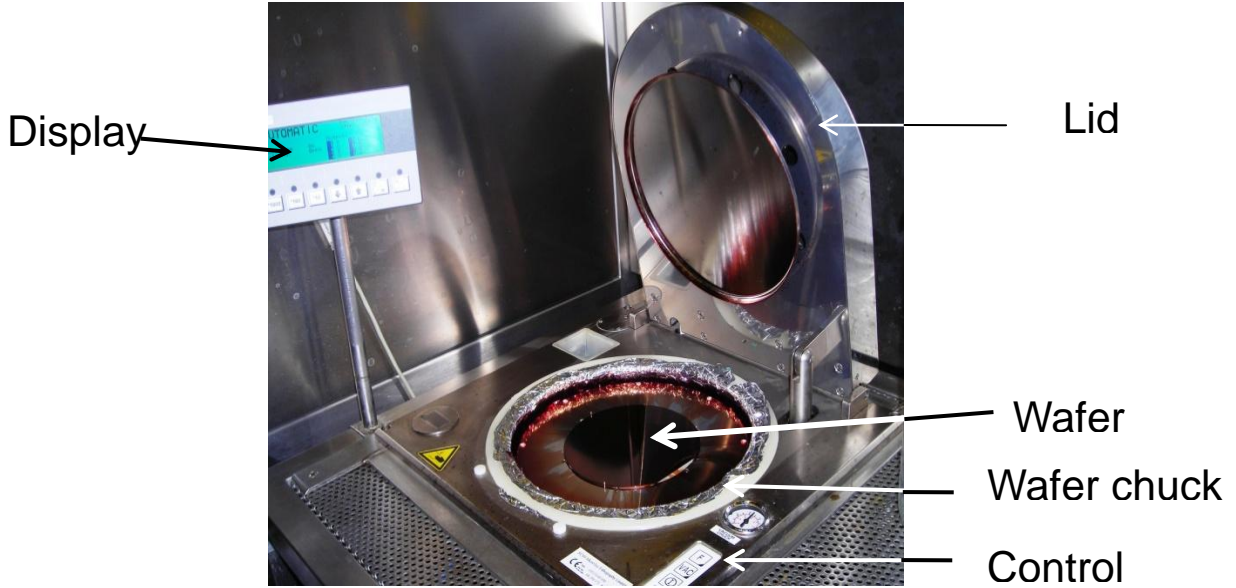


Fig. 6.7 DELTA 80 BM Spin Coater used in the present work

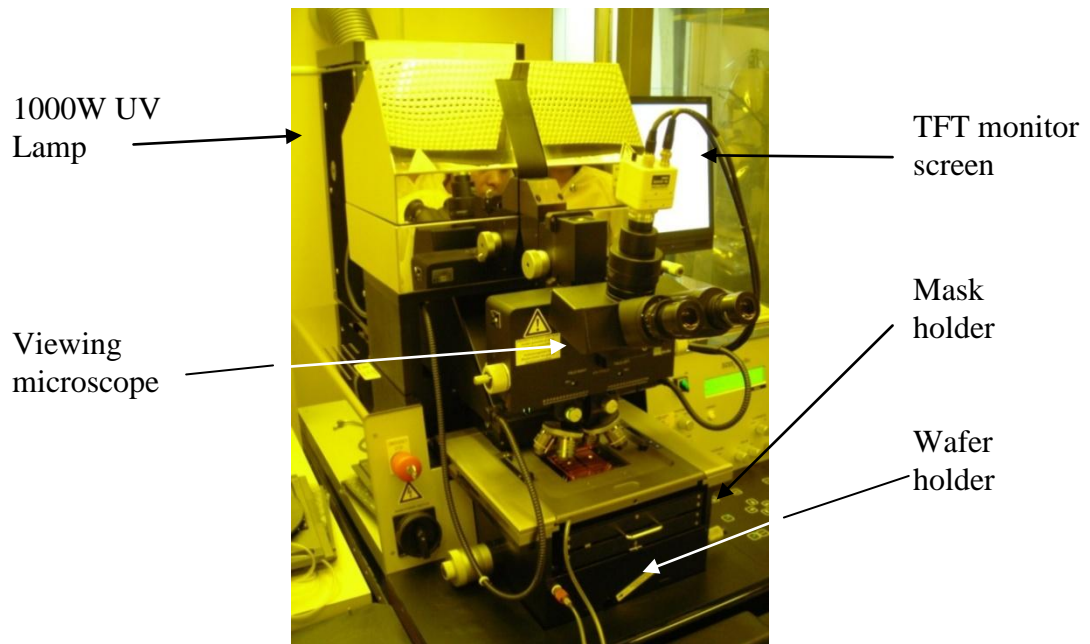


Fig.6.8 SUSS MA6 Mask Aligner used in the present work

6.6.11 RIE of PolySi

The wafers are now ready for PolySi etching. Etching of the polysilicon has been done in RIE tool 320 PC STS RIE system, Fig.6.8. Here we need an anisotropic low undercut RIE process for the etching of polysilicon. To achieve this extensive experimentation was carried out and a recipe based on CCl_2F_2 plasma has been characterized.

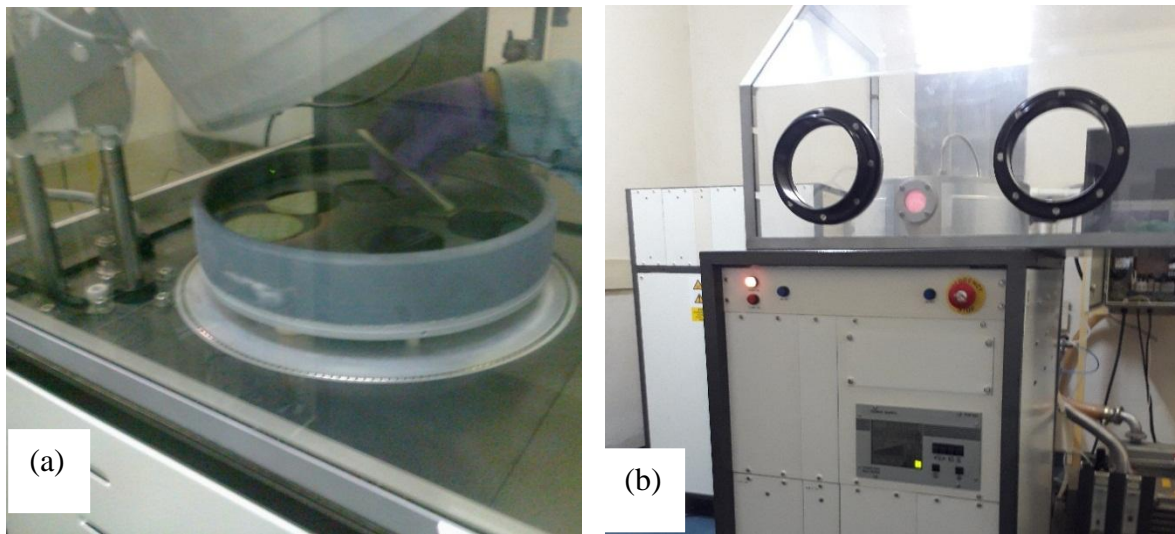


Fig. 6.9(a) Wafers loading in RIE machine (b) Plasma etching during process.

6.6.12 Oxide etching for Diaphragm

The polySilicon deposited on the back side of the wafers is removed by a high etch rate blanket RIE process.

After removal of polycrystalline silicon from the back side of the wafers, patterning of the thick oxide from back side for the etching of diaphragm is carried out. For this, lithography on the backside of the wafer through back side alignment (BSA) using mask number 2 was carried out. Consequently, circular windows in the positive resist are opened.

For etching of silicon dioxide up to the thickness of one micron, we have used BHF (buffered hydrofluoric acid). BHF is commercially available. It can also be prepared by mixing Ammonium Fluoride and HF in volume ratio of 6:1 respectively. For the etching of SiO₂ in BHF following reaction takes place:



At room temperature the etch rate is approximately 1000 Å/min. For an oxide of one micron thickness, it takes roughly 10 minutes. One has to take an extreme care while etching with BHF, it is extremely corrosive, and moreover no glass beakers should be used as it etches glass. Polyethylene or teflon beakers have to be used. Specialty chemical bench, Fig. 6.3, is used for this purpose. Photoresist is now removed from the wafers thoroughly followed by acid cleaning.

6.6.13 PECVD oxide deposition

After the patterning of oxide for the diaphragm is over, the wafers are thoroughly cleaned and then a 0.2 micron silicon dioxide was deposited using PECVD process tool from M/s Plasma Lab, U.K. It consists of a cylindrical vacuum chamber with high speed vacuum pumping station and having parallel plate electrodes.

Heating of the substrate is accomplished by means of resistance heated system mounted under substrate holder. The temperature of the substrate holder is measured by a K-type thermocouple. The top electrode which is made of Aluminum is water cooled. The power to the electrode is supplied by a 13.56 MHz R.F. generator. The exhaust gases from the pump are passed through water scrubber before being thrown out in the atmosphere.

6.6.14 Contact opening in PECVD oxide

Next step is the opening of contact holes in PECVD oxide so that the contacts from the polySi piezoresistors may be taken out. For this, lithography was carried out using Mask No. 3. Subsequently, the etching of PECVD oxide was carried out through RIE process.

6.6.15 Metalisation

After opening the contact holes in the oxide, the photoresist was removed and wafers were thoroughly cleaned. Then the wafers were loaded in Magnetron Aluminium sputtering system. An aluminium layer of 1.0 micron thickness is deposited.

6.6.16 Formation of Si Diaphragm

After the metallization with aluminium, we proceed to the formation of silicon diaphragm. It is done through Bulk micro-machining of Si from backside of the wafer using DRIE technique. Aluminium coated surface of the wafer acts as a conducting surface and helps in clamping of the wafer to the wafer chuck of the DRIE tool through electrostatic clamping. Therefore, Aluminium patterning is done after the fabrication of the Silicon diaphragm.

Now, the wafers are loaded in DRIE machine for the dry bulk micromachining of silicon from the back side. The circular opening in the oxide mask as already been done earlier. Silicon is etched through 575 microns in a number of process steps, initially using High Etch Rate (HER) recipes, Table 6.11, but at a later stage switching between HAR processes, Table 6.13, to obtain a 50 Micron thick Silicon diaphragm. After every DRIE process, the depth of the diaphragm was measured with the help of a DEKTEK Surface Profiler shown in Fig.6.9.

Fig.6.10 (a) is the block diagram of the DRIE tool, Fig.6.10 (b) is a schematic of the different blocks. The DRIE process parameters are tabulated in Table 6.11

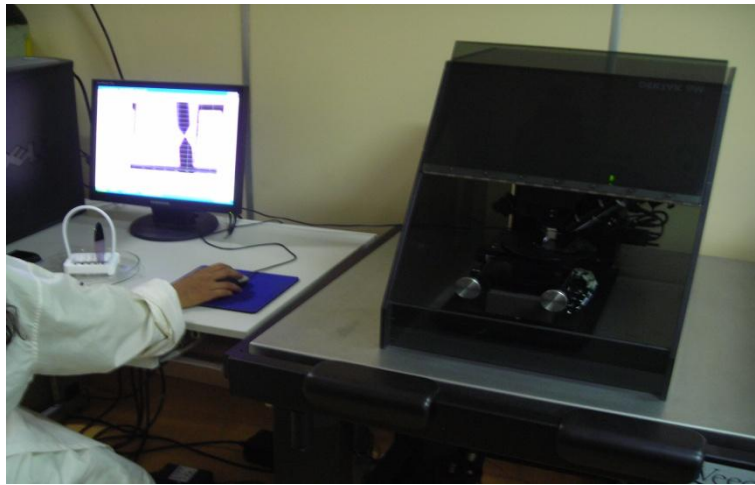
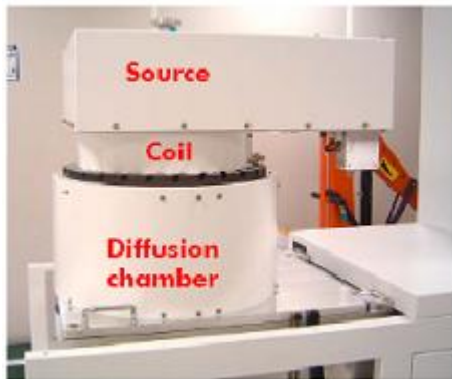
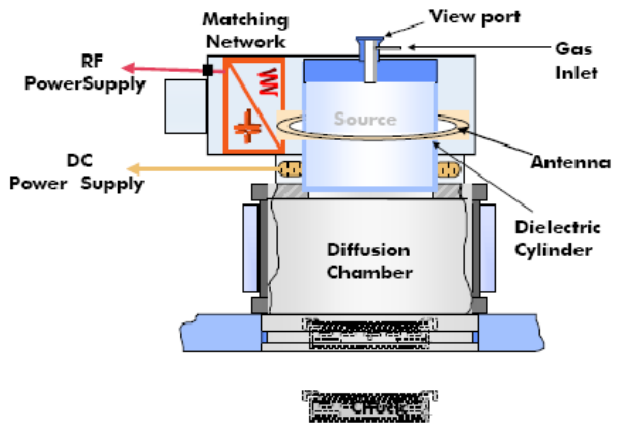


Fig.6.10 DEKTEK Surface Profiler: Measurement of Etch Depth of Si



(a) Reactor Chamber



(b) Schematic: different blocks

Fig. 6.11 AMS 100 DRIE Tool (Alcatel Micro Machining System)

Table 6.11 HER Process Recipe

S.No.	Process Parameters	Unit	Value
1.	Source Power	W	2800
2.	SF ₆ Flow	SCCM	700
3.	SF ₆ pulse	s	7
4.	SF ₆ pressure	Pa	10
5.	C ₄ F ₈ Flow	SCCM	300
6.	C ₄ F ₈ Pulse	s	3
7.	C ₄ F ₈ Pressure	Pa	7
8.	Platen Power	W	110
9.	He Pressure	mb	20
10.	ESC Voltage	V	1500
11.	ESC Time Switch	s	0
12.	SH Position	Mm	200
13.	Process limit	Min.	20

Table-6.12 Process Results

S.No.		Unit	Average Value
1.	Etch Rate	Micron/min	10
2.	Etch uniformity	%	<±3
3.	Selectivity to oxide mask		>400
4.	Selectivity to PR mask		> 90

Table 6.13 HAR Process Recipe

S.No.	Process parameters	Unit	Value
1	Source Power	W	2000
2	SF ₆ Flow	SCCM	300
3	SF ₆ pulse	s	3
4	SF ₆ pressure	Pa	4
5	C ₄ F ₈ Flow	SCCM	250
6	C ₄ F ₈ Pulse	s	2
7	C ₄ F ₈ Pressure	Pa	3
8	Platen Power	W	60
9	He Pressure	mb	20
10	ESC Voltage	V	1500
11	ESC Time Switch	s	0
12	SH Position	mm	200
13	Process time	Min.	20.5

Table-6.14 Process Results

S.No.		Unit	Average Value
1	Etch Rate	Micron/min	2.8
2	Etch uniformity	%	>±2
3	Selectivity to oxide mask		~90
4	Profile Angle	Degree	89.75°

The SEM micrographs of the etched cavity and Si diaphragm are shown in Fig. 6.11.

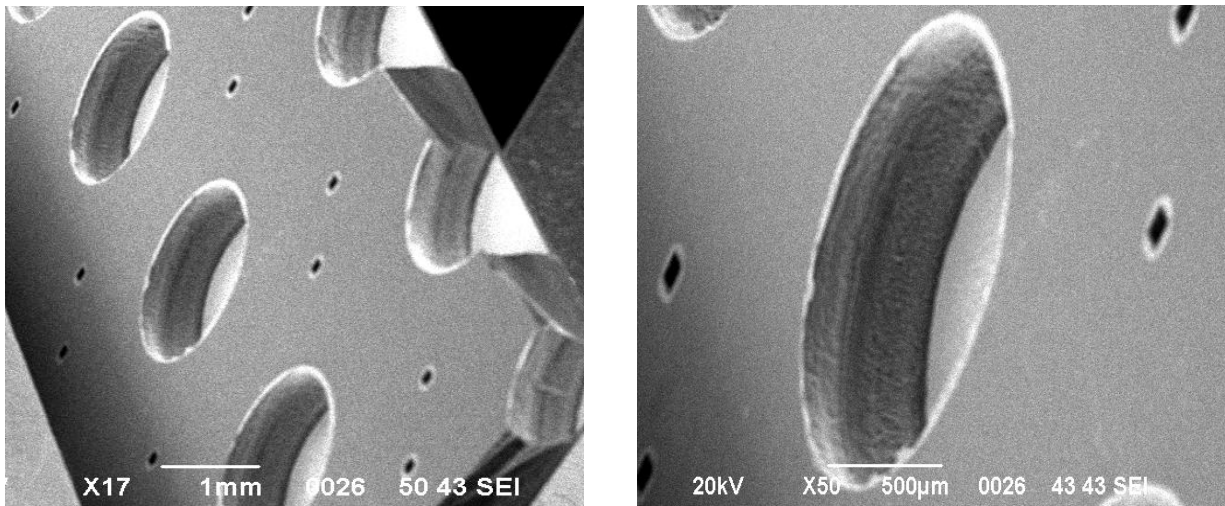


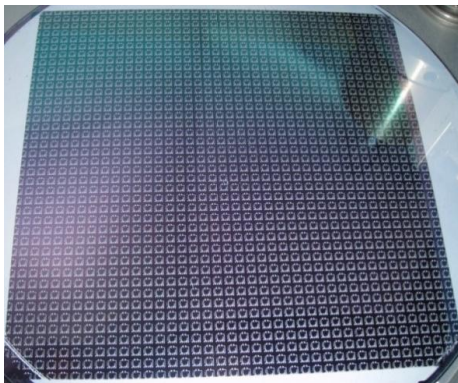
Fig. 6.12 Si Circular Diaphragm with cavity etched from backside of the wafer using DRIE

6.6.17 Patterning of Aluminum

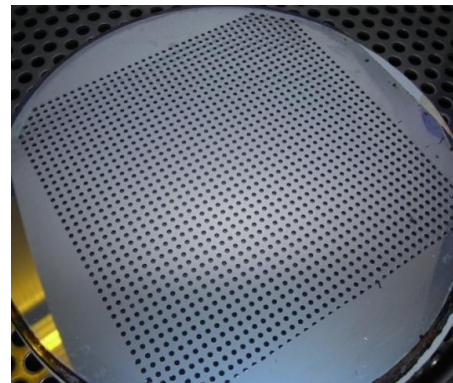
After the fabrication of Si diaphragm, patterning of the Al at the front side of the wafers is carried out. Lithography using Mask No.4 was carried out. The subsequent etching of Al is carried out in hot H_3PO_4 .

After the etching of aluminum, photoresist is removed with acetone. A blanket exposure of the deep UV light for 30 second is given to the wafers using the Mask Aligner MA-6 and the photoresist residues are dissolved in the developer. As the next step is the aluminum sintering, no organic (photoresist) should be left on the wafers. Sintering of the aluminum has been done in MRL Bandit furnace at $450^{\circ}C$ in forming gas ambient. The process makes aluminum more stable and mechanically strong.

After the patterning of Aluminum is over, a passivation layer of PECVD Silicon dioxide of thickness 0.5 Micron is deposited. The purpose of this passivation is to protect all the layers over the device. In order to take the contacts of the device to the outer world we have to open the contact pads for this, we go for lithography mask number 5. It is followed by RIE of silicon dioxide. The contact pads are now open. The processing of the Silicon wafers for the device fabrication is now complete. The top side of the wafer consists of an array of diaphragm with piezoresistors over it, connected in Wheatstone bridge configuration along with the connecting Aluminum lines and contact pads placed at the periphery of the device, Fig.6.12(a). The back side of the wafers contains an array of circular cavity of 1400 Micron in diameter and depth of 575 microns, Fig.6.12 (b). This cavity now needs to be closed.



(a) Top side array of the device



(b) Back side array of the Si cavity

Fig. 6.13 Fully processed 150 mm Si wafer

6.6.18 Anodic Bonding with Pyrex Glass

To close the Si cavity, anodic bonding with a glass wafer of the same size and thickness 0.7mm was carried out with the Silicon wafer.

6.6.19 Dicing of the Fabricated Chips

After bonding of glass wafer with silicon wafer we go for dicing. It is done using a double spindle dicing machine model DFD 6450 from M/s Disco, Japan. The glass side is kept down and silicon side is kept up. The dies are cut along grid line. The step size is 2.4 mm in both X as well Y direction.

The diced chips were then thoroughly cleaned. Fig.6.13 shows the diced chips, front and back side.

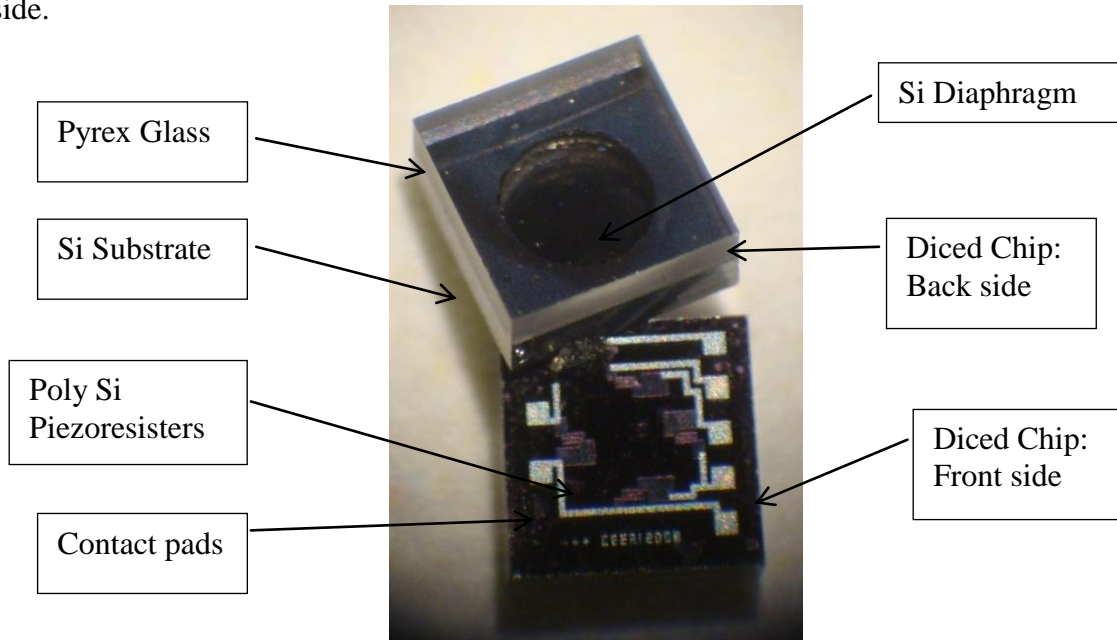


Fig. 6.14 Diced Chips: Si Force Sensor

6.7 Packaging of the Device

The cleaned devices were initially tested individually under a variable force indenter. Although, some of the devices could be tested successfully, but being an improper way, most of the devices were damaged. Therefore, a procedure for testing of these devices was evolved out which required proper packaging of the device. For this task, a printed circuit board (PCB), as shown in figure 6.14 was designed and fabricated. The device was glued to the PCB and contact pads were wire-bonded with the connecting pads of the PCB, fig. 6.15. The bonding

wires are very fragile and hence they are covered with an epoxy, very carefully, so that the Silicon diaphragm remains open as shown in figure 6.16.

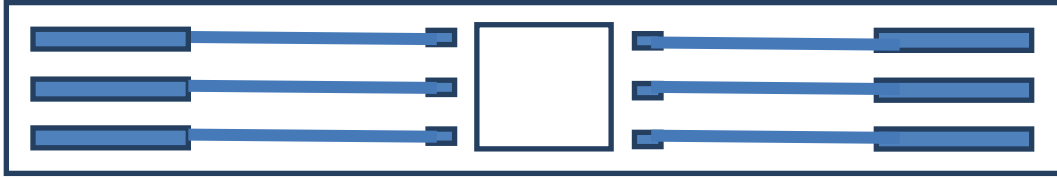


Fig.6.15 PCB Layout for packaging of Force Sensor

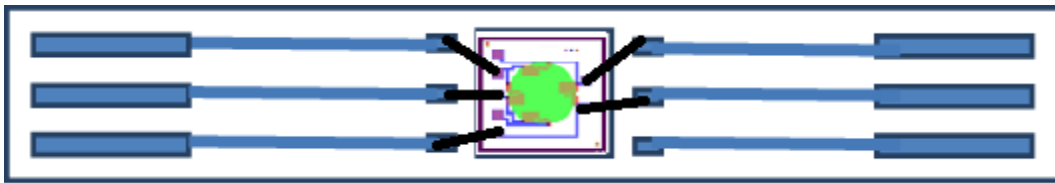


Fig.6.16 PCB Layout with Force Sensor image



Fig.6.17 Force Sensor packaged on PCB and packed cover with epoxy with open diaphragm

The device is now fully packaged and ready for metrological characterization and testing.

6.8 Investigations of a of Silicon diaphragm for Metrological characteristics

A dedicated investigational calibration setup is developed for metrological characterization of Silicon diaphragm force transducers from 10 Newton to 50 Newton force ranges at an equal force step of 10 N. Three sets of calibration series are observed from (10 N to 50 N) for each Silicon force sensor developed (figure 6.17). A digital indicator of high resolution has been used for observing the output readings on an excitation voltage of 1 Volt. A special

frame designed for loading and unloading of weights. For the experiment three force chips were selected from a batch for metrological investigations, calibrated weights of uncertainty better than $\pm 0.01\%$ at ($k=2$)

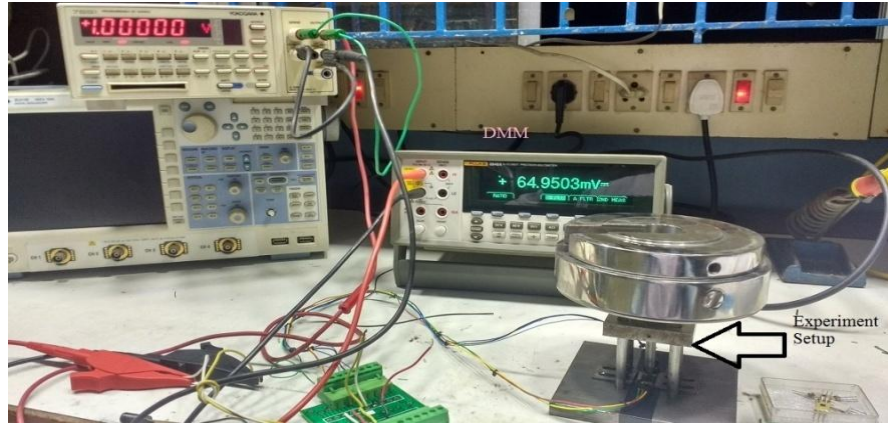


Fig.6.18 Experimental setup for MEMS force sensor

The various applicable uncertainty components considered for measurement uncertainty components and their calculation for MEMS silicon force sensor is mentioned in the table 6.15, 6.16 given below and the calculated uncertainty budget depicted in the table 6.17.

Table 6.15 Associated uncertainty components along with their relative (%) contribution

Sl. No.	Relative Uncertainty Component	Probability Distribution, Type of Error	Estimated Relative Variances of Input Quantities
1	Repeatability	Rectangular, type B	$w_{\text{rep}} = a^2 / 3$
2	Zero offset	Rectangular, type B	$w_{\text{zer}} = a^2 / 3$
3	Resolution	Rectangular, type B	$w_{\text{res}} = a^2 / 3$

Table 6.16 Different factors pertaining to metrological characterization with uncertainty of measurement of MEMS force sensor

Applied Force (N)	%age deviation due to uncertainty components				Measurement uncertainty (%) at $(k=2)$
	Zero offset error (2a)	Repeatability error (2a)	Resolution error (2a)	Uncertainty associated with the calibrated weights W_{REF}	
10	0.00534	0.3825	0.021	0.010	0.22
20	0.00534	0.1253	0.011	0.010	0.07
30	0.00534	0.1654	0.007	0.010	0.10
40	0.00534	0.0390	0.007	0.010	0.03
50	0.00534	0.0534	0.005	0.010	0.03

**Table 6.17 Maximum Measurement Uncertainty budget (%) of MEMS silicon force sensor at
10 N**

Source of Uncertainty	Estimate X1 (2a)	Limits ± X1 (a)	Probability Distribution / Divisor	Standard Uncertainty	Sensitivity Coefficient (ci)	Uncertainty Contribution	Degree of Freedom
Repeatability	0.38	0.19	Rectangular/ √3	0.11	1.0	0.11	∞
Zero offset	0.005	0.003	Rectangular/ √3	0.0015	1.0	0.0015	∞
Resolution	0.02	0.011	Rectangular/ √3	0.006	1.0	0.006	∞
Relative combined standard Uncertainty)						0.11	
$w_c(tra) = \sqrt{(w_{rep}^2 + w_{rpr}^2 + w_{int}^2 + w_{rev}^2 + w_{zer}^2 + w_{res}^2)}$							
Relative expanded uncertainty, $W_{(tra)} = k \cdot w_c(tra)$						0.22	
W_{REF}						0.01	
Relative uncertainty of measurement, $W = \sqrt{(W_{tra}^2 + W_{REF}^2)}$						0.22	

The metrological investigation revealed the maximum measurement uncertainty is found to be less than 0.25% at 10 N force step as depicted in table 6.16 for which the uncertainty budget is presented in table 6.17, for MEMS based transducer[106]. Further, uncertainty of MEMS based transducer can be reduced by appropriate change in mechanical experimental setup.

6.9 Summary

The chapter describes the detailed procedure for fabrication of silicon diaphragm and developing of piezoresistors on the spring sensing silicon diaphragm loading element of force sensor. The force sensor of rated capacity 50 N is fabricated. The force sensor is investigated for its metrological characterization as per standard calibration procedures. Applicable uncertainty contributing factors as discussed in the previous chapters have been considered to evaluate the overall measurement uncertainty of the force sensor.

Chapter 7

Conclusion and Future Scope of Work

7.1 Introduction

This chapter bestirs to talk about the significant characteristics of the investigative completed job. The chapter briefs the main accomplishment of the investigation over and above the foremost achievement of investigation in requisites of socio-economic effect besides the findings of study-wise investigation / learning process. This chapter additionally briefs about the restrictions of the current investigation made together with the possibility of upcoming investigations, which can be taken up in future by the other researcher for further solutions.

7.2 Summary of these Investigations Findings

The most important aim of this investigative effort is to plan to carry out a design method for the development of force measuring transducers/devises, which can facilitate the researchers to build up the precise and accurate force measuring transducers. The prime conclusions of the investigation are as follow:

- The diaphragm shaped force measuring transducers are designed and developed on the base of traditional theories available through literature survey.
- Deflection studies of diaphragm shaped force transducers show variation in results of analytical approach and computational results.
- The steel diaphragm shaped force measuring transducers are fabricated and strain gauges are pasted at appropriate chosen locations.
- Metrological investigative analysis of steel force transducer has been done in accordance

with standard calibration procedures derived from IS 4169 – 88 (reaffirmed 2003) and ISO 376-2004/ 2011 and given suitable outcome. Measurement uncertainty is found up to 0.05 %.

- On the other hand, in low down range another diaphragm shaped force transducers made of silicon for nominal capacity of 50 N are designed, developed and fabricated using MEMS Technology. Measurement uncertainty is found to be less than 0.25 %.

7.3 Study-wise Learning's and Conclusions

- The exhaustive literature evaluation and retrospective investigation involved learning of various types of force measuring transducers/devises, force realizing and measurement techniques, analogue dial gauge force transducers, strain gauged digital force transducers, some other force transducer based on principles like tuning fork based force transducers and Hall Effect based force transducers, special purpose force transducers for some specific intent applications, and different calibration procedures based on ISO/IS standards etc. Although many varieties of force transducers are developed so far, but all of them are restricted to few explicit jobs. The force transducers are fabricated mostly for field applications like monitoring cutting forces during a machining process or studies related to agriculture field. This review study indeed has helped in deciding the research goals.
- The analogue dials gauged ring shaped force transducers had been invented and in inception since 1927 and are currently extensively used in developing economies like India due to cheaper cost in comparison to digital strain gauge force transducers. The force transducers when used with dial gauges are found to have poor metrological

properties due to nonlinearity and poor resolution of the dial gauges in terms of measurement uncertainty of force realization in comparison to strain gauged force transducers. Hence the force transducers with strain gauges prove to be a better measuring system for force realization and have optimal metrological performance. The strain gauged circular diaphragm digital force transducers have been investigated by analytical methods available through literature (Classical plate theory of bending of circular plates) for its design related studies. Another small diaphragm made of silicon using deflection theory of very small MEMS silicon devices are taken into account. The systematic approaches are found to be very useful for computation of the most important parameter e.g. deflection for the design of diaphragm shaped circular force transducer under the action of the nominal static force applied.

- The computational studies are done on circular diaphragm force transducers. The computational studies consist of the finite element analysis (FEA) of circular diaphragm force transducer using the software ANSYSTM. Due to axis-symmetry of circular diaphragm force transducer, the whole body of circular diaphragm force transducer for both the cases i.e. steel and silicon are taken into account along with appropriate assumptions are considered, as mentioned in the analytical methods also. The finite element analysis assists in investigating the stress – strain and deflection models of the whole circular diaphragm force transducer. The finite element analysis discloses that there is prominent diversity in the values of deflection computed by analytical approach and the finite element analysis. Therefore, the investigations doubt about the legality of the analytical perspective and imply that it may be applicable for some limited situations only.

- The circular diaphragm shaped force transducers of unlike material like steel and silicon of different estimated capacity in lower and medium range (50 N and 5000 N) are made-up and strain gauged by hand for steel diaphragm whereas strain gauged with special technique of MEMS technology in case of silicon diaphragm. The fabricated force transducers are then calibrated for their metrological categorization in accordance with standard calibration methods like ISO 376-2004 / 2011 and 4169-88 (reaffirmed 2003) by means of 50 kN dead weight force standard machines for steel diaphragm whereas a special calibration set up was made for handling and testing of small silicon chip force device arrangement . The measurement uncertainty of the force devices has been investigated by considering the %age uncertainty of unlike components such as zero deviation, resolution, reproducibility, repeatability, interpolation, reversibility, etc. pertaining to the measurement uncertainty of the force devices, as per the standard procedure adopted.
- The finite element analysis is very useful in finding out the locations for the strain gauges on the basis of stress – strain patterns found with the help of finite element analysis of the circular diaphragm shaped force devices. The maximum value of stress and strain are found at the centre of both the steel and silicon diaphragm's loading point hence the maximum stress point location at the centre of the diaphragm have not been considered due to practical constraints and design considerations, therefore the second maximum stress location has been chosen with the help of fem model as the most appropriate locations for fixing up resistors.
- The circular diaphragm shaped force transducers are the simplest shaped force transducers in comparison to other shapes like cantilever, hollow cylindrical, sphere,

square, hexagonal, octagonal and other complex shaped elastic sensing membrane force devices for which the strain gauging is a very difficult task. The circular diaphragm shaped force transducers are basically a flat circular ring from inside, and have the smoothed flat surface for pasting the strain gauges with much ease whereas the outer surface of the diaphragm carries the loading point for the applied force.

- The uncertainty of measurement for circular steel diaphragm force transducer is found up to 0.05 % whereas the uncertainty of measurement for circular silicon diaphragm force transducer is found up to 0.22%.
- On the whole, the current investigation bestirs to present an in detail unify of design and development investigations of diverse types of force transducers. These developed force transducers shall be exceptionally useful for manufacture of very easy shaped and reasonably priced force transducers with low measurement uncertainty.

7.4 Key conclusion of Research

- The research bestows a simplified method for design and development of force transducers and applies the analytical as well as computational methods.
- The circular diaphragm shaped force transducers of varied estimated range for low and medium capacities have been designed and developed. The force transducers are further calibrated in accordance with standard calibration methods and found with good quality metrological characterization.
- The function of finite element analysis has also been analyzed and found to be very useful for practically viable different locations for pasting of strain gauges in order to achieve the minimum measurement uncertainty.

- The circular shaped Diaphragm force transducers are simple shaped force transducers, which demonstrate good quality metrological features.
- The circular shaped Diaphragm force transducers fabricated possesses uncomplicated deliberation of design, as well as manufacturing considerations including their instrumentation.
- The investigative research effort confers a comprehensive outline work, relating to the unlike aspects associated to the design, development and metro logically characterization of force transducers, which is very rarely found to be reported.

7.5 Research's Socio-Economic Impact

- Although the force transducers are commercially obtainable for a rated capacity started from 1 Newton to a few some Mega Newton range, however these are found of very intricate shapes and sizes and further their manufacturing machining process including strain gauging of these complex load sensing elements is a very tricky and complicated job.
- The investigate work led to the development of a very simple circular diaphragm shaped force transducers, on the basis of the analytical expression and computational techniques. The force devises fabricated have an uncomplicated design and ease in manufacturing considerations. The commercially available precise force transducers, by various manufacturers throughout the globe, are generally consisting of multiple Wheatstone bridge made up of a combination of a number of strain gauges. The force transducers fabricated following a line of investigation, are having only one Wheatstone bridge, however demonstrate good quality metrological characteristics as par to commercially

available force transducers.

- The unlike force transducers as fabricated during the investigation, their metrological characterization is indicative of good quality metrological presentation and are capable to serve up for particular precise force measurement linked applications. The measurement uncertainty of the force transducers is found well within the limits of various relative components of uncertainty, according to the particular referred standard procedures.
- The steel diaphragm force transducers developed are having maximum measurement uncertainty up to 0.06 %, which are further improved up to 0.05% by double the number of strain gauges in each arm of the Wheatstone bridge. The measurement uncertainty of the steel force transducers is found well within the permitted limits for the majority of the precise measurement allied applications whereas the uncertainty of measurement for circular silicon diaphragm force sensor is less than to 0.25% and overall repeatability below 1% which is widely accepted for the applications in this range.
- If additionally follow a line of investigation work led to decrease in the measurement uncertainty of force transducers, subsequently the force transducers may exhibit enhanced metrological features than the present commercially accessible force transducers.
- This is necessary to have more and more industry - academia interaction for more research and investigations related to the developed force transducers of various types and their active partaking, help and support may assist in reducing in the uncertainty of force transducers, over and above growth of a number of simple shaped precise force transducers.

- The force transducers processed and fabricated are very cost efficient in contrast to the commercially obtainable force transducers, which makes this investigative effort commendable to a larger extent.
- The force transducers developed by this investigative work could be easily available in the Indian market at a very cheap cost with the help of large level commercialization keeping in view the current market costs of commercially easy available force transducers.
- The investigative effort provides a well-ordered recorded work, discussing different facets correlated to the design, development and metrological research of force transducers.

7.6 Important investigation Contribution

- The most important noteworthy role of the investigation is to help within the country to stop the monopoly and to break the trade barricade by provided an option to especially intricate shaped globally available commercial force transducers.
- The usefulness of investigative force transducers has been proven by its metrological characterization results, thus endorses it's capabilities of demonstration for use regarding a variety of applications linked to requirement of precise force measurement.
- The force transducers, because of having exceptionally easy design along with ease mechanized considerations can be fabricated with a very simple machining facilitation and without any extremely difficult instrumentation for data acquisition system.
- The force transducers fabricated in this current investigation could be further modified and developed commercially, credited to the low fabrication cost and small measurement

uncertainty at par with commercially available transducers.

- The investigative effort reports the development of the low cost circular diaphragm shaped steel force transducer with a low measurement uncertainty of 0.06% good to be used as a transfer standard for verification of forces, particularly for static force measurement of site testing machines, another silicon diaphragm sensor has been developed by MEMS technology for the first time in India for precise force measurement applications in low range bio-medical field.
- Further by means of available amenities of industry for manufacturing and instrumentation and their appropriate participation and support could help out in bringing more cost effectiveness of the force transducers.
- Constantly interaction with industry could promote help in growth of a few advance force transducers to meet some specific purposes by modifications in adding up together to the existing reported investigations.

7.7 Limitations of the Investigative Work

- The role of end bosses in conjunction with self-aligning compression pads or tension shackles make easy submission of concerted or tip force to the force transducers. Barely, there is debate at anyplace regarding influence of end bosses over the existing design of the force transducers. All neither through the investigation, the function of end bosses has been taken into account for analytical as well as computational investigations. There is further need for vigorous discussion to find the role of end bosses over the design of force transducers and its overall significant effect on the measurement uncertainty of force transducer to be investigated.

- The circular steel diaphragm shaped force transducers are fabricated to cover up the medium range of nominal of 5 kN only. The measurement uncertainty of this force transducers is establish up to 0.06 %, also circular silicon diaphragm sensor of low range of 50 N only with an overall measurement uncertainty of 0.22% (excluding the %age uncertainty owing to reversibility), which is found as good as and superior in comparison to a few commercially accessible force transducers. Owing to simplicity of design and mechanized techniques, it is desirable to put greater stress over the big scale growth of circular diaphragm shaped force transducers by means of the support and interactions with industry. Owing to some realistic constraints, the investigation could limit to some few circular shaped force transducers.
- Strain gauged force devises be the majority and extensively used for various applications related to precise force measurement, in spite of recently newly added transducers like Hall Effect, laser and MEMS based transducers for force measurement have been investigated and established, however, could not be implemented on a very large level. Proper consideration is also necessary to look into the fitness of non-conventional transducers similar to the conventional strain gauged force transducers, which is already proven to become the most adaptable for force measurement.
- Research investigation has been capable to confer many varieties of transducers for force measurements in different ranges from low to medium ranges from 50 N to 5000 N, however force measurements in micro and sub micro range are required in a good number for engineering applications like tactile, micro hardness, bio-medical related applications measurement, presently there is requirement to have force measurement in ranges below 10 Newton e.g. sub-Newton range. Therefore for this reason, appropriate

efforts should be applied for the growth of force transducers in the sub-Newton range.

7.8 Scope for Future Research Work

- Although the current investigative effort is a mixture of both analytical and computational methods along with the investigational findings from experimental results of metrological characterization of circular diaphragm made of steel and silicon force transducers, but there is still possibility for further prospect research work, which could guide for enhanced clarifications in relation to a number of unthinking technical and methodical aspects of force transducers in much detail:
- This is the high time to undertake the studies regarding the role of end bosses and there consequences on the design work of force transducers, as these are the part from where the applied load transfer takes place as a point line load to the elastic sensing element of the force transducer. Up to the best of information, barely any effort has been done to examine the consequence of end bosses to the force transducers. The analytical and computational examinations have overlooked every feature associated to the end bosses. It will be very fascinated to observe the effect of end bosses over the computational result of the circular diaphragm shaped force transducers.
- The elastic load sensing elements of force transducers of different materials, shapes and sizes are studied for their computational investigations by Ansys software. The software has already been deliberated by some of the researchers earlier also. Presently there are a number of very dedicated software's accessible for finite element analysis of mechanical components. Efforts may be made to examine the force transducers by the different software's and an assessment can be made for the detections achieved by the Ansys

software and the other one. A close conformity in the results would put in extra confidence about the computational analysis done by the researchers.

- The circular diaphragm shaped force transducers have been designed and developed for low and medium rated range using different material and size. Both the force transducers provide a flat surface for ease in applying of the strain gauges. Further efforts may be made to develop the circular diaphragm shaped force transducers in the higher ranges, which is also very important related to a variety of industrialized applications.
- So far a very limited research has been done on the use of non-conventional techniques like Laser based, Hall Effect for the development of force transducers. Therefore, there is need to put more efforts to develop a new class of force transducers based on non-conventional techniques to find out their suitability as precise force transducer to meet the requirements related to various industrial applications.
- Efforts in dedicated manner are required for improvement in the uncertainty of measurement of the MEMS force sensors on continuous basis to achieve it up to 0.1 % or better to provide an alternative to strain gauged force sensors, which are being implied globally for more than five decades.

7.9 Summary

This chapter summing up the research findings related to the development of the force transducers in the past. The most important features of the investigative work have been summarized and discussed all along with the major contributions of the investigation. The socio-economic aspects along with limitations of the research work have been discussed and summarized. The scope of future work also has been discussed and need to have more

emphasize on industry interaction is highlighted for successfully adoption of the investigative findings.

BIBLIOGRAPHY

- [1] Guide to the measurement of force (1998), The Institute of Measurement and Control, United Kingdom.
- [2] Technical Bulletin (1987), National Physical Laboratory, New Delhi, India.
- [3] R J Godwin (1975), An extended octagonal ring transducer for use in tillage studies, *Journal of Agricultural Engineering Research*, Vol. 20, 347-352.
- [4] S Yaldiz and F Ünsaçar (2006), A dynamometer design for measurement of cutting forces on turning, *Measurement*, Vol. 39, 80-89.
- [5] Ferreira H P (2009), Force Measurement, *NRCS – Legal Metrology Division (Technical Report)*.
- [6] G B Anderson (1969), Studies of calibration procedures for load cells and proving rings as weighing devices, *NBS Technical Note – 436*, USA.
- [7] National Institute of Standards and Technology (NIST), The Proving Ring, <http://www.nist.gov/pml/div684/grp07/provingring.cfm> (Downloaded on 03.11.2013)
- [8] National Institute of Standards and Technology (NIST), How did the Proving Ring Come About?, <http://www.nist.gov/pml/div684/grp07/provingringhow.cfm> (Downloaded on 03.11.2013)
- [9] H Kumar and A Kumar (2011), Investigations on measurement uncertainty and long term stability of dial gauged force proving instruments, *NCSLI Measure – the Journal of Measurement Science*, Vol. 6, 64-68.
- [10] <http://www.omega.com/literature/transactions/volume3/strain2.html> (Downloaded on 15.07.2013)

- [11] <http://www.gtm-gmbh.com/en/products/force-transducers.html> (Downloaded on 15.08.2013)
- [12] F J Cangnan (1996), Displacement / force measurement transducer utilizing Hall Effect sensors, US 5339699A (Patent).
- [13] C W Richest (2006), Design and characterization of a low cost dual differential proving ring force sensor utilizing Hall Effect sensors, Massachusetts Institute of Technology, USA (B S Thesis).
- [14] T Hayashi, Y Katase, K Ueda, T Hoshino, H Suzawa and M Kobayashi (2008), Evaluation of tuning fork type force transducer for use as a transfer standard, *Measurement*, Vol. 41, 941-949.
- [15] J N Libii (2004), Design Analysis and testing of a force sensor for use in teaching and research, *World Transaction on Engineering and Technology Education*, Vol. 5, 175-178.
- [16] H Kumar and A Kumar (2011), "Stability studies of force proving instruments", *Proceedings of Asia Pacific Symposium on Measurement of Mass, Force and Torque*, Xi'an, China.
- [17] J L Dorrity and B E Gilliland (1977), A digital force transducer, *IEEE Transactions on the Instrumentation and Measurement*, Vol. 26, 411-414.
- [18] C Rohrbach and J Lexow (1986), Miniature force transducers with strain gauges, *Measurement*, Vol. 4, 93-100.
- [19] E K J Chadwick and A C Nicol (2001), A novel force transducer for the measurement of grip force, *Journal of Biomechanics*, Vol. 34, 125-128.
- [20] D M Stefansu (2006), N shaped axisymmetric elastic elements for strain gauged force

- transducers, *Proceedings of XVIII IMEKO World Congress*, Rio de Janeiro, Brazil.
- [21] S S K Titus, K K Jain, S K Dhulkhed and P Yadav (2009), Design and development of precision artifact for dissemination of low forces of 1 N and 2 N, *Proceedings of XIX IMEKO World Congress*, Lisbon, Portugal.
- [22] A Pusa (2005), Long-Term Observation of Force Transfer Transducers as a Tool to Confirm the Measurement Capability of Force Standard Machines, *Mapan – Journal of Metrology Society of India*, Vol. 20 (3), 231-237.
- [23] A Pusa (2007), The long term behaviour of force transducers as a criterion for the selection of a new transfer standard, *Proceedings of IMEKO 20th TC3, 3rd TC 16 and 1st TC 22 International Conference*, Merida, Mexico.
- [24] H Kumar (2013), A study of the long term stability of force transducers, *NCSLI Measure – the Journal of measurement Science*, Vol. 8, 40-44.
- [25] J Andrea, C Hons and A Sawla (2003), High precision force transducers with new method for online compensation of parasitic effects, *Measurement*, Vol. 33, 173-178.
- [26] T Ueda, F Kohsaka and E Ogita (1985), Precision force transducers using mechanical resonators, *Measurement*, Vol. 3, 89-94.
- [27] C Gehin, C Barthod and Y Teisseyre (2000), Design and characterization of a new force resonant sensor, *Sensors and Actuators A- Physical*, Vol. 84, 65-69.
- [28] C Barthod and C Gehin (2000), New force sensor based on a double ended tuning fork, *IEEE / EIA International Frequency Control Symposium and Exhibition*, Kansas City, USA.
- [29] Z Wang, H Zhu, Y Dong and G Feng (2004), Development of a high resolution quartz resonator force and weight sensor with increased reliability, *IEEE / ASME Transactions*

- on Mechatronics*, Vol. 9, 399-406.
- [30] J M Friedt and E Caary (2007), Introduction to the quartz tuning fork, *American Journal of Physics*, Vol. 75, 415-422.
- [31] A Cheshmehdoost, B E Jones and B O'Connor (1991), Characteristics of a force transducer incorporating a mechanical DETF resonator, *Sensors and Actuators A: Physical*, Vol. 26, 307-312.
- [32] A Cheshmehdoost and B E Jones (1996), Design and performance characteristics of an integrated high-capacity DETF-based force sensor, *Sensors and Actuators A: Physical*, Vol. 52, 99-102.
- [33] S. Mäuselein, O. Mack, R. Schwartz, G. Jäger (2009), Investigations of New Silicon Load Cells with Thin-Film Strain Gauges, XIX IMEKO World Congress Fundamental and Applied Metrology, Lisbon, Portugal.
- [34] S. Mäuselein, O. Mack, R. Schwartz, G. Jäger (2008), Single crystalline sensors with thin-film strain gauges for force measurement and weighing technology, *International Conference on Precision Measurement*, Ilmenau.
- [35] K. D. Wise, (2007), Integrated sensors, MEMS, and Microsystems: reflections on a fantastic voyage, *Sensor. Actuat. A - Phys.*, Vol. 136, 39-50.
- [36] R. Kumme, O. Mack, B. Bill, H.R. Haab, C. Gossweiler,(2002), Dynamic Properties and Investigations of Piezoelectric Force Measuring Devices, VDI-Bericht 1685, VDI Verlag GmbH, Düsseldorf, ISBN 3-18-091685-0, 161–172.
- [37] S. Mäuselein, O. Mack, R. Schwartz, (2006), Investigations into the use of single-crystalline silicon as mechanical spring in load cells, *XVIII IMEKO World Congress*, Brazil.

- [38] A A Barlian, W T Park, J R Mallon, Jr., A J Rastegar, and B L Pruitt . (2009), Review: Semiconductor Piezoresistance for Microsystems, Proceedings of the IEEE, IEEE 97, No. 3.
- [39] A S A Mohammed, A M Walied and L Edmond (2008), High Sensitivity MEMS Strain Sensor, Design and Simulation, *Sensors* , Vol. 8, 2642-2661.
- [40] L Daniel , S D Ricardo, F Ephraim, E K Dennis (2005) , MEMS-Based Force Sensor: Design and Applications, *Bell Labs Technical Journal*, Vol. 10(3), 61–80.
- [41] S Beeby, G. Ensell, M. Kraft, and N. White (2004) *MEMS Mechanical Sensor*, Norwood, MA: Artech House.
- [42] L Beccai, S Roccella, A Arena, F Valvo, P Valdastrì, A Menciassi, M C Carrozza, P Dario (2005), Design and fabrication of a hybrid silicon three-axial force sensor for biomechanical applications, *Sensors and Actuators A*, Vol. 120, 370–382
- [43] B Massa, S Roccella, R Lazzarini, M Zecca, M C Carrozza, P Dario (2002), Design and development of an underactuated prosthetic hand, Proceedings of the 2002 IEEE International Conference on Robotics and Automation, Washington.
- [44] P Dario, C Laschi, A Menciassi, E Guglielmelli, M C Carrozza, L Zollo, G Teti, L Beccai, F Vecchi, S Roccella (2002), A Humanlike robotic manipulation system implementing human models of sensory-motor coordination, Proceedings of the IARP 2002, 3rd International Workshop on Humanoid and Human Friendly Robotics, Tsukuba, Japan, 97–103.
- [45] J B David , D D Denton, R G Radwin (1998), *IEEE* and J G Webster, A Silicon-Based Tactile Sensor for Finger-Mounted Applications *IEEE Transactions On Biomedical Engineering*, Vol. 45 (2), 151.

- [46] R Wiegerink, R Zwijze, G Krijnen, T Lammerink, M Elwenspoek,(1999) Quasi Monolithic Silicon Load Cell for Loads up to 1000 kg with Insensitivity to Non-homogeneous Load Distributions, MEMS'99, Orlando, Florida, Jan. 17-21.
- [47] J Lin, K Walsh, D Jackson, J Aebersold, M Crain, J Naber, W Hnat,(2007), Development of capacitive pure bending strain sensor for wireless spinal fusion monitoring *Sensors and Actuators A: Physical* , Vol. 138, 276-287.
- [48] W Ko, D Young, J Guo, M Suster, H K Chaimanonart (2007) A high-performance MEMS capacitive strain sensing system, *Sensors and Actuators A: Physical* , Vol. 133, 272-277.
- [49] C Liu, Recent developments in polymer MEMS, (2007) *Adv. Mater.*, Vol. 19, 3783-90.
- [50] L Cao, T Kim, S Mantell, D Polla,(2000), Simulation and fabrication of piezoresistive membrane type MEMS strain sensors *Sensors and Actuators A: Physical*, Vol. 80, 273-279.
- [51] K Yongdae, K Youngdeok , L Chulsub , K Sejin (2008), 3D Force and Displacement Sensor for SFA and AFM Measurements, *Langmuir* , Vol. 24, 1541-1549
- [52] K Kristiansen, P McGuiggan, G Carver, C Meinhart, J Israelachvili,(2010), Thin Polysilicon Gauge for Strain Measurement of Structural Elements, *IEEE Sensors Journal*, Vol. 10(8). .
- [53] R Kumar, S Rab, B. D. Pant, S Maji (2018), Design, development and characterization of MEMS Silicon diaphragm Force sensor Vacuum, Vol. 153, 211-216.
- [54] M A Rehman and S Rehman (2007), A computer program for designing circular proving rings of uniform strength, *Journal of the Institution of Engineers (India) Mechanical Engineering Division*, Vol. 88, 3-7.

- [55] S Fank and M Demirkol (2006), Effect of microstructure on the hysteresis performance of force transducers using AISI 4340 steel spring material, *Sensors and Actuators A – Physical*, Vol. 126, 25-32.
- [56] B Aydemir, E Kaluc and S Fank (2006), Influence of heat treatment on hysteresis error of force transducers manufactured from 17-4PH stainless steel, *Measurement*, Vol. 39, 892-900.
- [57] S Karabay (2007), Design criteria for electro-mechanical transducers and arrangements for measurement of strains due to metal cutting forces acting on the dynamometers, *Materials and Design*, Vol. 28, 496-506.
- [58] S Karabay (2007), Analysis of drill dynamometer with octagonal ring type transducers for monitoring of cutting forces in drilling and allied process, *Materials and Design*, Vol. 28, 673-685.
- [59] M O’gherty (1996), The design octagonal ring dynamometers, *Journal of Agriculture Engineering Research*, Vol. 63, 9-18.
- [60] S Yaldiz, F Ünsaçar, H Sağlam and H Işık (2007), Design, development and testing of a four-component milling dynamometer for the measurement of force and torque, *Mechanical Systems and Signal Processing*, Vol. 21, 1499-1511.
- [61] I Korkut (2003), A dynamometer design and its construction for milling operation, *Materials and Design*, Vol. 24, 631-637.
- [62] S Yaldiz and F Ünsaçar (2006), Design, development and testing of a turning dynamometer for cutting force measurement, *Materials and Design*, Vol. 27, 839-846.
- [63] S Karabay (2007), Performance testing of a constructed drill dynamometer by deriving empirical equations for drill torque and thrust on SAE 1020 steel, *Materials and Design*,

- Vol. 28, 1780-1793.
- [64] G Barbato and F Franceschini (1994), Performance indicators for multicomponent dynamometers, *Measurement*, Vol. 13, 297-306.
- [65] M Askari and S Khalifahamzehghasem (2013), Draft Force Inputs for Primary and Secondary Tillage Implements in a Clay Loam Soil, *World Applied Science Journal*, Vol. 21, 1789-1794.
- [66] Y Chena, N B McLaughlinb and S Tessier (2007), Double extended octagonal ring (DEOR) drawbar dynamometer, *Soil and Tillage Research*, Vol. 93, 462-471.
- [67] S A Masroor and L W Zachary (1991), Designing an all-purpose force transducer, *Experimental Mechanics*, Vol. 31, 33-35.
- [68] A Balakeborough, D Clément, M S Williams and N Woodward (2002), Novel load cell for measuring axial force, shear force, and bending movement in large-scale structural experiments, *Experimental Mechanics*, Vol. 42, 115-120.
- [69] M J Dixon (1991), Development of a load-cell compensation system, *Experimental Mechanics*, Vol. 31, 21-24.
- [70] R A Mitchell (1991), Misalignment sensitivity test for load cells, *Experimental Mechanics*, Vol. 31, 140-143.
- [71] R Skelton and J A Richardson (2006), A transducer for measuring tensile strains in concrete bridge girders, *Experimental Mechanics*, Vol. 46, 325-332.
- [72] D Diddens, D Reynaerts and H V Brussel (1995), Design of a ring shaped three axis micro force / torque sensor, *Sensors and Actuators A - Physical*, Vol. 46-47, 225-232.
- [73] J W Joo, K S Na and D I Kang (2002), Design and evaluation of a six component load cell, *Measurement*, Vol. 32, 125-133.

- [74] R J Wood, KJ Cho and K Hoffman (2009), A novel multi-axis force sensor for microrobotics applications, *Smart Material Structures*, Vol. 18, 125002.
- [75] D Lopez, R S Decca, E Fischbach and D E Krause (2005), MEMS - based force sensors: design and applications, *Bell Labs Technical Journal*, Vol. 10, 61-80.
- [76] G N Bakalidis, E Glavas, N G Voglis and P Tsalides (1996), A low cost fiber optic force sensor, *IEEE Transactions on the Instrumentation and Measurement*, Vol. 45, 328-331.
- [77] Gab-Soon Kim (2002), Uncertainty evaluation of a multi-axis force / moment sensor, *International Journal of the Korean society of Precision Engineering*, Vol. 3, 5-11.
- [78] Oliver Mack (2007), Investigations of piezoelectric force measuring devices for use in legal weighing metrology, *Measurement*, Vol. 40, 746-753.
- [79] H M Aguilar and F A Aguilar (2009), A force transducer from a junk electronic balance, *Physics Education*, Vol. 44, 652.
- [80] K Li and C Zhu (2010), Design and measurement of hollow cylinder type force transducer with ultra-low height, *Proceedings of International conference on Electronic and Control Engineering*, Wuhan, China.
- [81] G P Behrmann, J Hiddler and M S Mirotzink (2012), Fiber optic micro sensor for the measurement of tendon forces, *Bio Medical Engineering Online*, Vol. 11, 77.
- [82] B Chen, X Wu and X Peng (2007), Finite element analysis of ring strain sensor, *Sensors and Actuators A - Physical*, Vol. 139, 66-69.
- [83] H Kumar and S K Jain (2009), Evaluation of axial sensitivity of circular ring shaped force proving ring using finite element analysis (FEM), *Proceedings of 7th International Conference on Advances in Metrology (Admet)*, New Delhi, India.
- [84] S Kumar, N Hasan, H Kumar and A Kumar (2011), Finite element analysis of a force

- transducer, *Indian Journal of Science and Technology*, Vol. 4, 1246-1247.
- [85] D M Stefanescu and D I Kang (2003), Selection criterion for the elastic elements of very large force transducers, *Proceedings of Asia Pacific Symposium of Mass and Force – Theory, Practice and Applications*, Shanghai, China.
- [86] D M Stefansu, L Dolga and A Marinescu (2003), Parametrical modeling of the strain gauged force and or pressure transducers, *Proceedings of XVII IMEKO World Congress*, Dubrovnik, Croatia.
- [87] J H Antkowiak and J J Rencis (1994), Geometric nonlinearities in the design of force transducers, *Advances in Engineering Software*, Vol. 21, 11-16.
- [88] Method for calibration of force proving instruments used for verification of uniaxial testing machines, *IS 4169-1988 (re-affirmed 2003)*.
- [89] Metallic materials – Calibration of force proving instruments used for verification of uniaxial testing machines, *ISO 376-2004 / 2011*.
- [90] D I Kang and C S Hong (1994), Rotation effects of force transducers on the output of a build-up system, *Measurement*, Vol. 14, 147-156.
- [91] A Bray, G Barbetto, F Franceschini and E Xhomo (1996), Rotational and end effects: a model for uncertainty evaluation in force measurement by means of force dynamometers, *Measurement*, Vol. 17, 279-286.
- [92] M K Dass Gupta (1987), Calibration of the force measuring devices, *MAPAN – Journal of Metrology Society of India*, Vol.2, 131-134.
- [93] D E Marlowe (1975), A study of the national force measurement system, National Bureau of Standards, USA.
- [94] T W Bartel, S L Yaniv and R L Seiforth (1997), Force measurement services at NIST:

- equipment, procedures and uncertainty, *Proceedings of NCSL Workshop & Symposium*, USA.
- [95] <http://www.ptb.de/cms/en/fachabteilungen/abt1/fb-12/ag-121/measuring-devices.html>
(downloaded on 15.03.2013)
- [96] K K Jain, S K Jain, J K Dhawan and A Kumar (2005), Realization of force scale up to 50kN through dead weight force, *MAPAN – Journal of Metrology Society of India*, Vol. 20, 249-257.
- [97] S S K Titus, S K Dhulkhed, P Yadav and K K Jain (2009), Development and performance evaluation of a dead weight force machine in 2 – 50 N range, *Mapan – Journal of Metrology Society of India*, Vol. 24, 225-232.
- [98] H Kumar, A Kumar and P Yadav (2011), Improved performance of 50 kN dead weight force machine using automation as a tool, *Measurement Science Review*, Vol. 11, 67-70.
- [99] H Kumar and A Kumar (2013), Inter-comparison as a measure of the performance evaluation of the force standard machines at National Physical Laboratory, India (NPLI), *Current Science*, Vol. 105, 1038-1043.
- [100] R Kumar, H Kumar, A Kumar and Vikram (2012), Long term uncertainty investigations of 1 MN force calibration machine at NPL, India (NPLI), *Measurement Science Review*, Vol. 12, 147-150.
- [101] C Ferrero (2005), Multicomponent Force Sensors, *Mapan – Journal of Metrology Society of India*, Vol. 20(3), 213-221.
- [102] Y K Park and D I Kang (2005), Build-Up Force-Measuring System and its Applications, *Mapan – Journal of Metrology Society of India*, Vol. 20(3), 223-229.
- [103] C Schlegel, O Slanina, G Haucke and R Kumme (2012), Construction of a standard force

- machine for the range of 100 μN –200 mN, *Measurement*, Vol. 45, 2388-2392.
- [104] S Niehe (2005), Force Measuring Facility from the Range of 1 mN to 10 N, *Mapan – Journal of Metrology Society of India*, Vol. 20(3), 239-248.
- [105] R Kumar and S Maji (2016), Force transducers – a review of design and metrological issues, *Engineering Solid Mechanics*, Vol. 4, 81-90.
- [106] R Kumar, S Rab, B D Pant, S Maji and R. S. Mishra (2018), FEA based design studies for development of diaphragm force transducers, *Mapan – Journal of Metrology Society of India*. (**Accepted**).
- [107] S. Timoshenko and S. Woinowsky-Krieger, (2010), Theory of plates and shells Tata McGraw Hill Education Private Limited, 2nd Edition.
- [108] W Yun, X Rongqiao and D Haojiang, (2010), Three dimensional solution of axisymmetric bending of functionally graded circular plates, *Elsevier Composite Structures*, Vol. 92, 1683–1693.
- [109] S.J Wang. (2010), Overload Protection Design of Silicon Pressure Sensor, *Instrument technique and sensor*, Vol. 35, pp 7-8.
- [110] L Zhao, X Fang, Y Zhao, Z Jiang, and L Yong, (2011), A High Pressure Sensor with Circular Diaphragm Based on MEMS Technology *Key Engineering Materials*, Vol. 483, 206-211.
- [111] S.M. Shaby, A.V. Juliet, (2012), Design and analysis of MEMS pressure sensor by using ANSYS, Proceedings of the 2nd International Conference on Mechanical, Automotive and Materials Engineering (MAME, 12), Bali (Indonesia),pp 132–135.
- [112] A Bray, (1981), Role of stress analysis in the design of force standard transducers, *Experimental Mechanics*, Vol. 21, 1–20.

- [113] Guidelines for Estimation and Expression of Uncertainty in Measurement, *NABL 141*.
- [114] International Standards Organization (1995), Guide for Expression of Uncertainty in Measurement, *ISO GUM Document*.
- [115] R Kumar, B D Pant, and S Maji (2016), Design, Development and Metrological Characterization of a Force Transducer, *Journal of Scientific & Industrial Research*, Vol. 75, 320-321.
- [116] R Kumar, B D Pant, and S Maji,(2017), Development and Characterization of a Diaphragm-Shaped Force Transducer for Static Force Measurement, *MAPAN-Journal of Metrology Society of India*, Vol. 32(3), 167–174.
- [117] M J Madou, Fundamentals of Microfabrication, FL, Boca Raton, CRC Press, 2002.
- [118] P R Choudhury (Ed), *Handbook of Microlithography, Micromachining, and Microfabrication*, Vol. (1-2), SPIE Press and IEE Press 1997, ISBN 0-8529-6906-6 (Vol. 1) and 0-8529-6911-2 (Vol. 2)
- [119] G Kovacs, *Micromachined Transducers Sourcebook*, McGraw-Hill 1998, ISBN 0-0729-0722-3.
- [120] Stephen D Senturia, *Microsystem Design*, Kluwer 2000, ISBN 0-7923-7246-8
- [121] E Gentili L, Tabaglio F Aggogeri, Review of Micromaching Techniques, *Advanced Manufacturing Systems and Technology*, Springer Wien New York, 2005.
- [122] Babak Ziaie, Antonio Baldi, Ming Lei, Yuandong Gu and Ronald A Siege (2004), Hard and soft micromachining for BioMEMS: review of techniques and examples of applications in microfluidics and drug delivery, *Advanced Drug Delivery Reviews*, Vol. 56 (2), 145-172

- [123] An Introduction to MEMS (Micro-electromechanical Systems) ISBN 1-84402-020-7, Wolfson School of Mechanical and Manufacturing Engineering Loughborough University, Loughborough, Leics.
- [124] Julian W Gardner, Vijay K Varadan, and Osama O Awadelkarim, *Microsensors, MEMS and Smart Devices*, Wiley, 2001, ISBN 0-4718-6109-X
- [125] Nadim Maluf, *An Introduction to Microelectromechanical Systems Engineering*, Artech House, 1999, ISBN 0-8900-6581-0
- [126] G T A Kovacs, N I Maluf and K E Petersen (1998), Bulk micromachining of silicon, *Proc. IEEE*, Vol.86, 1536-1551.
- [127] Jack S Kilby, Semiconductor Solid Circuits, Texas Instruments, Inc. Dallas, Texas. *Electronics*, August 7, 1959. McGraw-Hill Pub. Co.
- [128] Remco J Wiegerink and Miko Elwenspoek, *Mechanical Microsensors (Microtechnology and MEMS)*, Springer Verlag, 2001, ISBN 3-5406-7582-5

BIO-DATA

Name	Rajesh Kumar
Date of Birth	November 09, 1967
Qualification	<ul style="list-style-type: none">• B. E. (Mechanical & Engineering), 1996 First Division, Jamia Millia Islamia, Jamia Nagar Okhla, New Delhi-110025.• Ph. D. (Mechanical Engineering), 2018 Delhi Technological University Shahabad Daulatpur, Main Bawana Road, Delhi-110042
Experience	31 Years (Research & Academic)
Current Designation	Principal Scientist
Organization	CSIR – National Physical Laboratory, Dr. K S Krishnan Marg, New Delhi, India
Areas of Interest	Mechanical Measurements & Metrology Manufacturing Engineering
Phone Number	+91-9871154967
E-mail	rajeshkumarh33@gmail.com; kumarr@nplindia.org